UNIVERSITÀ DELLA CALABRIA

UNIVERSITA' DELLA CALABRIA

Dipartimento di Ingegneria Meccanica, Energetica e Gestionale (DIMEG)

Dottorato di Ricerca in

Ingegneria Civile e Industriale

CICLO

XXXII

Development of a CAE-based approach for the concurrent design, manufacturing and testing of hybrid metal-composite spur gears

Settore Scientifico Disciplinare ING/IND 13

Coordinatore: Ch.mo Prof. Franco Furgiuele

Firma _____

Supervisore/Tutor: Ch.mo Prof. Domenico Mundo

Firma _____

Co-Supervisore: Dr. Alessandra Treviso

Firma _____

Dottorando: Dott. Piervincenzo Giovanni Catera

Firma _____

Declaration of Authorship

I, Piervincenzo Giovanni CATERA, declare that this thesis titled, "Development of a CAE-based approach for the concurrent design, manufacturing and testing of hybrid metal-composite spur gears" and the work presented in it are my own. I confirm that:

- This work was done wholly or mainly while in candidature for a research degree at this University.
- Where any part of this thesis has previously been submitted for a degree or any other qualification at this University or any other institution, this has been clearly stated.
- Where I have consulted the published work of others, this is always clearly attributed.
- Where I have quoted from the work of others, the source is always given. With the exception of such quotations, this thesis is entirely my own work.
- I have acknowledged all main sources of help.
- Where the thesis is based on work done by myself jointly with others, I have made clear exactly what was done by others and what I have contributed myself.

Signed:

Date:

26/11/2019

"Il viaggio alla scoperta di sé può essere pieno di mille insidie, ma dovrete compierlo in autonomia, senza evitare gli ostacoli. Cercate da soli la vostra strada, cambiatela tutte le volte che volete, seguite i vostri sogni. Non lasciate che l'educazione, le abitudini, i vostri stessi preconcetti diventino una prigione.
Abbiate sempre il coraggio di cambiare voi stessi- le vostre idee, il vostro approccio, il vostro punto di vista- perché è l'unico modo per cambiare le cose che non vanno e per migliorare la vostra vita e quella di tanti altri.
E mentre cercate la vostra strada, tenete a mente chi volete diventare. Pensate a quale impronta volete lasciare, a quale differenza volete fare. Rimanete ambiziosi nei vostri obiettivi, perché rassegnarsi a una vita mediocre non vale mai la pena."

Sergio Marchionne

Acknowledgements

The present work was one of the most exciting and, at the same time, fascinating challenges I dealt with in my life.

During these three years, I have understood that the scientific research does not only constitute a continuous progress of knowledge in a specific field, but it represents something of deeper and more complex. Here, two different perspectives, the scientific and the humanistic one, apparently conflicting each other, meet together in a perfect and incredible symbiosis, which defines the figure of the researcher.

At the end of this experience, I increased awareness about the fact that the researcher is brave. This strength, which is the capability to face a new challenge with perseverance and determination, was my daily incentive and the only certainty to restart from the several standstills, which characterized these troubled years. For this reason, I thank my family, my dad, my brother and, in particular, my mum who was for me an extraordinary example of strength and, I am sure, she will be for the rest of my life. I thank her for moulding my mind with her stubborn to not give up and with her continuous optimism when everything seems to be covered by the darkness of the defeat.

I thank Mara, my great support, my unlimited source of inspiration, for the realization of my goals. I thank her for sharing always with the same passion the pages of my life. I hope to live up to her extraordinary love for me.

I would like to express sincere gratitude to the Prof. Mundo, who allowed me to have all the great working chances.

I thank Francesco, for all the precious suggestions in my research field.

Special thanks to the Simulation division office of Siemens Industry Software, to Ali, Laszlo, Anna, Valene, Daehyun and Tommaso for their availability with my research, by allowing me to develop my work in the best possible way.

I thank the National Composite Centre and, in particular, Alessandra, for giving me the opportunity to know a different reality, by believing in my research and bringing me to acquire deeper competences in the field of composite materials.

I thank Mara's parents, for cuddling and supporting me in every moment, above all during the most difficult periods.

I thank my colleagues Mathijs, Shadi, Antonio, Giuseppe e Walter for sharing with me these years.

Ringraziamenti

Il presente lavoro ha rappresentato una delle più stimolanti e, allo stesso tempo, affascinanti sfide che ho affrontato nel corso della mia vita.

Durante questi tre anni, ho compreso che la ricerca scientifica non costituisce esclusivamente un continuo avanzamento delle conoscenze in uno specifico settore disciplinare, ma si figura come qualcosa di più profondo e complesso, in cui due aspetti apparentemente contrastanti, quali quello scientifico e umano, si incontrano in una perfetta e mirabile simbiosi, che definisce la figura del ricercatore.

Alla fine di tutto il percorso, ho maturato il pensiero che essere ricercatori significhi essere coraggiosi. Questo coraggio, ovvero questa capacità di affrontare con determinazione e perseveranza una nuova sfida, per quanto difficile, è stato il mio quotidiano stimolo e la unica certezza da cui ripartire dopo le tante battute d'arresto che hanno caratterizzato questi turbolenti anni. Perciò ringrazio la mia famiglia, mio padre, mio fratello e, soprattutto, mia madre, la quale è stata per me straordinario esempio di coraggio e che, sono certo, continuerà ad esserlo in ogni momento della mia esistenza. La ringrazio per avermi plasmato con la sua caparbia volontà di non arrendersi mai e il suo continuo ottimismo anche in situazioni in cui tutto sembra avvolto dalle tenebre delle sconfitte.

Ringrazio Mara, il mio conforto più grande, la mia sconfinata fonte di ispirazione per il raggiungimento di continui traguardi. La ringrazio per aver condiviso e continuare a condividere sempre e con la stessa passione le pagine della mia vita. Spero di poter essere sempre all'altezza del suo straordinario amore nei miei confronti.

Ringrazio con sincerità il Prof. Mundo, per avermi concesso delle grandi opportunità lavorative durante questi anni.

Ringrazio Francesco, per tutti i consigli preziosi ricevuti nell'ambito della ricerca.

Un ringraziamento speciale all'ufficio Simulation Division della Siemens Industry Software, a Ali, Laszlo, Anna, Valene, Daehyun e Tommaso per la loro disponibilità riguardo alla mia attività di ricerca e per avermi permesso di svolgere al meglio il mio lavoro con i loro preziosi consigli.

Ringrazio il National Composites Centre e, in particolare, Alessandra, per avermi dato l'opportunità di conoscere una diversa realtà e aver creduto nello sviluppo della mia ricerca, portandomi ad acquisire più profonde competenze nel campo dei materiali compositi.

Ringrazio i genitori di Mara, per avermi coccolato e supportato in ogni momento, facendomi sentire la loro continua vicinanza, soprattutto nei periodi più difficili.
Ringrazio i colleghi Mathijs, Shadi, Antonio, Giuseppe e Walter per aver condiviso con me questi anni di dottorato.

Contents

Abstract

Trends in emission limitations and fuel efficiency impose a more efficient energy exploitation in many application fields of mechanical systems. In this direction, the lightweighting of mechanical structures represents a powerful strategy, above all in the transportation industry, where geared transmissions play a key role. Here, these components are designed in such a way that performance criteria are met at the minimum weight, without compromising the requirements of reliability and safety.

In this context, the aim of the present work is the development of new strategies for the design of geared systems, where the concept of gear body lightweighting with geometrical modifications is substituted by the one applied to the material, in order to improve the strength-to-weight ratio and reduce vibrations in the overall mechanical system. In particular, the research is focused on innovative methods for the simulation, manufacturing and testing of a hybrid gear, in which a metal rim is joined with a composite body. In detail, the contribution of the gear body stiffness is studied by means of a multi-scale approach, which starts from the interaction between matrix and fibres at the micro-scale to derive the lamina properties at the macro-scale. In this way, the anisotropy of the composite material can be accounted for, leading to an accurate modelling and evaluation of the mechanical properties of the gear. Additionally, two assembly techniques are used for joining the rim part to the body, which include adhesive bonding and interference fitting. Both techniques are analysed with experimental modal tests to characterize dynamic stiffness and damping in comparison to a lightweight metal gear with the same mass.

At the same time, non-linear finite element (FE) simulations are executed for the evaluation of the static transmission error and meshing stiffness.

Finally, the last part of the work deals with the experimental analysis of a hybrid gear pair during meshing in a dedicated test-rig, where the dynamic behaviour is analysed with respect to the variation of applied torque and rotational velocity. Noise and vibration behaviour of a solid-hybrid gear pair is compared to that of a pair composed by a solid and a lightweight metal gear. Experimental results show the great potentiality of the multi-material approach in mechanical power transmissions.

Sommario

La necessità di ridurre in modo sempre maggiore consumi di carburante ed emissioni di sostanze inquinanti comporta una ricerca di soluzioni ingegneristiche efficaci nell'ambito dei sistemi meccanici. In questa direzione, il processo di alleggerimento di strutture meccaniche rappresenta una potente strategia, soprattutto nel settore dei trasporti, in cui i sistemi di trasmissione del moto mediante ruote dentate giocano un ruolo chiave. Di conseguenza, i moderni criteri di progettazione si scontrano con la necessità di ridurre il peso dei componenti, senza mai compromettere i requisiti di affidabilità e sicurezza.

In questo contesto, lo scopo della ricerca è lo sviluppo di nuove strategie di progettazione per sistemi di trasmissioni a ruote dentate, con il passaggio dal concetto di alleggerimento della geometria del corpo ruota a quello applicato al materiale, al fine di migliorare l'indicatore di prestazioni rigidezza-peso e mitigare le vibrazioni nell'intero sistema meccanico. In particolare, la ricerca si focalizza su innovativi metodi per la simulazione, prototipazione e test di un modello di ruota dentata ibrida, caratterizzata da una corona metallica e un corpo ruota in materiale composito. Nel dettaglio, il contributo alla rigidezza del corpo ruota è studiato mediante un approccio multi-scala, che parte dall'interazione tra fibra e matrice alla micro-scala fino ad esaminare la disposizione delle lamine in una macro-scala. Ciò permette di considerare l'anisotropia del materiale composito per un'accurata valutazione delle proprietà meccaniche della singola ruota. Inoltre, due tecniche di assemblaggio sono analizzate per l'unione del corpo ruota alla corona metallica, che comprendono l'incollaggio mediante utilizzo di adesivi e il collegamento con interferenza. Entrambi gli approcci sono valutati sperimentalmente attraverso test modali per la determinazione di rigidezza dinamica e smorzamento e confrontati con il caso di ruota metallica alleggerita con uguale massa. Parallelamente, simulazioni statiche non-lineari agli elementi finiti sono eseguite per la valutazione di errore di trasmissione statico e rigidezza di ingranamento per entrambe le tecniche.

Infine, la parte conclusiva del lavoro è focalizzata sull'analisi dell' ingranamento delle ruote ibride su un banco prova in cui il comportamento dinamico è analizzato al variare della velocità di rotazione e della coppia applicata. I valori di vibrazione e rumore sono analizzati nel caso di una trasmissione con ruote dentate ibride e confrontati con

quelli ottenuti mediante l'utilizzo di ruote in metallo alleggerite. I risultati mostrano le grandi potenzialità dell'approccio multi-materiale nella progettazione e nella realizzazione di trasmissioni meccaniche.

List of Figures

List of Tables

List of Abbreviations

NVH	Noise, Vibration, Harshness
CAE	Computer Aided design
FE	Finite Element
TE	Transmission Error
CFRP	Carbon Fibre Reinforced Polymers
VMC	Virtual Material Characterization
UD	Unidirectional
ELST	Equivalent Single Layer Theory
LWT	Layer-Wise Theory
CLT	Classical Lamination Theory
FSDT	First Order Shear Deformation Theory
ZZT	ZigZag Theory
FRP	Fibre Reinforced Polymers
RUC	Representative Unit Cell
N&V	Noise and Vibration
2D	Two-Dimensional
3D	Three-Dimensional
FRFs	Frequency Response Functions
Tg	Glass Temperature
DMA	Dynamic Mechanical Analysis
DOF	Degree of Freedom
STE	Static Transmission Error
DTE	Dynamic Transmission Error
MB	Multibody

A mia Madre, a mio Padre, a mio Fratello, a Mara,
presenze costanti di infinito valore nella mia vita.

Chapter 1

Introduction

1.1 The spread of composite materials for lightweight structures

Nowadays, the human society is facing the global warming as one of the most critical problems. The carbon dioxide (CO_2), mainly generated by the burning of fossil fuels, is the primary responsible of the climate change. It behaves like a glass of a greenhouse remaining in the atmosphere longer than other emitted gas and contributing to the growth of the earth temperature. In this direction, the European Union has defined a set of emission standards that all new vehicles must meet [1], which require a continuous research on efficient solutions on different industrial scales to minimize the air pollutants released into the atmosphere. In the transportation sector, which has a great impact on the fuel consumption and CO_2 emissions, the development of lightweight structures can be seen as one of the possible answers to the always more stringent limitations.

In the last decades, multilayer materials have been introduced as a viable alternative to the use of metals in structural applications. Since graphite fibres were first developed around 1960s, the importance of composite materials increased quickly over the years [2], mainly due to their intrinsic properties of high strength and stiffness, low density and high damping capability. This development was possible thanks to the combination of two or more components, classified as matrix and fibres, which combine different characteristics. Generally, the function of the matrix, made of polymers, metals or ceramics is to hold and protect fibres from external damages and, often, to contribute some properties like ductility and toughness. On the other hand, the strength and stiffness properties are typical of fibrous reinforcement. Their use arises from the idea that a material is stronger and stiffer in fibre form of very thin diameter than in the bulk form [3].

In this context, a large number of market sectors benefited from the introduction of composite materials and their employment has been in continuous growth, especially in aerospace, automotive and wind energy sectors. Aerospace industry has always been in a leading position for the development of primary and secondary composite structures for military and commercial aircrafts, with the main purpose of reducing the overall weight.

In the renewable energy industry, the application of composites in wind turbines blades allows reaching a higher energy efficiency.

The last years have seen the increase of multilayer materials in automotive vehicles for weight saving and reduction of emissions and consumption, ranging from wheels to drive-shafts, ending with the development of composite chassis in supercars, much stiffer and lighter than it would be if made of steel.

However, the introduction and the employment of composite materials has implied the need for understanding new complex phenomena that were not considered in the design of conventional metallic structures, like steel or aluminium. Differently from homogeneous and isotropic metals, where material properties are independent of the position in the body, in composites, which are heterogeneous, the properties differ along different directions. In this context, the design is complicated because the material properties depend on a large number of parameters, like the type of the reinforcement, the orientation of the lamina, the percentage of matrix and fibre, the type of architecture used, etc. Moreover, multilayer materials are very often brittle due to the presence of the fibres and subjected to delamination and cracks, because of the rising stresses at the interface of adjacent laminae, that add a further level of difficulty in the determination of material laws. Traditional experimental techniques have been redefined, as in the case of aerospace and aeronautic industries, where an extensive validation work led to the definition of new international standards.

From the manufacturing point of view, the fabrication processes are various according to the type of the fibre reinforcement, the final geometry or the production rate that need to be achieved. For short fibres reinforced polymers, the processes are derived from those of polymers, while long fibres components generally require manual work, like hand-layup techniques. This approach, which introduces a remarkable variability in the final properties, represents a drawback that needs to be considered in the manufactured part, since the actual tailored properties can be sometimes different from the predicted during the design stage.

1.2 Multi-material design for right-weighting

A multi-material approach has been considered to overcome both the limits of the metals and composite materials, while joining the advantages. Especially in the aerospace and

automotive sectors, the frequently need of reliable and durable structures is always linked to the reduction of weight. In this way, it is possible to move from the concept of lightweighting to that of right-weighting, which aims at achieving the wished performance targets by applying the right amount of the right material in the right region of the system. This approach finds its full application in the modern vehicle spaceframe where a mix of multiple materials is used in the weight-bearing body structure.

Here, the most used material is often the aluminium for its low mass density and high impact absorption. High strength steel contributes to provide enhanced safety to the passengers, while magnesium and carbon fibre composites are used with the function of giving a better stability and weight distribution to the structure. It is clear that such an approach introduces several additional complexities in the design and production, mainly due to the complexity of the connection between different materials, which requires unconventional joining techniques.

1.3 Need of lightweight geared transmissions and relative issues

Recently, composite materials have been applied in gearboxes to the housing and shafts [4] and [5] for weight reduction and acoustic insulation, with the identification of several critical issues, which include metal-composite attachment, corrosion, strength, etc.

In motor vehicles, such as passenger cars, or rotorcrafts, the geared power transmissions represent a significant amount of the overall mechanical system weight and, hence, the study of the transmission of motion with a multi-material approach and the relative problems of Noise, Vibrations, Harshness (NVH) and durability become of essential interest.

Gearing mechanisms have been used for millennia, so that they have been perceived to be the icon of Mechanical Engineering [6]. Gears are mechanical components that can transmit power from a driving shaft to a driven shaft resulting in a faster or slower rotation. The multiplication or the reduction of rotational speed and torque can be realized with extremely different shapes and arrangements, according to the specific technical requirements. Gears with very high dimensions can be found in wind turbines or in the naval industry, while complex architectures are typical of automotive and aerospace gearboxes, where rotational speeds are of thousand of revolutions per minute (rpm).

Although the use of gears is widespread in the mechanical industry, there are still several complex phenomena that are poorly understood and constitute an actual research topic. The continuous effort in investing resources on the development of modern technologies for geared transmissions, implies the definition of new challenges that need to be addressed in order to improve NVH behaviour, acoustic comfort, durability and efficiency, which strongly depend on a series of factors, ranging from manufacturing and assembly errors to the teeth's deflections and thermal distortions during working conditions. In this context, the constant push toward lightweight design and downsizing of structures represents an additional aspect that has to be considered.

Gear lightweighting represents one of the most powerful strategy to reduce weight in transmissions, even though this implies the consideration of additional dynamic effects, which increase complications in the design and product development. The dynamics of gears, which is becoming increasingly more important, dramatically changes with the modification of the body, due to the variation in the meshing compliance [7]. In particular, this effect can have influence when gears mesh with and without loss of contact.

In the former situation there is an impact induced-noise caused by the unloaded gear pairs, which excite the system over a frequency range, i.e. "rattle" phenomena. In the second case, gear vibration has a modulated tonal component related to the meshing frequencies, i.e. "whine".

Then, the challenge is to address NVH reduction through novel approaches, which increase energy dissipation in the overall mechanical system.

An efficient way to reduce weight and to damp the system at the same time is represented by the use of composite materials joined with metals.

1.4 Context and problem statement

In a context where the technology advancement is growing rapidly and immediate solutions to newer problems are required, the definition of adequate strategies for the design, simulation and testing of transmissions at system level is becoming crucial. Moreover, industry is requiring methodologies to analyse the system dynamics with an high-fidelity models and in a faster way, to reduce the time-to-market, which is the length of time it takes from a product being conceived to its availability on the market.

Additionally, companies cannot spend resources in developing and testing expensive prototypes. For this reason, the introduction of computer aided engineering (CAE) methodologies have enabled the analysis of the system dynamics with different mathematical models to approximate the real-life behaviour as accurately as required.

As a consequence, researchers are investigating various methodologies in order to simulate the behaviour of transmission components with different degree of fidelity, ranging from analytical [8] to multibody models [9], ending with FE ones [10], which are the most accurate but, at the same time, computationally expensive.

Hybrid metal-composite design in gears is one of the most advanced approaches for multilateral optimization of transmission systems.

More recently, efforts have been spent to expand the use of composite materials to gears and a new concept of hybrid gear, where a composite web is attached to the metal toothed part, was proposed and investigated in [11]. Here, the proposed model enabled a weight reduction of 20% with respect to the conventional steel gear with the same macro-geometry but numerical investigations with classical FE approach were not satisfying. That was mainly due to the need of different competences in mechanical fields, going from the simulation of system dynamics to materials analysis and manufacturing, which traditionally have always been relatively far from each other. For this reason, new methodologies of analysis are necessary for the understanding of the static and dynamic behaviour of hybrid gears and for their multilateral optimization.

1.5 Research objectives

The present dissertation aims at establishing a complete framework for the development of multi-material gears made of steel and composite materials, which account for the design, simulation manufacture and testing of gears as stand-alone component and at system-level.

Huge gaps to cover are identified both in the simulation models, which should be enhanced to properly model the interface between metal and composite parts to take into account the anisotropic behaviour of the composite web, and model validation. Numerical models are still preliminary and lack an adequate characterization of the proposed gear technology.

The overall objective is to stimulate the transition from the well-known concept of gear lightweighting to a more-advanced right-weighting approach. The desired performances of transmissions will be reached with a multi-objective optimization of the hybrid system by means of the development of efficient solutions from computational point of view, linked to the definition of reliable and safe mechanical joining techniques between composite and steel.

These purposes will be achieved by addressing and covering the following research objectives in hybrid gear technology:

- Accurate generation of hybrid gear models, which take into account the technology used for the composite gear body properties, as well as fibre volume fraction and orientation of the laminae;
- Identification of efficient strategies for the joining of metal and composite parts;
- Research on a new manufacturing approach of hybrid metal-composite gear to overcome the limitations of the existing proposed solutions;
- FE-based study for the determination of static and NVH properties of composite materials with different architectures;
- FE-based and MB-based estimation of mesh stiffness and numerical assessment of transmission error (TE) in hybrid gears;
- Experimental tests for the evaluation of modal properties at the component level and TE at gear-pair level.

1.6 Thesis contributions to the state of the art

The main contributions described in the dissertation can be summarized as follows:

- **Multi-scale modelling of the composite web in hybrid gears.** The anisotropy of the composite gear body is considered by means of a multi-scale modelling. It is essentially based on the definition of the unit cell model with different architectures (unidirectional, woven, triaxial, etc.) and analysed through multiple scales: the micro-scale, in which fibre geometry, packing and interaction between fibres and matrix are considered; the meso-scale, where the architecture of the composite unit cell is defined. Yarn geometry, local fibre direction, fibre volume fraction inside yarns, interactions between the yarns and between the yarns and the surrounding matrix are also taken into account.

- **Definition and manufacturing of a novel model of hybrid gear and validation at component level.** The modelling of the metal-composite interface is important to understand how it affects the working behaviour of gears. Adhesive bonding and interference fitting are analysed in terms of stiffness and damping contributions in modal analyses. In particular, experimental tests are carried out to characterise the modal behaviour of the hybrid gears with the two mentioned techniques.

- **Design of hybrid gear pairs and FE-based and MB-based estimation of mesh stiffness and numerical assessment of the static TE.** In order to simulate the meshing behaviour of hybrid gears, an integrated approach is used for the design and simulation of meshing gears under an applied torque. The influence of the composite body on the non-linear time-varying mesh stiffness is considered through non-linear FE simulations, where a cohesive modelling technique is used to account for damage at the metal-composite interface. MB simulations are also considered to show how the computational time of the analysis can be reduced with respect to the full FE with similar accuracy in the results.

- **Experimental analysis of the manufactured gear models at gear pair level.** Hybrid gears models are tested in an experimental campaign, where a dedicated precise test-rig is used for NVH analyses. A pair of designed hybrid gears is considered to analyse static and dynamic TE with different rotational speeds and applied torques.

1.7 Dissertation structure

The current section provides an overview on the structure of the dissertation, which is divided in six chapters.

Chapter 2 presents a brief introduction of multilayer laminated materials and the mechanical properties of interest, from both static and dynamics point of view. Different architectures of carbon fiber reinforced polymers (CFRP) laminates are shown and the

current methodologies for the analysis of their anisotropic behaviour are reviewed, based on analytical or more sophisticated theories. Multi-material approaches applied to several mechanical applications are reviewed and the related industrial needs are discussed.
Additionally, different strategies for gear lightweighting are described with an accurate review of the first applications of composites to gears and the main issues from both manufacturing and simulation sides. The chapter concludes with the main analysis models of gears.
Chapter 3 deals with the multi-scale analysis applied to composite materials. It is introduced for the evaluation of orthotropic properties used in the FE simulations of metal-composite gears. In particular, Virtual Material Characterization (VMC) is employed in the analysis of complex structures, namely triaxial braided composites, which are used into hybrid gears. The obtained results are compared to those presented in literature.
Chapter 4 is dedicated to the description of a comprehensive approach for the design and prototyping of metal-composite gears, where manufacturing aspects are analysed and discussed. This section describes two assembly techniques for joining composites to metals based on interference fitting and adhesive bonding. Moreover, both technologies are tested experimentally at gear-level for the evaluation of eigenfrequencies and modal damping. FE simulations are used to show how these quantities can be predicted with high accuracy by considering the homogenization of the composite web. The chapter ends with the study of gear meshing by means of FE simulations for static analysis of the TE.
Chapter 5 discusses the experimental gear pair analysis in a dedicated test-rig. Here, two different geared transmissions are compared: the first is with a solid metal gear driving a metal thin-rim one, while the second is with the same solid gear driving the composite one with the same mass of the metal thin-rim. The tests are executed at different rotational speeds and applied torque in order to understand how the composite body influences acceleration, noise and TE. The latter is considered as one of the main indicator able to describe deviations from a perfect transmission motion. FE and MB simulations are used to validate experimental results.
Finally, *Chapter 6* draws the main conclusions and discusses future work for possible improvements.

Chapter 2
Composite materials and their applications in mechanical transmissions

2.1 Definition and properties of composite materials

A composite material is constituted by two or more different solid phases that remain macroscopically separate, assembled together to lead to a material with better mechanical properties of its constituents. In the most general case, a composite material can be seen as composed by a continuous phase, called matrix, and a discontinuous one, the reinforcement. The role of the matrix is to transfer loads and to protect the reinforcement, while the fibres act as the load-carrying member. Composites are classified with respect to the nature of the matrix, (i.e. polymeric, metallic, etc.), and the reinforcement properties (geometry, nature and orientation). Among all the classes of composites, CFRP (carbon fiber reinforced polymer) represent the most popular class of composites for structural applications. In this case, long carbon fibres with very small diameter in the order of microns are assembled in a polymer resin, thermoplastic or thermoset, to define a material with high mechanical properties, such as great stiffness and strength, vibrations absorption and lightness.

For practical use, fibres are gathered together in a bundle called strand or yarn, which generally are provided in the form of thin sheets, laminae or plies, used to create a laminate. According to the yarn's architecture, different laminae can be created to fulfil technical requirements. In unidirectional plies, (UD), fibres are aligned together along one direction, while woven fabrics consist of two sets of interlaced yarns in the lengthwise direction, warp, and in the crosswise direction, weft, mutually orthogonal, where the fabric is woven on a loom. Braiding is also a popular textile production technique, in which fibres are interlaced over a cylindrical mandrel to produce bi-axial or tri-axial textiles.

The main advantage in designing with composite materials is that mechanical properties can be tailorable by changing the amount of fibres, i.e. their volume fraction, their packing in the matrix or the disposition of the laminae inside the laminate. In general, the higher is the amount of fibres, the higher is the stiffness and the strength of the material. On the other hand, a high fibres volume fraction contributes to an increased brittleness of the laminate.

It is clear that the right design of multilayered structures cannot exclude a multi-objective optimization, which needs to account for the weight of the component, its stiffness and strength and, from the dynamic point of view, the damping capacity. In fact, it is well known that polymers, or in general viscoelastic materials, are used for vibration damping purpose. In a linear elastic material, the deformation is fully recoverable, while in a viscous one, typical of fluid, it is irreversible. In viscoelastic material, a part of the deformation is completely recovered while another part is lost. Additionally, this property is dependent on time and temperature [12]. This damping capacity makes them considered in applications where the primary purpose is the dissipation of energy.

2.1.1 Analysis of UD lamina

The lamina properties are defined in the material coordinate system *(1,2,3)*, where *1* is the direction along the fibres, *2* is the one perpendicular to the fibre direction and *3* is the through-the-thickness direction. The direction *1* of this system, referred as local, differs from an angle θ from the x-axis of the global axis system, positive in counter clockwise direction, Figure 2. 1 .

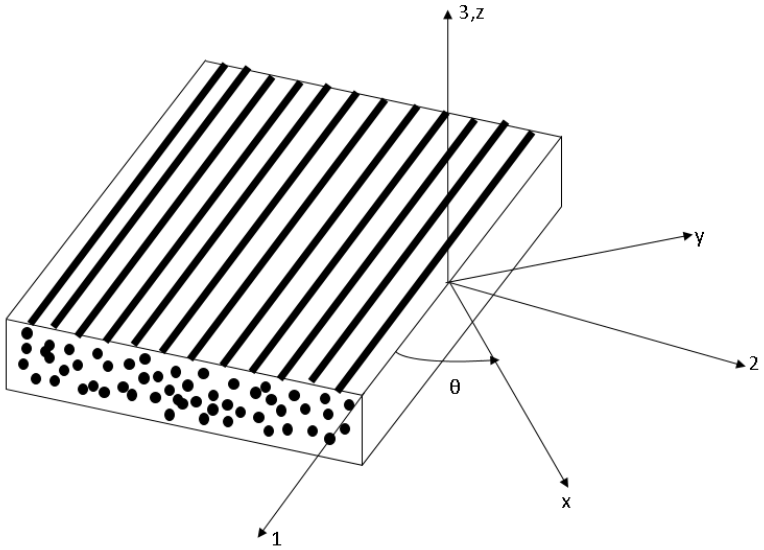

Figure 2. 1 Global and local coordinate system.

In a UD composite lamina, the analysis of stress-strain relationship can be expressed by the generalized Hooke's law. For its application, the lamina is assumed to be continuous and linear elastic. This implies that the relation between stress and strain can be written as follows:

$$\sigma_i = C_{ij}\varepsilon_j \tag{1}$$

where,

$$C_{ij} = \begin{bmatrix} C_{11} & C_{12} & C_{13} & C_{14} & C_{15} & C_{16} \\ & C_{22} & C_{23} & C_{24} & C_{25} & C_{26} \\ & & C_{33} & C_{34} & C_{35} & C_{36} \\ & SYM & & C_{44} & C_{45} & C_{46} \\ & & & & C_{55} & C_{56} \\ & & & & & C_{66} \end{bmatrix} \tag{2}$$

The elastic tensor C_{ij} is symmetric and, in the most general case, it will contain 21 independent elastic constants. When materials present planes of symmetry, the number of independent constants is reduced, as visible from Table 2. 1.

Material	**Number of nonzero coefficients**	**Number of independent coefficients**
3D case		
Anisotropic	36	21
Generally orthotropic (non-principal coordinates)	20	9
Transversely isotropic	12	5
Isotropic	12	2

Table 2. 1 Elastic coefficients for different materials *[13]*.

Most laminae are orthotropic, which means that they have three mutual orthogonal planes of symmetry, and the number of independent constant is *9*, that is *3* Young's moduli, *3* Poisson's ratios and *3* shear moduli, as it is visible from the following equation:

$$\begin{Bmatrix} \varepsilon_1 \\ \varepsilon_2 \\ \varepsilon_3 \\ \gamma_{23} \\ \gamma_{13} \\ \gamma_{12} \end{Bmatrix} = \begin{bmatrix} 1/E_1 & -\upsilon_{12}/E_2 & -\upsilon_{31}/E_3 & 0 & 0 & 0 \\ & 1/E_2 & -\upsilon_{32}/E_3 & 0 & 0 & 0 \\ & & 1/E_3 & 0 & 0 & 0 \\ SYM & & & 1/G_{23} & 0 & 0 \\ & & & & 1/G_{13} & 0 \\ & & & & & 1/G_{12} \end{bmatrix} \begin{Bmatrix} \sigma_1 \\ \sigma_2 \\ \sigma_3 \\ \tau_{23} \\ \tau_{13} \\ \tau_{12} \end{Bmatrix} \quad (3)$$

The above relation between stresses and strains is valid for the local coordinate system of the laminae $\{1,2,3\}$ (l). However, while very often laminates are constituted by plies oriented at different angles. For this reason, the global system $\{x, y, z\}$ (g) is considered and a transformation matrix [T] is used to transform quantities from local to global axis in the following way:

$$\{\sigma\}_g = [T]\{\sigma\}_l = [T][C]_l\{\varepsilon\}_l = [T][C]_l[T]^T\{\varepsilon\}_g = [C]_g\{\varepsilon\}_g \quad (4)$$

where $[C]_g$ is the laminate stiffness matrix.

2.1.2 Analysis of laminated structures

Laminates are constituted by a sequence of laminae, which can differ each other by constituents or angles. Depending on these two options, laminates exhibit different behaviour in terms of mechanical and thermal properties.

When analysing multilayer structures, different approaches can be used to study the variation of the mechanical properties through the thickness, which provide a certain level of accuracy depending on the assumptions made. In particular, it is possible to make a distinction of Equivalent Single Layer Theories (ELST) and three-dimensional elasticity theories, i.e. Layer-Wise Theories (LWT) and 3D elasticity formulations. The first deals with laminated structures as if it is an equivalent material, relating stresses and strains to a single equivalent stiffness matrix of the laminate. In this context, the Classical Lamination Theory (CLT) [14], which is the first proposed approach for the analysis of multilayer structures, relies on the assumptions that laminae are perfectly bonded together, so that they behave as a unitary and anisotropic plate. No interfacial slip occurs and displacements across the laminae are assumed to be continuous. Figure 2. 2 shows the coordinate system used for the CLT analysis, which is assumed to have its origin in the middle surface of the plate. The theoretical assumptions for the analysis are:

1. Laminae are orthotropic and perfectly bonded together, with principal material axes oriented at arbitrary angles with respect to the *x*, *y* axes:
2. The thickness of the plate *t* is much smaller than in-plane dimensions, *a* and *b*;
3. The displacements *u*, *v* and *w* are assumed to be small compared to the plate thickness;
4. The in-plane strains $\varepsilon_x,\ \varepsilon_y,\ \gamma_{xy}$ are <<1;
5. The transverse strains γ_{yz}, γ_{xz} and the normal strain ε_z can be neglected (plane-stress hypothesis)
6. The in-plane displacements *u*, *v* are linear functions of the thickness coordinate z;
7. Each ply is analysed with Hooke's law;

8. The plate thickness is constant;
9. Transverse shear stresses τ_{xz}, τ_{yz} vanish at the outer free surfaces.

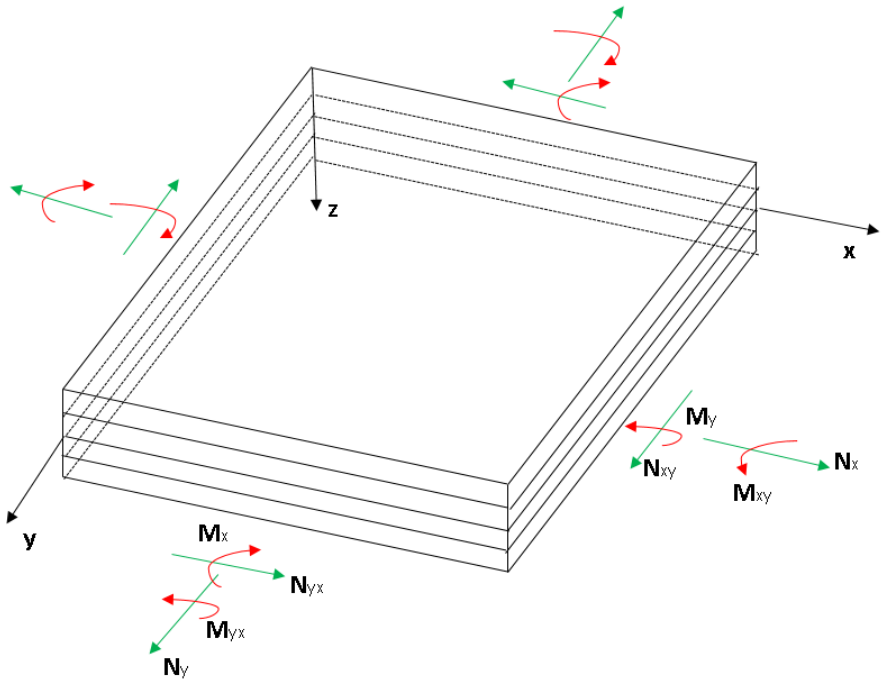

Figure 2. 2 Coordinate system and stress resultants in the laminated plate.

The hypotheses 5 and 6 implies that the lines normal to the middle plane remain straight and normal after the deformation, according to the Kirchoff deformation hypothesis. The displacement field can be expressed as follows:

$$u(x,y,z) = u_0(x,y) - z\frac{\partial w}{\partial x} \tag{5}$$

$$v(x,y,z) = v_0(x,y) - z\frac{\partial w}{\partial y} \tag{6}$$

$$w(x,y,z) = w_0(x,y) \tag{7}$$

where u_0 and v_0 are the displacements of the middle surface along x and y directions respectively. The transverse displacement w is constant over the thickness. From that, the strains on the mid-plane are:

$$\varepsilon_x = \frac{\partial u}{\partial x} = \varepsilon_x^0 + zk_x \tag{8}$$

$$\varepsilon_y = \frac{\partial v}{\partial y} = \varepsilon_y^0 + zk_y \tag{9}$$

$$\gamma_{xy} = \frac{\partial u}{\partial y} + \frac{\partial v}{\partial x} = \gamma_{xy}^0 + zk_{xy} \tag{10}$$

where

$$\varepsilon_x^0 = \frac{\partial u_0}{\partial x} \quad \varepsilon_y^0 = \frac{\partial v_0}{\partial y} \quad \gamma_{xy}^0 = \frac{\partial u_0}{\partial y} + \frac{\partial v_0}{\partial x} \tag{11}$$

are the strains on the mid-plane and

$$k_x = -\frac{\partial^2 w}{\partial x^2} \quad k_y = -\frac{\partial^2 w}{\partial y^2} \quad k_{xy} = -\frac{2\partial^2 w}{\partial x \partial y} \tag{12}$$

are the curvatures of the mid-surface. In this way, the stresses along an arbitrary *x, y* axis in the *kth* lamina take the form:

$$\begin{Bmatrix} \sigma_x \\ \sigma_y \\ \tau_{xy} \end{Bmatrix}_k = [\bar{C}]_k \begin{Bmatrix} \varepsilon_x^0 + zk_x \\ \varepsilon_y^0 + zk_y \\ \gamma_{xy}^0 + zk_{xy} \end{Bmatrix} \tag{13}$$

In the laminate plate analysis, it is useful to relate the strains of the eq. 13 to the applied forces and moments of Figure 2. 2 per unit of length. In particular:

$$N_x = \int_{-t/2}^{t/2} \sigma_x dz = \sum_{k=1}^{N} \int_{z_{k-1}}^{z_k} (\sigma_x)_k \, dz = \tag{14}$$

$$= \sum_{k=1}^{N} \int_{z_{k-1}}^{z_k} \{(\bar{C}_{11})_k \varepsilon_x + (\bar{C}_{12})_k \varepsilon_y + (\bar{C}_{16})_k \gamma_{xy}\} dz$$

$$M_x = \int_{-t/2}^{t/2} \sigma_x z dz = \sum_{k=1}^{N} \int_{z_{k-1}}^{z_k} (\sigma_x)_k z \, dz = \tag{15}$$

$$= \sum_{k=1}^{N} \int_{z_{k-1}}^{z_k} \{(\bar{C}_{11})_k \varepsilon_x + (\bar{C}_{12})_k \varepsilon_y + (\bar{C}_{16})_k \gamma_{xy}\} z dz$$

where t is the laminate thickness, $(\sigma_x)_k$ is the stress at the k*th* lamina, z_{k-1} the distance from the middle surface to inner surface of the k*th* lamina and z_k the corresponding distance from the middle surface to the outer surface of the k*th* lamina.

Finally, the laminate extensional, coupling and bending stiffnesses are given respectively as:

$$A_{ij} = \int_{-t/2}^{t/2} \left(\bar{C}_{ij}\right)_k dz = \sum_{k=1}^{N} \left(\bar{C}_{ij}\right)_k (z_k - z_{k-1}) \tag{16}$$

$$B_{ij} = \int_{-t/2}^{t/2} \left(\bar{C}_{ij}\right)_k z dz = \frac{1}{2} \sum_{k=1}^{N} \left(\bar{C}_{ij}\right)_k (z_k^2 - z_{k-1}^2) \tag{17}$$

$$D_{ij} = \int_{-t/2}^{t/2} \left(\bar{C}_{ij}\right)_k z^2 dz = \frac{1}{3} \sum_{k=1}^{N} \left(\bar{C}_{ij}\right)_k (z_k^3 - z_{k-1}^3) \tag{18}$$

As visible from eqs. 16-18, the integration over the laminate thickness becomes a discrete summation over the number of layers N. The same relation can be expressed in matrix form as:

$$\begin{Bmatrix} N_x \\ N_y \\ N_{xy} \\ M_x \\ M_y \\ M_{xy} \end{Bmatrix} = \begin{bmatrix} A_{11} & A_{12} & A_{16} & B_{11} & B_{12} & B_{16} \\ A_{12} & A_{22} & A_{26} & B_{12} & B_{22} & B_{26} \\ A_{16} & A_{26} & A_{66} & B_{16} & B_{26} & B_{66} \\ B_{11} & B_{12} & B_{16} & D_{11} & D_{12} & D_{16} \\ B_{12} & B_{22} & B_{26} & D_{12} & D_{22} & D_{26} \\ B_{16} & B_{26} & B_{66} & D_{16} & D_{26} & D_{66} \end{bmatrix} \begin{Bmatrix} \varepsilon_x^0 \\ \varepsilon_y^0 \\ \gamma_{xy}^0 \\ k_x \\ k_y \\ k_{xy} \end{Bmatrix} \tag{19}$$

Alternative form is:

$$\begin{Bmatrix} N \\ \dots \\ M \end{Bmatrix} = \begin{bmatrix} A & \vdots & B \\ \dots & \dots & \dots \\ B & \vdots & D \end{bmatrix} \begin{Bmatrix} \varepsilon^0 \\ k \end{Bmatrix} \tag{20}$$

The matrix [A] links the in-plane forces {N} to the midplane strains $\{\varepsilon^0\}$ and the bending stiffness matrix [D] relates the moments {M} to the curvatures {k}. The [B] matrix couples the in-plane forces with the curvatures and the moments with the in-plane strains. The matrix [B] is therefore responsible of bending or twisting of laminate under in-plane loads. Some particular situations for matrices [A], [B] and [D] can be considered:

- [B]=0 in symmetric laminate. A symmetric laminate is characterized by both material and geometric properties symmetric about the middle plane. This means that the ply thickness, ply material and ply orientation at a certain distance z from the middle surface are identical to the ones at the same distance in the negative z direction. In this way, the coupling phenomena of bending-twisting and bending-stretching are avoided. This becomes important in structures subjected to a change in temperature, or during the cure process, where unbalanced loads in plane can cause warping phenomena.
- $B_{11}=B_{22}=B_{12}=B_{66}=0$; B_{16} and B_{26} are non-zero in an antisymmetric angle-ply laminate. Angle-ply laminates have all the plies oriented at $\pm\theta$, while a cross-ply has only laminae at 0 and 90 degrees.
- [A] is with isotropic behaviour in quasi-isotropic laminates. In fact, if the application requires to have an isotropic material, it is possible to use orthotropic laminae to build up a laminate that exhibits an isotropic behaviour in the plane. These laminates are called quasi-isotropic, where the angle between adjacent laminae is kept constant.

. Figure 2. 3 gives an example of the mentioned types of laminates.

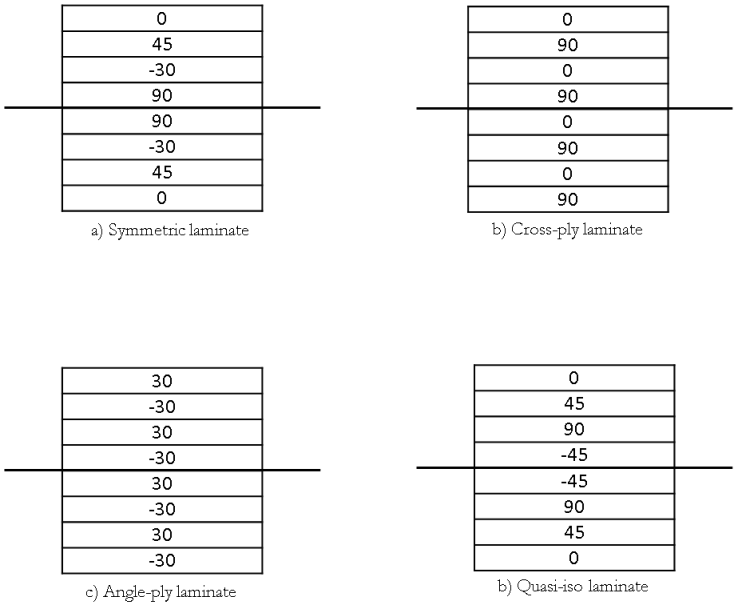

Figure 2. 3 Example of laminates.

The CLT is still the reference model when dealing with composites, although its accuracy decreases as the thickness of the structure increases, since the transverse shearing can no longer be neglected.

The First Order Shear Deformation Theory (FSDT) overcomes the limit of assumptions 5 and 6, allowing the cross-section to rotate independently of the transverse deflection [15], [16]. All ELST consider the continuity in the thickness direction, implying the discontinuity of transverse shear stresses. The main purpose of LWT is to consider a piece-wise variation of displacements through the thickness and transverse shear stresses continuity [17], [18]. Further developments of Zigzag Theories (ZZT) deal with the combination of low computational cost of ELST with the accuracy of LWT [19].

2.1.3 Multi-scale modelling of composite materials and homogenization techniques

The development of a new product made of composite material requires the definition of a multi-stage design process at different scales, which can be depicted as a pyramid approach (Figure 2. 4).

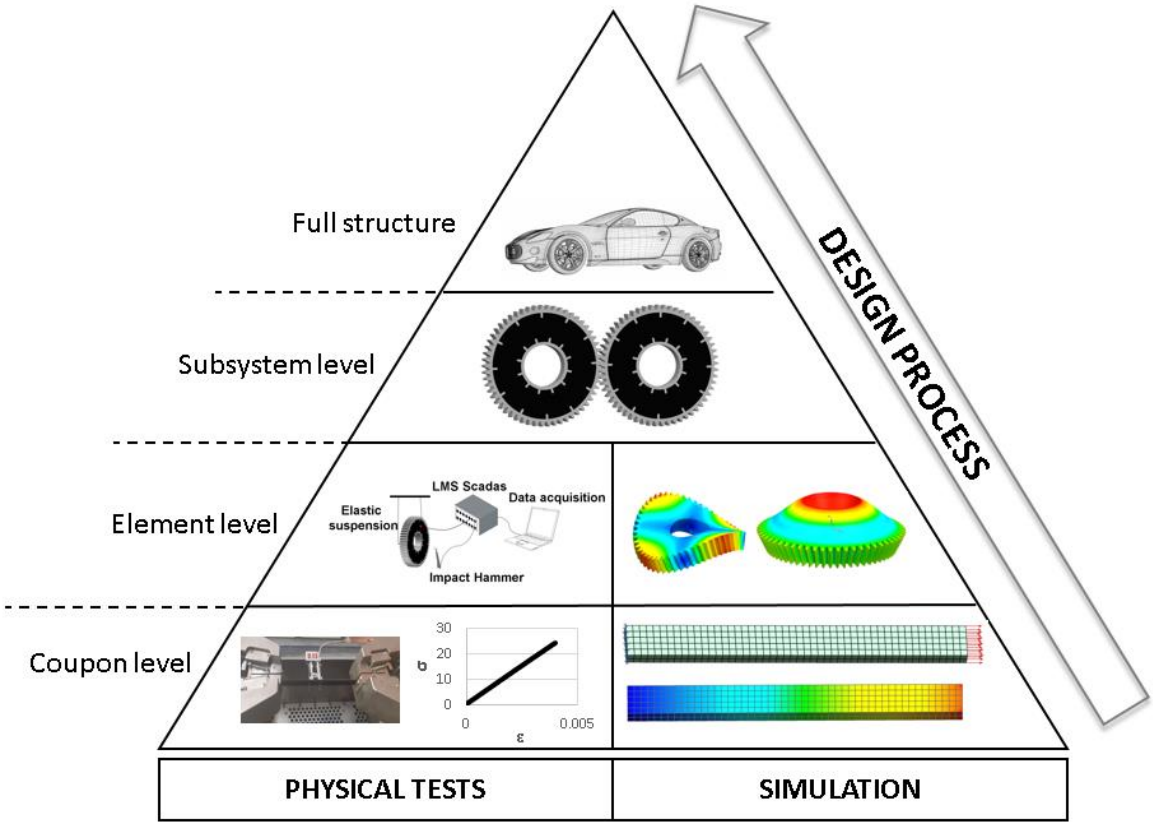

Figure 2. 4 Design process for the development of a new product.

As visible from Figure 2. 4, the base of the pyramid is constituted by the analysis and validation of material properties at coupon levels to be used in subsequent simulations for more complex components or assembly at system-level. This implies that a large number of tests is carried out in order to generate material properties, like stiffness, strength, fatigue, etc. As a consequence, new engineering approaches, which overcome the classical analysis of material properties, need to be defined to reduce computational time and efforts and decrease the time-to-market of a product. This assumes even a greater importance in the case of composite materials, where it is necessary to optimize several parameters, like fibre volume fraction or stacking sequence.

In this context, the application of multi-scale modelling techniques becomes a powerful solution to model the material behaviour by considering different aspects at different scales. This method is based on the definition of different scales of analysis, micro-meso, and a representative unit cell (RUC), which can be defined as the smaller volume of the material over which a measurement can be made that will yield a value representative of the whole (Figure 2. 5).

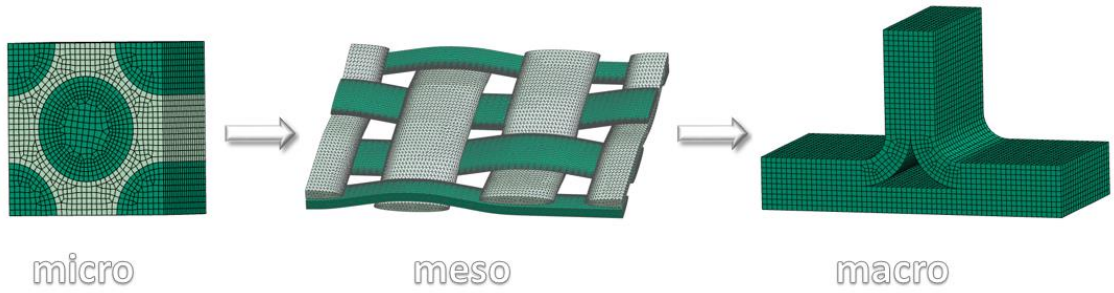

Figure 2. 5 Multi-scale modelling.

The micro-scale allows to consider fibres geometry, their packing and interaction with the surrounding matrix. At meso-scale, the architecture of the RUC is analysed trough the definition and the application of periodic boundary conditions for material homogenization. The macro-scale exploits the material properties, derived from micro and meso analysis, as input in full-scale simulations. Depending on the complexity of the laminate architecture, analytical or more sophisticated theories, like FE-focused approach, are used with multi-scale techniques. All these approaches rely on the hypothesis of the continuity of the material. The latter, which is heterogeneous, is considered as being effectively homogeneous and the solution is obtained by considering the average properties of the RUC measured at the meso-scale.

In case of UD laminates, analytical formulations at the three scales enable a complete representation of the material behaviour. At the micro-scale, the rule of mixture can be used to account for orthotropic moduli of fibres [20]. Then, the three-dimensional laminate is studied with an approach that replaces the heterogeneous medium by an equivalent homogeneous material [21] to evaluate effective moduli [22].

For more complex architectures, analytical formulations [23] are not always possible or lack an adequate level of accuracy. In these cases, FE approaches [24] and [25] are introduced to overcome the aforementioned issues. In ref. [25] a virtual material characterization technique associated with a multi-scale modelling of composites is used to determine the material properties. Here, the micro-scale can account for random packing [26] and analytical or FE techniques are used to evaluate fibres effective moduli. At the meso-scale, a FE-based homogenization procedure [24] is employed. This considers yarn geometry, local fibre direction, fibre volume fraction inside yarns, interactions between the yarns and between the yarns and the surrounding matrix. The result is the evaluation of macro-scale material elastic constants, calculated by the volume-

averaging technique applied on the stress-fields [27]. The described technique will be used in the Chapter 3 for the analysis of triaxial braided materials applied to hybrid gears.

2.1.4 Damping in composite materials

Damping is the dissipation of energy during a dynamic deformation. In metallic structures, the damping capacity is very low and higher levels are reached with add-on surface treatments. CFRPs have increased in popularity thanks to their good damping characteristics, which comes from viscoelastic effects.

Viscoelasticity is a concept known for decades. Differently from ideal elastic solids, capable of accumulating and giving back all the energy under load without dissipation, and fluid, able to dissipate all the mechanical energy, viscoelastic materials present an intermediate behaviour. This means that they can both store and dissipate energy. By considering constant loads in time domain, in viscoelastic materials, such as constant stresses or constant strains, the resulting strain and stresses exhibit the well-known creep and relaxation phenomena, respectively [14]. In order to describe their rheological behaviour, different formulations are used [28], all of them based on the series, parallel or a combination of springs and dashpots, i.e. Maxwell, Voigt or Zener models.

Additionally, by referring to the frequency domain, when the structures are subjected to dynamic loads, damping can present a frequency dependence. As described in [29], the hypothesis of linear viscoelastic behaviour is valid when both stiffness and damping are independent of the amplitude of vibrations. In this way, for a given sinusoidal force/stress input with a certain amplitude and frequency, the material response will result in a sinusoidal output with a phase lag.

A useful way to describe stiffness and damping properties as function of the frequency is to use the complex modulus notation [14]. From this point of view, when considering a viscoelastic material subjected to a general sinusoidal varying stress $\sigma_a(t)$, to which corresponds a sinusoidal varying strain $\varepsilon_b(t)$, the relation between stress and strain can be expressed in the following way:

$$\sigma_a(t) = C^*_{ab}(\omega)\varepsilon_b(t) \tag{21}$$

where a, b=1, 2…6 and $C^*_{ab}(\omega)$ is the complex stiffness. The latter can be expressed as follows:

$$C^*_{ab}(\omega) = C'_{ab}(\omega) + iC''_{ab}(\omega) \tag{22}$$

in which $C'_{ab}(\omega)$ is defined as the storage modulus, which relates to the material's ability to store energy elastically, and $C''_{ab}(\omega)$ as the loss modulus, which is related to the material's ability to dissipate stress through heat. Finally, the relation between the storage and the loss modulus can be described as follows:

$$\eta_{ab}(\omega) = \frac{C''_{ab}(\omega)}{C'_{ab}(\omega)} = \tan[\delta_{ab}(\omega)] \tag{23}$$

where $\eta_{ab}(\omega)$ is the loss factor and $\delta_{ab}(\omega)$ is the phase lag between the sinusoidally varying stress and strain. Figure 2. 6 shows the relation between C'(ω) and C"(ω).

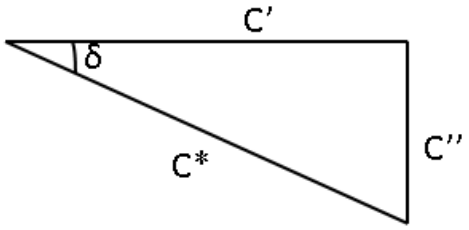

Figure 2. 6 Relation between storage and loss factor for viscoelastic materials.

It is relevant to notice that when the phase lag δ between stress and strain is equal to zero, $C^* \rightarrow C'$ (linear elastic solids), while δ is equal to $\pi/2$ in case of Newtonian fluids. An in-depth investigation of the dissipation energy of composites under impact loading will be described in Chapter 4.

2.2 Multi-material design in mechanical applications

When designing complex engineering structures, which need to satisfy several requirements, great advantages can be obtained by using hybrid structures made of metals and composites, thanks to their different material properties. These can be combined to improve the overall mechanical behaviour of the system in which they are introduced.

Generally, metals, like steel and aluminium, are well-known in terms of design parameters and manufacturing processes. Metals have high modulus, high yield strength, and high ductility. Additionally, they are relatively cheap and easy to fabricate. On the other hand,

composites, like CFRPs, have low density, high stiffness and strength and damping properties, with the possibility of tailoring the stacking sequence for optimal mechanical response. Moreover, they are more expensive than metals and difficult to fabricate, especially in case of complex structures. During these years, the research has been very often focused on hybrid structures, which aim at combining the benefits of metals and composites. The simplest hybrid component is represented by a beam or plate. Kim [30] makes a comparison of box beams made of aluminium, FRP and hybrid materials in terms of performance and costs. Here, hybrid design allows to have a lighter component than the one made of aluminium and less expensive to produce. Additionally, other advantages are the increased ductility and high fatigue resistance. Moreover, metal-composite architecture can be exploited to enhance damping behaviour by means of the application of rubber or epoxy adhesive [31]. In [32] Liebig et al. investigate how modal and damping behaviour of hybrid laminates with an elastomer ply changes with its thickness and stiffness.

The following paragraphs discuss the current application of metal-composite structures in different sectors.

2.2.1 Hybrid structures in the transportation sector

The research of structures made of metal and composites has grown fast during the last decades in the automotive sector. First applications of hybrid design have interested drive shafts. In [33], Cho et al. showed how it was possible to manufacture a hybrid metal-composite drive shaft with aluminium and CFRP with a co-curing technique. Here, a pre-load is applied to the aluminium to reduce thermal residual stresses after the cure process. The aluminium has the function of sustaining the applied torque while the composite provides additional bending stiffness. In the same context, Kim and Lee [34] have studied a reliable assembly process capable of joining aluminium and CFRP in a hybrid drive shaft with a mass reduction of about 50% with respect to the conventional steel drive shaft.

The application of composite material to metal structures in wheels may have the strong benefit of increasing the NVH indicators for the enhancement of the overall ride comfort. In particular, Bae et al. [35] presented a novel model of hybrid wheel, fabricated as to have the same shape of a conventional aluminium one. The damping capacity in terms of damping ratio has been greatly improved thanks to the use of friction damping layer

inserted between the composite and aluminium parts. Moreover, the dynamic stiffness of the hybrid wheel was increased by 30% thanks to the application of CFRP. NVH tests provided a reduction of the noise level compared to the aluminium wheel, while no structural problem, like crack initiation and delamination, occurred.

In the automotive and aerospace industry, the absorption of energy in structures is an important requirement that needs to be considered. Recently, Zhu et al. [36] investigated the crashworthiness of hybrid metal-composite tubes under quasi-static axial loading compared to an empty aluminium tube and CFRP tube. They found that, in general, hybrid tube exhibits the best crushing behaviour with the highest absorbed energy. Additionally, hybrid tube lead to a reduction in cost by 30% compared to the CFRP tube, as well a 33% weight saving compared to the aluminium tube. Similarly, in [37] authors showed the benefit to use hybrid sandwich tubes to improve crashworthiness and performance to cost ratio. In the same field, Kalhor et al. [38] defined a methodology to analyse the crushing behaviour of hybrid square tubes as a function of FRP thickness and stacking sequence, while in [39] Tran et al. studied a novel lightweight and high performance anti-ram bollard system to prevent terror attacks. In particular, they focused the attention on a series of comparative studied of the bollard behaviour against the impulsive loading of a pick-up truck, finding the optimal design for the mitigation of localized impact and failure.

Recently, hybrid configuration has been used in the upper arm of a pantograph for high-speed trains. A first prototype is described in [40], where a steel pantograph was replaced by a hybrid configuration with aluminium and CFRP joined by means of an adhesive layer. The novel design allowed to reduce the weight of the structure by about 47% with an increase of bending and torsional stiffness by 17% and 20%, respectively. For the same application, in [41] a parametric study was performed to determine the best configuration of CFRP laminates for high stiffness and a friction layer of Teflon was applied between metal and composite during the cure process to avoid excessive thermal stresses at the interface. Authors in [42] carried out experimental tests at different temperature to check the durability of the hybrid pantograph arm. Results showed that the fabricated arm could work in safe conditions up to 300 Km/h.

2.2.2 Hybrid structures in the industrial sector

In industrial operations, high precision of tools, which rotate at very high speed, is always required and the level of the generated vibrations needs to be as low as possible. This can be possible with the design of hybrid machines made of metal and composites. Chang et al. [43] investigated the use of composites in a headstock of a precision grinding machine to decrease thermal expansion and to enhance dynamic stiffness and damping behaviour, a necessary requirement to reduce vibrations during the machining process and to improve the machined surface quality. Similar considerations can be found in [44], where authors show how mass reduction and improvement of dynamic stiffness can be achieved with the use of hybrid circular plate cutting tools, which are employed for rough machining of bearing sites in crankshafts or camshafts.
Similarly, in [45] and [46] authors investigated the application of composites and metals in the machine tool structures by optimizing the laminate thickness and the stacking angle in order to increase their stiffness and reduce their weight.

2.2.3 Joining of hybrid structures

A critical point in the design of hybrid metal-composite structures is the joining technique. Basically, three main connections can be used: adhesive bonding, interference fitting and mechanical fastening. Adhesive bonding uses a very thin layer of adhesive with a relatively low cure temperature (from room temperature to hundreds of degrees) able to ensure a shear strength around 30-50 MPa. The major drawback of this technique is that the layer thickness is very often small and it is difficult to control during the joining process. Additionally, adhesive bonding is not suitable for applications where high temperatures are required because it cannot withstand extreme environments. A careful surface preparation is needed and premature failures due to peel stresses can occur. A study on the damage behaviour of adhesive layer can be found in [47], where authors showed the damage and crack growth analysis of a lap joint made of metal and composite.
Interference fitting enables a safer connection between components, but it may not be feasible if complex structures are considered. Additionally, this process, based on the heating and the following cooling of the surfaces in contact, may generate residual stresses that can contribute to in-service failures. This technique is typically used in hybrid drive shafts [34].

Mechanical fastening uses different fasteners to connect parts. The process is based on the local deformation of the parts in contact due to the applied pressure on the fasteners. The two main process variables to take into account are the tapering angle and the punch diameter [48]. This technique is often used in aerospace applications, especially for aircraft lap joint repairs [49]. Sometimes all these joining methods are used in combination to increase the performance of the connections. For example, in [50] a novel hybrid joint is analysed, where the metallic and composite components are adhesively bonded together and pins are added to the overlap region.

2.3 Multi-material design for gear lightweighting

Mass reduction is one of the main innovation drivers in several industrial sectors, including gear transmissions. The use of lightweight gears originated in the aerospace industry, where weight optimization has always been a key topic, and is recently extending to mechanical transmissions, where huge benefits are expected in terms of mass reduction and compliance with the increasingly stricter regulations on fuel efficiency and emissions. Common lightweighting strategies are based on the reduction of gear thickness as well as on the manufacture of holes in the web of the gear. The continuous increase of lightweight gears in the transportation and industrial sectors requires the development of simulation models capable of representing the contribution of different design choices, e.g. web thickness, number, position, and shape of the holes.

In [51] and [52] a methodology has been proposed to analyse the dynamic behaviour of lightweight spur gears through the evaluation of the variable meshing stiffness, while in [53] the effects of holes in spiral bevel gear body have been considered. The major drawback of considering lightweight gears with geometrical modifications of the gear body is the possible introduction of additional dynamic excitations, which can increase vibrations in the mechanical system.

A newer approach for weight reduction in mechanical systems and, specifically, in geared transmissions, is based on the exploitation of composite materials as standalone components or in a hybrid metal-composite design. Recently, efforts have been spent to expand the use of composite materials to the geared bodies and a new concept of hybrid gear, where a composite web is attached to the metal-toothed part, has been proposed and investigated [11]. This combines the excellent contact stress and fatigue resistance of

high-performance steel with the high strength-to-weight ratio of composite materials. In fact, from a functional, load-related standpoint, a gear can be split into three main regions, as shown in Figure 2. 7: the rim (including the teeth), which is the outer region of the gear; the web, or central portion; and the hub, which is the internal part, connecting the gear to the shaft.

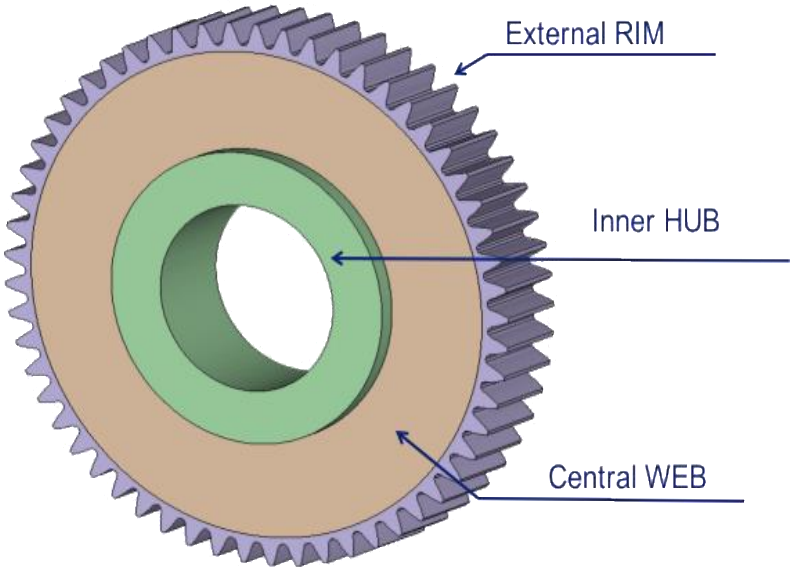

Figure 2. 7 Gear zones definition.

To enable the fulfilment of a set of requirements linked to precise geometry, fatigue and wear resistance, the toothed part of the gear is the region where most of the design standards are applied, while the web is usually less prone to failure mechanisms. Being far from the local area of direct contact between teeth, the web is not subjected to impacts, wear and other friction-related phenomena. Moreover, it contributes significantly to the overall mass of the gear and hence it offers a great potential for both mass reduction and noise and vibration enhancement, which is fully exploited in the hybrid gear design.

Recent research efforts have focused on the applicability and the advantages of a hybrid design approach for weight and noise reduction in small transmissions, consisting of a pair of identical gears [11]. In particular, in [11] an innovative gear design was proposed and investigated, based on the replacement of the metal web of the gears with triaxial braided composite material. The latter is characterized by high-strength properties and quasi-isotropic behaviour in plane, which makes it suitable especially in aerospace drive system applications. A hexagonal design of the composite region was used to replace the

steel web with three ply stacks, each of 12 layers. Two of them were cut as to have an overlap onto the surface of the outer rim, while the third was machined to fit the gear web region. Then, the complete assembled gear was cured in a mold at 350 °F for 1 hr. Two different experimental studies were carried out. The first was at component level, where the baseline steel gear and the hybrid gears were tested with an impact hammer and accelerometer to analyse their modal behaviour in free-free conditions, in terms of natural frequencies and damping. Results showed that the fundamental frequency in hybrid gear was lower than the one measured for steel gear, while higher structural damping was noticed.

The second test was executed in dynamic conditions to measure vibration and noise at different speeds and levels of torque in a dedicated test-rig, which showed how hybrid gears could reduce the transmitted vibrations, although not drastically as expected. This was mainly due to the introductions of manufacturing errors during the assembly of gears. Additionally, an endurance test demonstrated a very good fatigue resistance of such hybrid gears, in which no detectable damage were identified in a post-test inspection after $300x10^6$ cycles at 10000 rpm. In [54] authors analysed the same gear pairs by correcting the geometry of the cured gears through a regrind process in order to maintain aerospace gear quality. In particular, the hybrid driving hybrid configuration exhibited the lowest vibrations, but only at higher speeds and loads. For the same gears, in [55] authors developed a multi-objective optimization technique to minimize shear stresses and mass with a sinusoidal interlock design.

A critical point of hybrid gears is the severe environment in which they may operate. In fact, gear pairs must be able to work under normal operating conditions but, at the same time, they must also withstand adverse events, like a loss-of-lubrication situation, which determines an increase of temperature in the components. LaBerge at al. [56] investigated this situation with experiments in which oil supply was disconnected during working conditions. A post-test inspection showed the rise of a gap between steel rim and composite web, due to the different coefficient of expansion of the two materials. This determined a relative rotation of the web with respect to the rim and some localized compression failure of the composite, suggesting the hexagonal interlock pattern is not suitable in severe working conditions, like loss-of-lubrication events.

The concept of hybrid gear has been applied to full-scale components used in real aerospace applications. In particular, in [57] authors described experimental tests of a full-

scale hybrid composite bull gear by recording and comparing vibrations, orbit and temperature to the baseline steel bull gear. The hybrid bull gear was successfully tested up to 3300 hp and results showed that there was no increase of vibration levels with hybrid gear design. Additionally, in some working conditions, the orbit changed shape, suggesting a change of the interface behaviour between metal and composite, probably due to a degradation of the adhesive connection. In any case, hybrid gears never lost their capacity to transmit torque and run within imposed vibration and orbit limits. In a newer design [58], authors presented a "stair stepped" solution for the composite web. In particular, to improve the stress distribution, the interlock pattern at the composite-metallic interface changed and the thickness at the inner hub was greater than the one at the outer steel radius. The static torsion test demonstrated how the maximum torque capacity was increased with respect to the old design, while dynamic tests were run up to 5000 hp. Finally, endurance tests have not revealed delamination phenomena.

From a simulation point of view, more in-depth investigations are needed to explain the complex phenomena involved in the application of this technology. In [11], authors used a FE approach to predict natural frequencies of a hybrid gear in free-free condition, by considering the composite web with isotropic behaviour, but without reaching a good correlation with experimental tests. In [59], Naffin et al. used FE analysis to determine the stress-strain field on the bull gear rim and body.

Despite these efforts, which were not entirely satisfying, there is still a lack of knowledge in modelling strategies for accurate predictions of the static and dynamic stiffness performance of hybrid transmissions compared to conventional steel gears. New simulation models are needed for the prediction of hybrid gears behaviour as stand-alone component and at system-level, which can consider the anisotropic nature of the gear composite web, from both static and dynamic point of view, and the importance of the metal-composite interface. These aspects will be examined in depth in the next chapters, while this one concludes with a brief review of the different models used for the analysis of geared transmissions.

2.4 Description of the models for the analysis of meshing gears

The first studies on the dynamics of spur gears arose from the works of Abramov [60] and Utagawa in the 50s [61]. A fundamental contribution to the understanding of the

sources of gear meshing vibrations was given by Harris [62], where he investigated the static behaviour of meshing gears. He introduced the concept of static error, which shows a variability due to the load transitioning from one tooth pair to the subsequent. Additionally, he highlighted the importance of damping in reducing the amplitude of vibrations close to the resonance. In a successive work, Gregory [63] introduced the static transmission error, defined as "the angular displacement of the mating gear from the position it would occupy if the teeth were rigid and unmodified". This definition makes the TE as one of the main sources of vibrations in meshing gears.

A distinction of the loads acting on gears was presented in [64], where dynamics loads that cause the vibration response of the system can be due to internal or external excitations.

When external excitations lead to contact loss and repeated teeth impacts, this condition is defined as *rattle*, in which the main characteristics of noise is a broadband frequency spectrum typical of impact events. This type of phenomena was analysed in the work of Kahraman [65].

When the internal excitation is dominant in the dynamic behaviour of the system and no contact loss is experienced, the acoustic response is represented by a tonal noise known as *whine*. In this condition, the behaviour is dominated by the periodic variation of the mesh stiffness, which generates a tonal excitation at the tooth-passing frequency.

In general, the approaches for the analysis of gear dynamics can be distinguished in the way the mesh stiffness variation is represented and the level of details used to describe the components of the transmission, either rigid or flexible, which is reflected by the number of the degrees of freedom in the model. The simplest approaches make use of few degrees of freedom with a spring-damper element to catch the rotation of the gears [66]. Additionally, bodies and supports are assumed rigid, as well as the meshing force, acting along the line of action, is considered one-dimensional. The goal of these simple approaches is to model the variable mesh stiffness for a gear whine study. It is clear that the simplicity in modelling reflects a lack of accuracy, which can be enhanced with FE-based techniques [67] and [68]. They offer the main advantage of including gear body flexibility and of capturing the non-linear nature of the contact problems in the simulation environment in a precise way. FE formulations often result in extremely long computational time, especially for dynamic analyses. A trade-off between the accuracy of the solution and the computational cost can be found using multibody simulation tools,

which have the advantage of modelling complex systems with an increased computational efficiency.

The following sections will give a brief overview of the principal classes of models used to analyse gears during meshing and the main applications.

2.4.1 Analytical models

The interest in the formulation and the use of analytical models stands on the fact that they are simple with low computational requirements and a small number of degrees of freedom. The drawback of this simplified but efficient approach is the low level of details in the representation of dynamic phenomena, which can lead to wrong results.

In this class of models, 1D formulations focus on the rotation of gears around their rotational axes neglecting the translational and the rotations out of the gear plane. 1D models have been used either for gear whine or contact loss. Generally, they consist of masses lumped into inertia moment around the rotational axis with a spring-damper element used to connect the two masses. The simplest approaches do not consider the time-varying mesh-stiffness, like in [65], where authors use constant stiffness formulation to study the non-linear response of a spur gear pair.

In [8] and [69] Cai included time-varying mesh stiffness in the analytical formulation, where TE is considered as the sum of two contributions due to the elastic deformations and the displacements caused by the deviation from theoretical involute shape. Other models that assume time-varying mesh stiffness and clearance-type nonlinearity have been described in [70] and [71] by Blankenship and Kahraman. They investigated the forced response of a mechanical oscillator reproducing the jump phenomena. In [72], Andersson offers a quantitative description of the contact pressure.

When the translational motion of the gears due to the deflection of bearings, shafts or other supporting structures is no longer negligible, additional compliance is included by adding spring-damper elements. An example can be found in [73], where effects of bearings and shafts compliance were introduced in the rotational formulation.

3D models are used to account for tilting motion out of the gear plane, misalignment effects and micro-modifications in axial direction. In [74] Velex considered the pressure distribution by introducing different springs in axial direction, each of them representing the stiffness of a thin slice of the tooth.

2.4.2 Finite Elements models

FE techniques are used to accurately simulate the gear meshing process without the restrictions imposed by the analytical formulations. In fact, the latter are based on the lumped formulation of the meshing stiffness, which introduce an approximation in the analysis. This approximation becomes important when analysing lightweight gears leading to incorrect results, since it is not possible to neglect the coupling between the deformation of the gear body and of the teeth.

In this context, FE formulations require a highly refined mesh in the contact area to account for the higher strain gradient generated by the Hertzian loads.

From the static point of view, FE tools are widely used to compute static TE and mesh stiffness. In [75] and [76], authors show how it is possible to analyse the local contact loads of the teeth during meshing with non-linear static analyses.

Additionally to the aforementioned advantages, FE techniques allow to consider other phenomena compared to the analytical tools, e.g. non-linearity with load, misalignments of the gears, variation of the local curvature due to the teeth profile modifications [77]. Moreover, they are very useful to decouple the teeth and body contribution in the gears deformation. The latter is particularly relevant when multi-material design is used, allowing to study of the gear body deformation as a consequence of the combination of different materials, as will be described in depth in the next chapters of this thesis.

Due to the long computational time required to solve non-linear FE models, dynamic FE analyses in time domain are unfeasible, and they can only be used for very short events in the order of few millisecond. With the aim of reducing the computational cost of contact problem, Abousleiman [78] presented an analytical formulation for the gear contact combined with a FE discretization of the deformable gear. An analytical description of the contact problem was also proposed by Vijayakar [79] who combined Bussinesq solution for a point load, which eliminates the need for highly refined mesh in the contact regions, with a FE representation of the global displacement field of the gear.

2.4.3 Multibody models

Multibody models represent a trade-off between the great accuracy of FE approaches and the low computational costs of the analytical techniques. They are based on the definition of different bodies, modelled through their inertia properties within a reference frame,

subjected to determined boundary conditions and mutually connected by joints. They are used to simulate the dynamic of the transmission at system-level, by considering a detailed modelling of the meshing forces. The representation of a body can be rigid or flexible. In [9] Palermo et al. developed a multibody element that can represent the meshing behaviour with a TE-based mesh stiffness coming from a pre-processing phase in gear dedicated tools. Different sets of TE curves, which correspond to different working conditions of the gears in terms of transmitted load and relative position, are generated. Then, the curves are interpolated in the dynamic analysis to obtain the actual value of the mesh stiffness. The approach allows to analyse gears at system-level. Other tools with integrated multibody capability are available in commercial products [80], [81] and [82].
Flexible multibody approaches allow to account for the distributed flexibility in the gear body, representing the most-detailing model for studying gear dynamics. However, they require high computational costs, which make them feasible only for simple cases.
Recently, a multibody approach combining FE and analytical representations of the gear stiffness has been presented in [83]. The multibody formulation provides high computational efficiency, allowing to precisely describe the time-varying mesh stiffness. This method will be used in the Chapter 5 to analyse and compare the meshing behaviour of a hybrid gear engaging with a metal gear with a second gear pair where the same metal gear engages with a metal thin-rim gear.

2.4.4 Industrial applications of geared transmissions

Gears play an important role and represent a critical component for the operation of the mechanical system in which they operate, especially in three main sectors, among all others: aerospace, automotive and wind turbine. The principal aim of gear analysis is related to the prevention of mechanical failures, due to the dynamic loads. Secondly, the analysis of geared transmissions has relevant importance for the noise and acoustic comfort, since gear meshing can be seen as a source of vibrations and noise, especially when gears operate at high rotational speed. Another significant aspect to be considered is the energy efficiency linked to the non-negligible source of losses, mainly due to the elasto-hydrodynamic lubrication and oil squeeze between meshing teeth.
The principal purpose of gears analysis [84] is the determination of dynamic loads arising from working conditions to avoid catastrophic failures in the mechanical system. In particular, two zones are considered critical: the first is the contact region, where high

contact stresses can arise; the second is the root fillet, which represents an area with high stress concentration [85]. The *pitting* phenomena are the most common gear failures, which are generated by the cyclic loads on the teeth. Basically, this is due to the high shear stress arising slightly below the tooth surface that determines the nucleation of small cracks, which lead to the detachment of small pieces of material with a formation of craters. Macropitting is a more severe condition of micropitting, whose pits are about an order of magnitude smaller. The phenomenon of *scuffing* happens when insufficient lubrication layer is provided between metal surfaces, leading them to slide each other and to cause superficial scratches.

On the other side, root cracks are generated by high stress concentration due to the tooth bending under cyclic loads. In this condition, fatigue guides the crack across the tooth root.

The exploitation of new solutions in gears application, including those for hybrid metal-composite structures, can help to improve the comfort level through the analysis of the acoustic pressure. Generally, acoustic and vibrational effects are related to each other. In the case of gear whine, the gear excitation propagates through the supporting structure and if the meshing frequency approaches a resonance frequency of the system, the noise and vibration may happen leading to a possible failure of the transmission.

In the automotive industry, the passengers comfort is greatly affected by transmissions problems. In particular, both gear whine and gear rattle represent important issues regarding noise. In modern electrical and hybrid vehicles, the combustion engine is no longer present and the removal of this source of noise leads to the domination of the tonal noise, which is a characteristic of gear whine. Additionally, gear rattle is really important in diesel engines, where torque fluctuations produces gear losses through repeated impacts. From the simulation perspective, manual transmissions models are quite easy to analyse because of the conventional arrangement of single gear pairs in a parallel two-stage. On the other hand, automatic transmissions [86], involving also hybrid vehicles, require planetary configurations, where the dynamic response of gears, coupled with the supporting structures needs to be correctly captured. For this reason, the system-level simulations represent a real challenge, even more with transmissions made of lightweight or hybrid metal-composite gears.

In the aerospace field, especially for helicopters and aviation jet engines, transmissions play key role, giving a strong contribution on the overall weight of the powertrain system.

In helicopters, the transmission connects the engine to the main rotor, to which blades are connected. The latter require low rotational speed, of hundreds of rpm, while the engine operates at ten thousand or more rpm. This situation brings to the development of gears configurations, which are able to ensure a reduction ratio of about 1:100, requiring one or more planetary gear stages. Typically, transmissions are composed by spur gear trains and spiral bevel gears, which aim at transmitting power between crossed-axis shafts. For this reason, durability becomes the main concern. Here, health-monitoring techniques, based on the applications of sensors, as close as possible to the excitation source, alerts crew in case of anomalies. To reduce inertia effects, the lightweight design is quite extreme, bringing to the development of complex gears geometries (holes, etc.), which can increase the level of vibrations in the system.

Based on all the considerations described so far, the development of mechanical transmissions made with lightweight composite materials, which can dissipate energy and mitigate vibrations, can be seen as a great opportunity to enhance the overall quality of the transmission. This is why the following chapters deal with strategies used to study hybrid gears from different perspectives

Chapter 3

Multi-scale modelling and analysis of hybrid gears

In this Chapter, based on the work published in [87] a predictive model for the mechanical behaviour of the composite gear body is developed through a FE multi-scale modelling approach that allows the evaluation of the orthotropic material properties to be used in the FE analysis. The proposed approach aims at reducing the efforts needed in hybrid gear development; an optimal design can be achieved by defining the geometry of the gear and the material itself, with no need for expensive and time-consuming experiments aimed at characterizing the composite material properties. The outline of the Chapter is the following: in Section 3.1 a brief review of the state of the art of triaxial braided composites is presented, while in Section 3.2 an overview of the proposed multi-step modelling approach is provided; Sections 3.3 is dedicated to the description of gear's FE model generation and Section 3.4 to the multi-scale approach used to compute homogenized, orthotropic properties of the composite web [25]. The accuracy of the resulting FE model is assessed in Section 3.5 by a comparison between the gear's natural frequencies predicted through a numerical modal analysis and the experimental values reported in [11]. Conclusions are summarized in Section 3.6 followed by the discussion of the achieved results. The latter show that the orthotropic description of the web material improves significantly the predictive accuracy of the FE model in comparison to an isotropic formulation.

3.1 Analysis methods for triaxial braided composites

In order to enable a simulation-driven design of hybrid gears with improved N&V behaviour, a methodology is proposed for an accurate FE modelling of hybrid gears described in [11] by taking into account the anisotropic nature of the composite web material and of the ply arrangement effects. The composite part of the gear was made of a polymer matrix reinforced with two-dimensional (2D) braided fabrics, for which a detailed description of architecture, manufacturing process, applications and predictive

models has been given in [88]. In order to test and model triaxial braided composites, different approaches have been investigated. An analytical method based on the rule of mixture for the evaluation of the stiffness properties of 2D triaxial braided composites has been presented in [89]. The architecture has been described as three separate layers, with the first two representing braided tows and the last being an axial tow. In [23] analytical models have been used to evaluate mechanical properties of quasi-isotropic triaxial braided composites made of glass fibres and epoxy resin.

A complete experimental characterization of the mentioned triaxial braided composite material has been described in [90], where a panel of six layers of plies has been tested to evaluate tensile and compressive moduli in axial (along axial yarns direction) and transverse directions, with the purpose of defining stress-strain curves. Moreover, a single RUC of such composite architecture has been split into four subcells and the CLT [14] has been applied to evaluate the equivalent unidirectional laminate properties needed for a subsequent FE simulation for material characterization and validation. In a subsequent step [91], the subcell representation has been improved with a more accurate model that allows to determine ply thickness and volume fraction.

In order to enable predictive analyses with higher accuracy and without losing information on local stress fields, the attention has been focused on micro and meso-scale modelling of triaxial braided composite panels, starting from the definition of a FE model of the RUC [92], which takes into account internal braiding architecture. In [93] and [94] a multi-scale FE model of a triaxial braided RUC has been developed for experimental and numerical correlations of axial and transverse tension response, while in [95] the 3D FE model at meso-level has been used to predict the progressive damage behaviour of single-layer braided composites. The application of FE techniques to different RUC models to support predictive analyses of the effective material properties as a function of the braiding angle has been described in [96].

3.2 Multi-scale modeling and simulation of hybrid gears: methodology overview for FE model generation

A modelling procedure is developed covering all steps needed for evaluating the modal properties of a hybrid gear. Since this process is strongly based on the use of CAD, CAE software [25], the proposed methodology can be applied in a generalized way to different

kinds of gears (e.g. spur, helical, bevel). In this work, all the considerations are done for a specific spur gear model, for which the results of experimental modal testing are provided in the literature [11] and [54].

The first step of the proposed approach is the setting of gear geometry based on the definition of the rim, the web and the hub parts. The geometric description of the gear, obtained from the data reported in [11], was used to generate the CAD model, which was subsequently translated in a FE model of the gear by using a commercial software Simcenter 3D [97]. In the analysis, the virtual model was enriched through a multi-scale approach. First, effective elastic orthotropic properties of the utilized triaxial braided composite were computed at the meso-scale. At this scale, the RUC was composed by interweaving yarns, braided according to the investigated composite. The geometry of the yarn, i.e. its cross-section, was reproduced in a CAD environment, considering the local fibre orientation and the fibre volume fraction. Then, a FE-based homogenization procedure was used to compute homogenized elastic properties of such composite at the meso-scale, to be used in the macro-scale analysis.

The flowchart of the overall methodology is presented in Figure 3. 1. The various steps carried out to perform the entire modelling procedure are detailed in the following Sections 3.3 and 3.4.

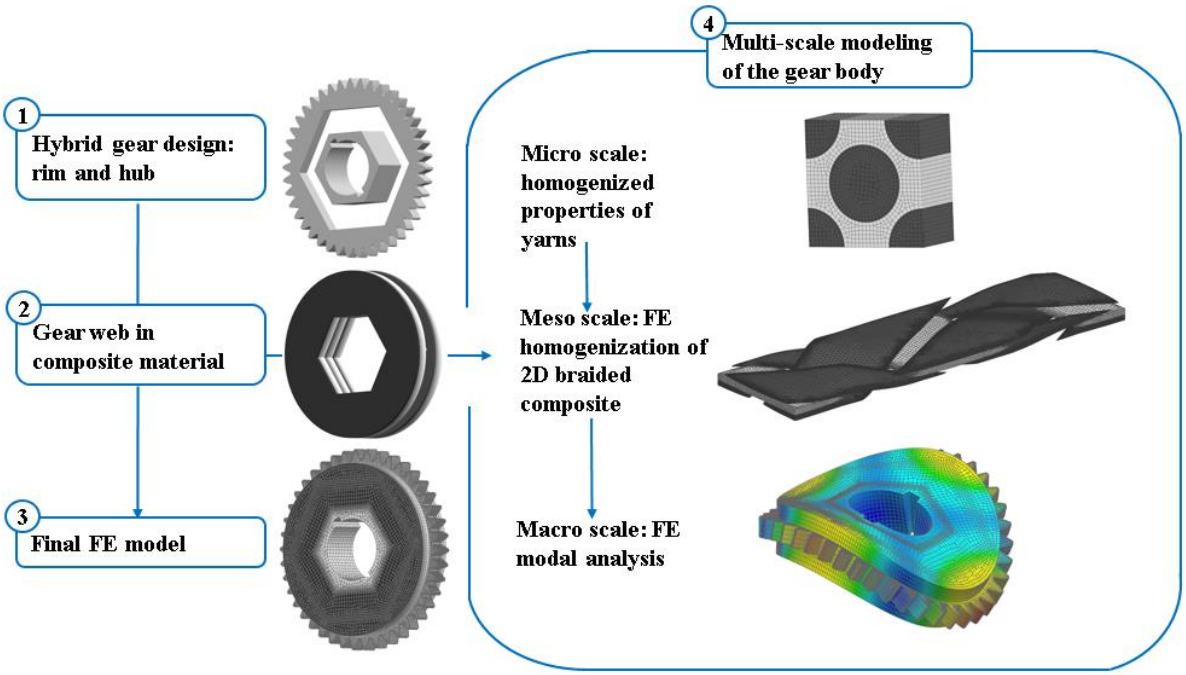

Figure 3. 1 Flowchart of the proposed methodology for hybrid gear modelling.

3.3 CAD and FE model generation of a hybrid gear

The design of the hybrid gear, based on the manufacturing process described in [11], started considering a detailed description of gear teeth surfaces. For this purpose, the FE model of the gear teeth was generated, in which all the gear specifications, such as number of teeth, addendum, dedendum, circular pitch, whole depth, pitch diameter and tooth profile modifications were considered. In such a way, an accurate model of the rim was created, which could be used for subsequent FE-based static and dynamic simulations of transmissions with hybrid gear pairs. In a next step, a parameterized CAD model of hub and web was generated, from which the FE models of those regions were derived and merged with the FE mesh of gear teeth to obtain a complete hybrid gear FE model description. The parametric approach facilitates the integration of the proposed workflow into an industrial design process allowing to easily change rim/web/hub CAD data. For model validation purposes, the FE model of the hybrid gear with the same isotropic material properties of the web as given in [11] (Young's modulus of 44 GPa, Poisson's ratio of 0.3 and mass density of 1522 Kg/m^3) was built and a modal analysis executed. Table 3. 1 shows a comparison between the model developed and the one analysed in [11] in terms of first 4 natural frequencies of the gear. The experimental results reported in [11] are illustrated as well.

FE-based predictions reported in [11]	**FE-based predictions with the proposed model**	**Difference**	**Experimental results**
[Hz]		%	[Hz]
7780	7851	+ 0.9	6270
7913	8014	+ 1.2	
13745	13656	- 0.6	9743
14592	14843	+1.7	10700

Table 3. 1 Comparison between predicted and experimental frequencies of the hybrid gear.

The results summarized in Table 3. 1 show that FE predictions on the proposed model are very close to FE-based estimations reported in [11]. Small differences are likely due to geometry uncertainties since few geometric parameters were unavailable. In addition, by comparison against test data, it can be noted that both FE models overestimate all

frequencies by a large amount, suggesting that an isotropic material formulation fails to catch the modal behaviour of the gear in the frequency range that has been analysed. For this reason, an improvement of the predictive accuracy was pursued through a multi-scale approach applied to the composite material of the gear web.

3.4 Multi-scale modelling of triaxial braided composite

As described in [11], [54], the model of the gear web is created as a stack of several braided composite prepregs. Each layer of such material consists of an axial yarn (24k carbon fibres in 0° direction) and bias yarns (12k carbon fibres in ±60° direction). Bias yarns are alternately passing above and under axial yarns with equal amount of material by weight in each direction. Figure 3. 2 shows a CAD representation of the braided architecture with axial and bias directions.

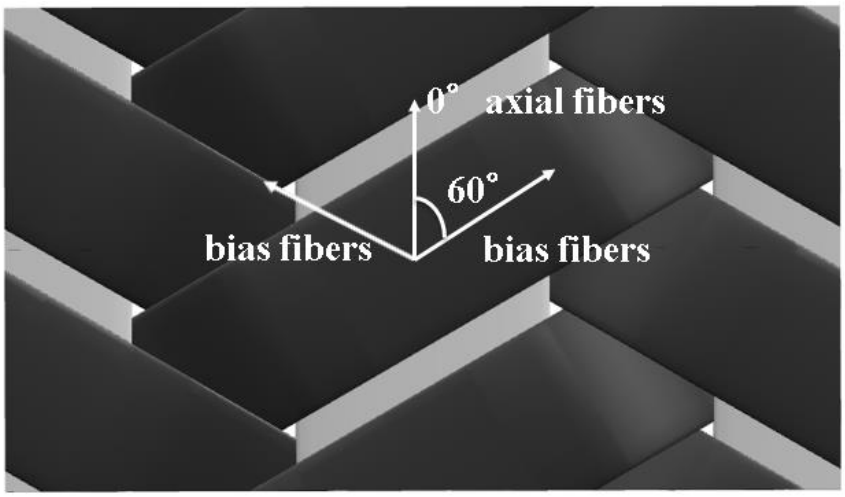

Figure 3. 2 Triaxial architecture.

With such a triaxial architecture, it was shown that a single layer of braided fabrics is balanced, symmetric and quasi-isotropic. It is known from laminates theory that a symmetric laminate is composed by plies in which material, orientation and thickness are symmetric about neutral axis [14]. This condition allows to avoid undesired effects due to unbalanced loads in plane, which could cause warping phenomena during fabrication.

The braided composite is analysed at micro and meso-scale to obtain the mascro-scale properties, as shown in Figure 3. 1:

Numerical homogenization of a triaxial composite unit cell is performed using the Simcenter™ VMC ToolKit (part of Siemens PLM Software): a set of software tools

developed for virtual material characterization [25]. The tool is used to obtain homogenised properties of the impregnated yarns on the micro-scale and subsequently link them to meso–level in order to compute the homogenised properties of plies. The main idea is to reduce modelling efforts and number of physical tests on coupons required to characterize mechanical behaviour of composites.

3.4.1 Micro-scale modelling

The multi-scale modelling approach started with the evaluation of local properties of impregnated yarns, taking into account local fibre volume fraction and orientation, based on Chamis formula [20]:

$$E_{11} = V_f E_{f11} + V_m E_m \tag{24}$$

$$E_{22} = \frac{E_m}{1 - \sqrt{V_f}(1 - \frac{E_m}{E_{f22}})} = E_{33} \tag{25}$$

$$G_{12} = \frac{G_m}{1 - \sqrt{V_f}(1 - \frac{G_m}{G_{f12}})} = G_{13} \tag{26}$$

$$G_{23} = \frac{G_m}{1 - \sqrt{V_f}(1 - \frac{G_m}{G_{f13}})} \tag{27}$$

$$\nu_{12} = V_f \nu_{f12} + V_m \nu_m = \nu_{13} \tag{28}$$

$$\nu_{23} = \frac{E_{22}}{2G_{23}} - 1 \tag{29}$$

where the subscripts *f* and *m* stand for fibres and matrix, respectively, while E_{ii}, ν_{ij} and G_{ij} (with *i, j =1,2,3* are the longitudinal, in-plane and out-of-plane transversal directions respectively) are the Young's moduli, Poisson's ratios and Shear moduli, while V_f and V_m are the volume fraction of the fibres and of the matrix, respectively.

Material data used in this work for the analysis of yarns properties of the braided composite material were taken from [11], [94] and are summarized in Table 3. 2. An important aspect of this micro-scale analysis is the definition of the fibre volume fraction in the yarns and in the entire unit cell, which has to be considered when using the Chamis formula. In [94], it is shown that the maximum volume fraction of the fibre (V_f) achievable in a single layer panel is 0.48 due to the limitations of the manufacturing process. In the RUC models described in [94], such a value is achieved by setting the fibre volume fractions in axial yarns and bias yarns to 0.86 and 0.69 respectively, while the values estimated experimentally are 0.77 and 0.745. In the model presented here the overall volume fraction of the single layer is set to 0.48, which is achieved by defining a fibre volume fraction of 0.86 for both the axial and the bias yarns.

Property	**Fibre**	**Matrix**
Material type	Carbon T700S	Epoxy E862
Longitudinal Modulus [GPa]	230	2.7
Transverse Modulus [GPa]	15	2.7
Shear Modulus [GPa]	24 Long./5.03 Transverse	1
Density [g/cm^3]	1.8	1.2
Single fibre diameter [μm]	7.0	--

Table 3. 2 Fibre and matrix properties.

3.4.2 Meso-scale modeling

The meso-scale analysis was performed starting from the CAD model construction. This model was further imported in the VMC ToolKit, capable to mesh the geometry, to define the material properties for both matrix and fibres and to set the periodic boundary conditions [97].

The geometric model of a triaxial braided composite unit cell provides a complete description of the internal geometric features, such as yarn cross section and interweaving and matrix dimensions. In detail, a parameterized CAD model was composed by multiple yarns built from a known elliptic cross section geometry. In order to obtain a solid volume

starting from sketches in different 2D planes, cross sections were repeated along a specified direction described by a heart line, which was linked to a predefined crimp value. The proposed approach allows to account for yarn width, thickness and spacing, in addition to the shape of the cross sections, as parametric features in the CAD model. A symmetric periodic unit cell is essential for the application of periodic boundary conditions. This requirement was met by trimming the overall geometry with specific symmetric planes and by extracting a solid 3D surrounding matrix, as shown in Figure 3. 3 and Figure 3. 4.

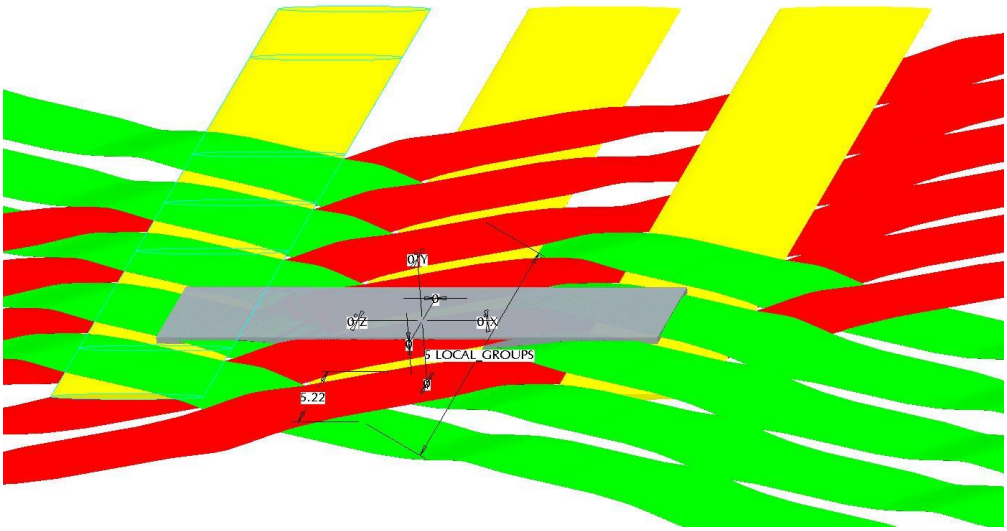

Figure 3. 3 Braided fabric pattern.

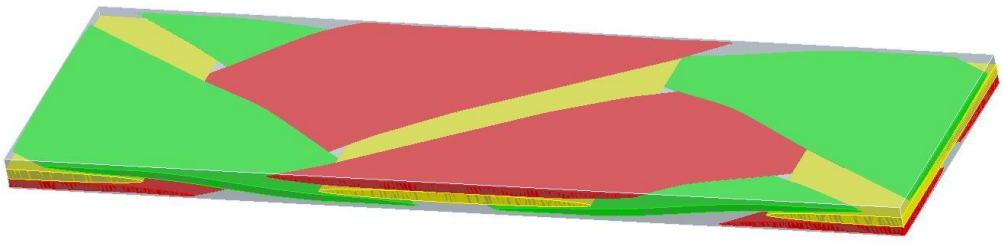

Figure 3. 4 Unit cell obtained after trimming.

The CAD model was parameterized to enable geometric modifications with reduced modelling effort and time, as to enable the generation of a RUC model with an adequate distance between two or more solid volumes to avoid interpenetration. All geometric features used in the case study presented here are reported in Table 3. 3 and are similar to those observed experimentally and considered in [94], as to enable a quality assessment of the resulting macro elastic material properties based on literature data.

Unit cell length	**Unit cell width**	**Unit cell height**	**Major dimension of axial elliptic cross-section**	**Major dimension of bias elliptic cross-section**	**Area of axial elliptic cross section**	**Area of bias elliptic cross section**
		[mm]			[mm^2]	
18.08	5.22	0.73	5.5	3.7	1.2	0.62

Table 3. 3 Unit cell geometry.

The main purpose in creating a mesh is to approximate properly the CAD geometry. In detail, yarns and matrix were meshed with linear tetrahedral solid elements, which can have very small dimensions and follow accurately the curvature of the yarns. Since the unit cell is characterized by a repetitive behavior in the plane, the mesh of the opposite faces was generated by imposing a constraint of identical discretization, both for yarns and matrix.

Figure 3. 5 and Figure 3. 6 show the generated meshes for the yarns and for the matrix respectively.

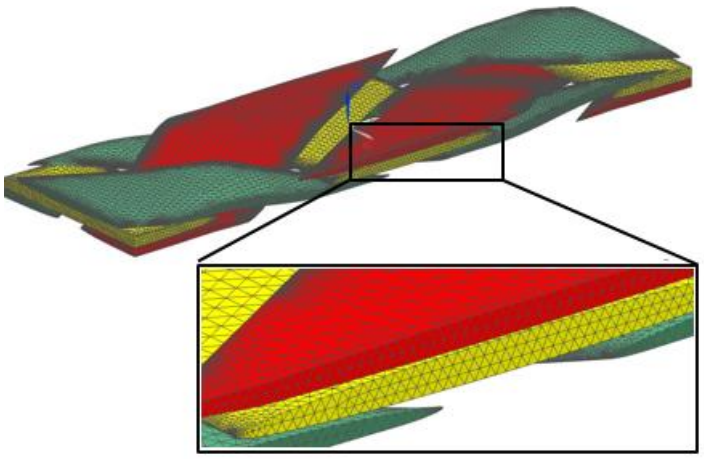

Figure 3. 5 Generated FE mesh of yarns only.

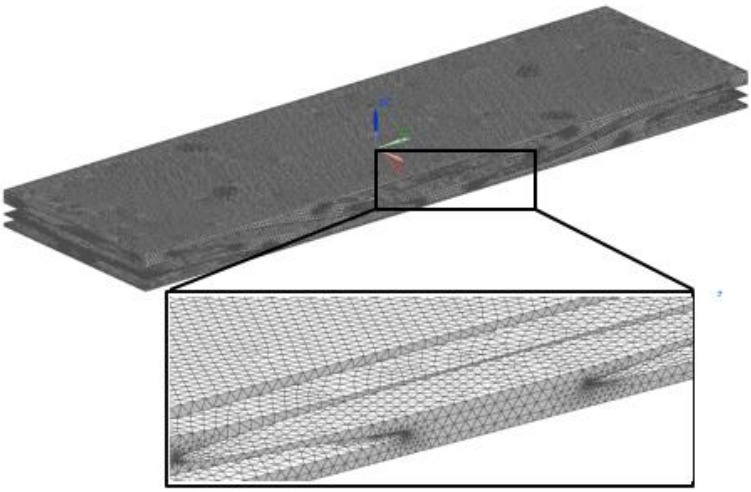

Figure 3. 6 Generated FE mesh of the matrix.

Yarn's material was considered with a transverse isotropic behaviour and its properties were derived using the Chamis formula, as described in Section 3.4.1. On the contrary, the matrix material properties were set according to the material specifications of Table 3. 2, with an isotropic behaviour. In order to complete the process of mesh generation of the analysed composite, local material orientation of the fibres has to be taken into account. This was achieved in CAD environment by selecting a heart line within a yarn created in the solid model. In this way, material orientation effects with respect to various crimp angles of the yarns can be accurately captured in the subsequent FE analysis. Figure 3. 7 shows how local material orientation is defined.

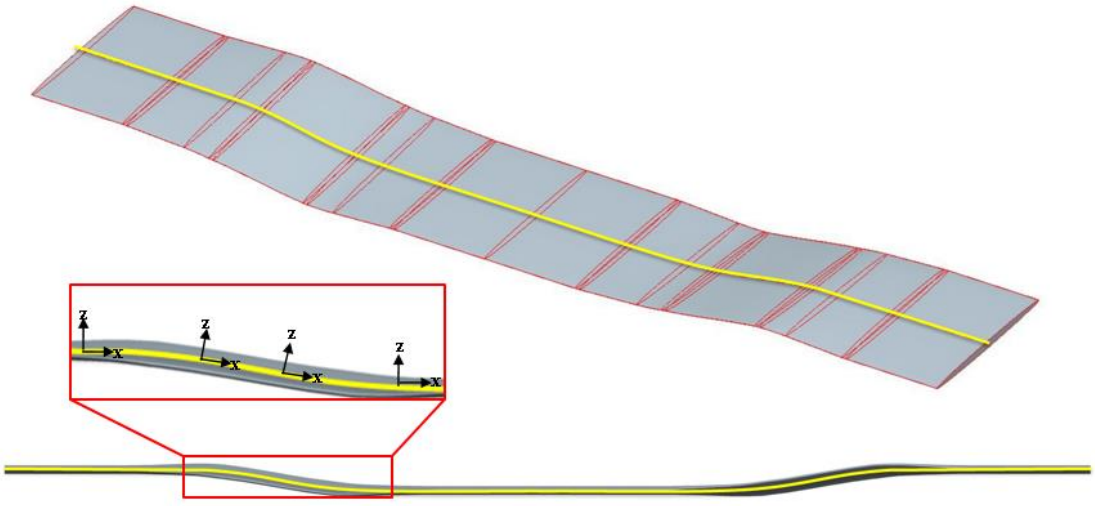

Figure 3. 7 Heart line and local material orientation.

Finally, the interaction between yarns and the matrix, which are in contact in normal working conditions, was defined through a surface gluing function. No relative movement between the nodes in contact of the matrix and of the yarns were, therefore, allowed.

As a last step of the overall multi-scale pre-processing analysis, periodic boundary conditions were applied to the model in order to simulate periodicity of a given unit cell geometry as described in [24]. Since the analysis was related to the single unit cell at the meso-level, the requirement of displacement continuity close to the opposite faces is fulfilled by imposing that any displacement on one side of the RUC is the same as in the opposite side plus or minus a constant value. Disregarding displacements and rotations of the unit cell, the displacement field can be written as:

$$u(\overline{x}) = \bar{\bar{\varepsilon}}\,\overline{x} + \tilde{u}(\overline{x}) \tag{30}$$

where $\bar{\bar{\varepsilon}}$ represents the macroscopic strain tensor and x the position vector of a material point in the RUC. The second term is a volume periodic term with zero average value, with ũ being the local displacement field in the RUC.

Six different subcases of linear static analysis, three tensile load cases and three shear load cases, were created and solved for subsequent homogenization process.

3.4.3 Material homogenization

The final goal of the proposed multi-scale modelling approach is the evaluation of homogenized elastic properties of the analysed unit cell. Such properties are calculated by post-processing the FE stress-strain results Figure 3. 8 shows the displacement fields for the six subcases.

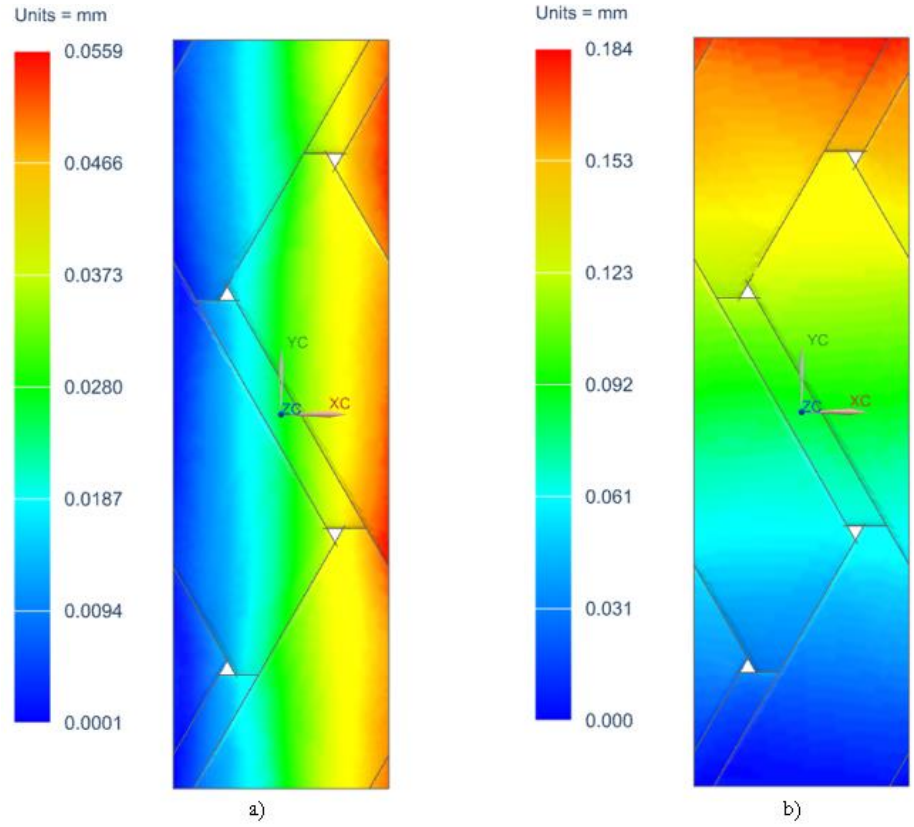
Units = mm
0.0559
0.0466
0.0373
0.0280
0.0187
0.0094
0.0001
YC
ZC
XC
a)
Units = mm
0.184
0.153
0.123
0.092
0.061
0.031
0.000
YC
ZC
XC
b)
Units = mm
0.0065
0.0054
0.0044
0.0033
0.0022
0.0011
0.0000
YC
ZC
XC
c)
Units = mm
0.094
0.078
0.063
0.047
0.031
0.016
0.000
YC
ZC
XC
d)

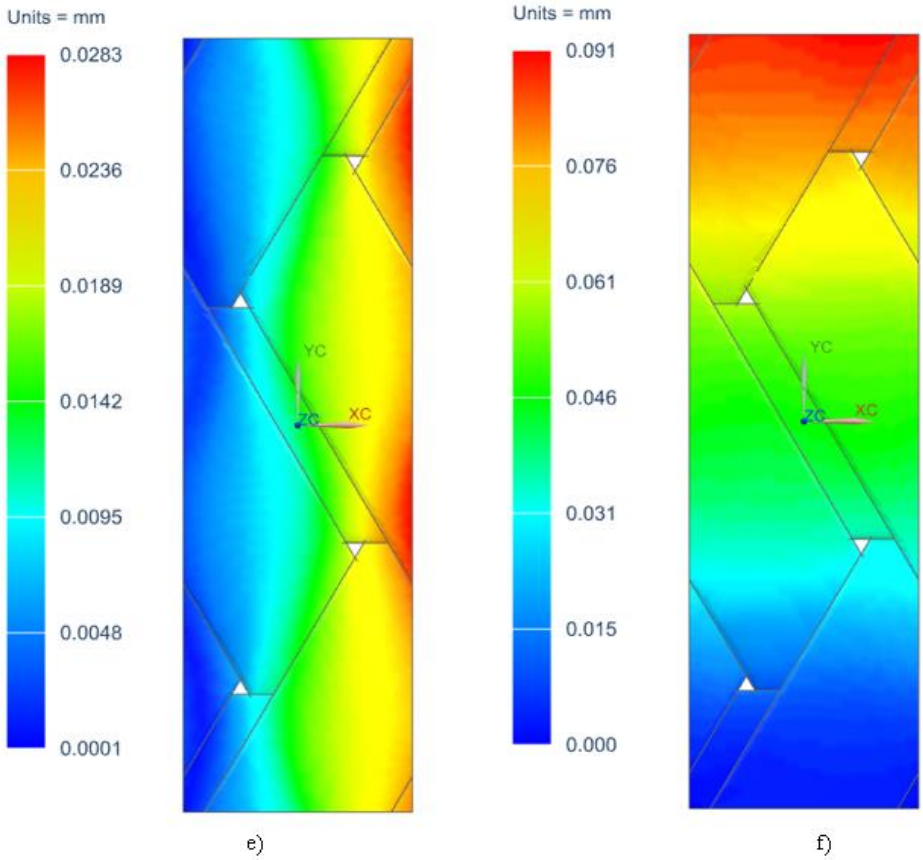

Figure 3. 8 Displacement field of the RUC yarns under the tensile static load case directions x a), y b) and z c); displacement fields of the yarns under shear static load case on planes xy d), xz e) and yz f).

The relationship between stresses and strains at the macro-level can be expressed as follows:

$$\sigma_{ij}^{H} = C_{ijkl}^{H}\, \varepsilon_{kl}^{H} \tag{31}$$

where C_{ijkl}^{H} represents the elasticity tensor at macro-scale. In order to obtain stiffness/compliance matrix and to derive elastic modulus values, the volume averaging technique was used, in which stresses are averaged over all the integration points of the elements:

$$\langle \sigma \rangle = \frac{1}{V} \sum_{p=1}^{n} \sigma^{p} V^{p} \tag{32}$$

where σ^{p} and V^{p} are the stresses and the equivalent volume of the integration points respectively.

In Table 3. 4, the homogenized macro-level elastic properties are compared to the experimental, the analytical and the numerical values reported in [94]. The latter are referred to a RUC model without axial fiber bundle undulation.

	RUC properties described in [94]**: Experimental**	**RUC model described in** [94]**: analytical approach**	**RUC model described in** [94]**: numerical approach**	**RUC properties with the proposed multi-scale approach**
			[GPa]	
$\mathbf{E_1}$	40.6	42.9	42.8	42.8
$\mathbf{E_2}$	38.5	42.5	38.9	41.4
$\mathbf{E_3}$	----------	---------	--------	7.4
υ_{12}	----------	---------	-------	0.3
υ_{23}	----------	---------	-------	0.39
υ_{13}	----------	---------	-------	0.36
$\mathbf{G_{12}}$	----------	15.88	15.9	14.2
$\mathbf{G_{13}}$	----------	------	------	2.06
$\mathbf{G_{23}}$	---------	------	------	2.03

Table 3. 4 Comparison of elastic material properties of RUC without considering axial bundle undulation *[94]*.

Table 3. 4 shows that the numerical results achieved with the proposed methodology are close to those presented in [94]. In addition, the axial fibre bundle undulation effect, which is currently neglected, can contribute to bring stiffness moduli much closer to the experimental values, as demonstrated in [94].

3.5 Macro scale FE modal analysis of a hybrid gear

A FE-based modal analysis was set up taking into account the gear model discussed in [11]. In detail, three thick plies, made of twelve layers of prepregs, were assembled in a hybrid gear model along the axial direction. The assembly was then attached to a steel gear rim through an adhesive bonding. Each layer was rotated by 60° around z-axis to increase through-the-thickness isotropic behaviour. As a result, the same stack configuration proposed in [11] was, finally, obtained. Furthermore, solid laminate

modelling, available in Simcenter Nastran, was used to simulate ply arrangement effect on the gear web, by considering transverse shear effects and out of plane stresses. The solid model was implemented with the calculated homogenized orthotropic elastic properties of the triaxial braided composite material. The results of the FE modal analyses of the proposed gear model in free-free conditions are presented in Figure 3. 9. Table 3. 5 summarizes the obtained hybrid gear eigenfrequencies for the two models (isotropic and anisotropic composite materials) comparing them with the experimental and numerical data published in [11].

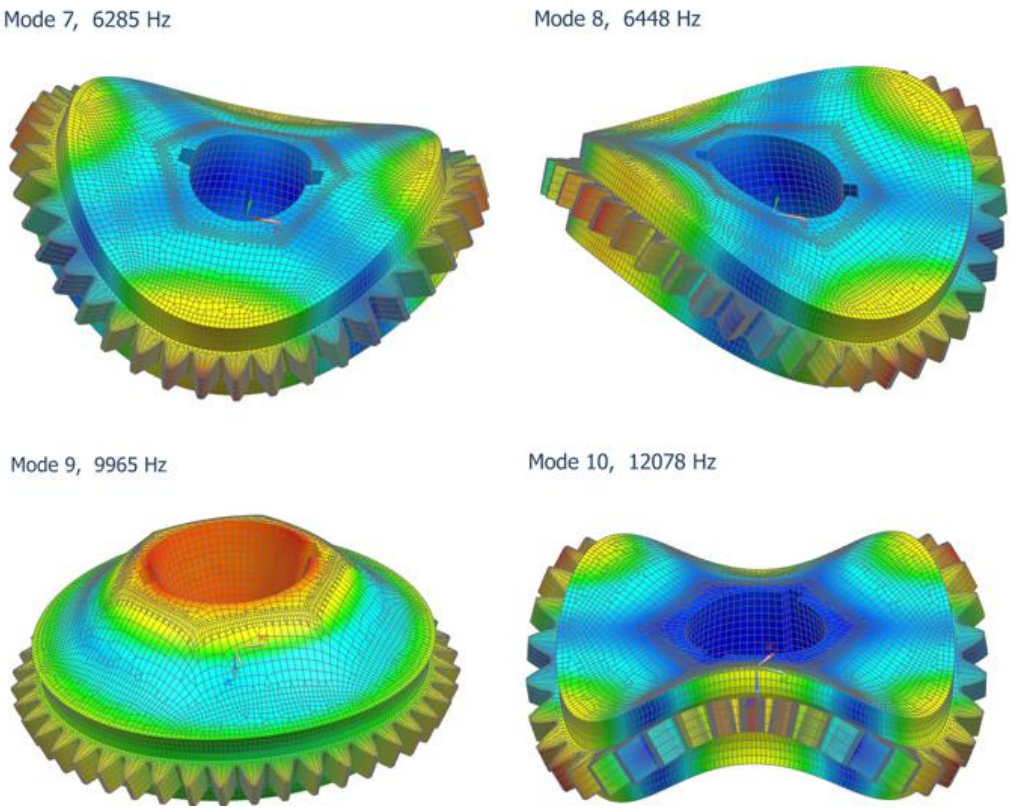

Figure 3. 9 First four shape modes evaluated with anisotropic web properties.

Experimental results in [6]	**FE results in [6]**	**FE results: proposed model with isotropic material**	**FE results: proposed model with orthotropic material**
		[Hz]	
6270	7780 (+24%)	7851 (+24.9%)	6285 (+0.2%)
	7913 (+26%)	8014 (+27.2%)	6448 (+2.8%)
9743	13745 (+41%)	13656 (+40.4%)	9965 (+2.3%)
10700	14592 (+36%)	14843 (+37.3%)	12078 (+12.8%)

Table 3. 5 Comparison of predicted and experimental natural frequencies for model validation.

As already commented in Section 3.3, the numerical model proposed in [11] and the one proposed in this work, implemented with isotropic material properties, generated frequency predictions that are very close to each other but significantly different from the experimental ones. This confirms the quality of the generated CAD and FE models of the gear. The FE model with the orthotropic formulation of the composite web material, achieved through the proposed multi-scale modelling approach for the triaxial braided composites, enabled more accurate predictions, which are much closer to the experimental results. This is more evident for the first two natural frequencies, where the difference between predicted and measured values is 0.2% and 2.8%, while differences of up to 41% are reported for the model with isotropic formulation of web material.

The model accuracy decreases when the third frequency was considered, with a difference slightly higher than 10% between experimental and orthotropic FE results, which is likely due to inaccuracies in the model linked to the web-rim interface and inter-laminar connection. Both factors, in fact, were neglected in the present model and are expected to play an important role on the overall modal response of the hybrid gear.

3.6 Conclusions

In this Chapter a multi-scale modelling approach was employed to predict natural frequencies of a hybrid gear. The gear was presented with web body made of stacks of braided prepregs. The composite web geometry was analysed by considering micro, meso and macro scales. At micro-scale, elastic properties of yarns were homogenized using analytical formulation taking into account the local fibre volume fraction. At meso-scale, the RUC of the braided composite was defined in a parameterized CAD model composed by multiple yarns built from a known elliptic cross section geometry. Then, the CAD geometry was accurately meshed and periodic boundary conditions were applied to simulate periodicity of the given unit cell. Finally, macro elastic properties were evaluated through a homogenization process, based on the volumetric stress averaging.

Two FE models were solved: in one, the composite body is represented by equivalent isotropic properties; in the other, orthotropic material properties are considered. In the latter case, effective homogenized orthotropic properties of the triaxial braided composite were considered. Even if the braided material has quasi-isotropic properties in plane and the ply stack configuration is set up to achieve the best isotropic behaviour along the axial direction of gear, by comparing the numerical results with the experimental data available in the literature, it was shown that the natural frequencies of the gear cannot be accurately predicted if anisotropy along axial direction is neglected. On the contrary, it was shown that the modal results achieved with a model with orthotropic material formulation are close to the experimental evidence for the first and second natural frequencies, while a more significant difference still exists for the third normal mode.

Even if further investigations are needed to explore the origin of this difference, the achieved results show the potential of the proposed approach to accurately model hybrid gears.

The presented approach can be used in subsequent FE-based simulations aimed at assessing the static and dynamic stiffness performance of such advanced transmissions in comparison to conventional, full metal gears. Moreover, the parametric definition of the hybrid gear geometry implemented in the overall multi-scale modelling procedure can be exploited to reduce modelling effort and time for further design optimization of the composite web part (stacking sequence, geometrical shape, etc.).

The next chapter is dedicated to the description of an innovative design, simulation and testing of a hybrid gear as a stand-alone component and during meshing.

Chapter 4

Innovative approach for the design, simulation and testing of hybrid gears

4.1 Introduction

This chapter, which is related to the work described in [98] and [99], presents a complete description of the steps required for the design, manufacture, testing and simulation of a novel hybrid metal-composite gear, assembled using two different joining technologies: interference fitting and adhesive bonding. The modal behaviour of two manufactured hybrid gears is compared to a traditional lightweight steel gear. In particular, Section 4.2 contains a schematic overview of the steps needed to design and analyse hybrid gears. Section 4.3 describes the design approach of the proposed hybrid gears that exhibit the same mass and macro-geometry properties of a lightweight metal gear assumed as reference gear.

Section 4.4 deals with the analysis methods for modal characterization. Here, experimental measurements of natural frequencies and damping of steel gear body and composite web as stand-alone components are correlated with FE simulations. Specifically, damping is evaluated for each natural frequency in the range of interest using the half power bandwidth method [100]. Section 4.5 describes the two different joining techniques used in the gear assembly process. Additionally, experimental and numerical frequency response functions (FRFs) are discussed and a numerical comparison against the modal properties of the steel lightweight gear with the same mass is provided. In Section 4.6, differences in terms of damping and dynamic stiffness are highlighted for the gears assembled by the two joining techniques.

Section 4.7 highlights different FE simulations of gear pairs to show how the composite body affects the behaviour of hybrid metal composite gears during meshing.

The obtained numerical and experimental results show how it is possible to design, manufacture, test and simulate a hybrid metal-composite gear with enhanced mechanical properties compared to a lightweight steel gear. The last section contains conclusions and provides an outlook of the next chapter.

4.2 Process overview for the design, manufacturing and analysis of hybrid metal-composite gears

The new concept of metal-composite mechanical transmissions imposes a general schematization of the process employed to design, manufacture and analyse the modal behaviour of the hybrid gear in a stand-alone configuration, before planning gear-pair and even system-level analyses. The two primary aims of the presented study can be summarized as follow:

1) To compare the modal behaviour, e.g. the natural frequencies and modal damping coefficients, of two metal-composite gears assembled by two different joining techniques against each other and with respect to the steel lightweight gear with the same mass;

2) To develop and validate an FE-based numerical approach for predictive modal analyses of such gears, thus enabling simulation-driven design of hybrid gears with optimized dynamic behaviour.

Figure 4. 1 shows the flowchart of the proposed approach that will be described in depth in the next sections.

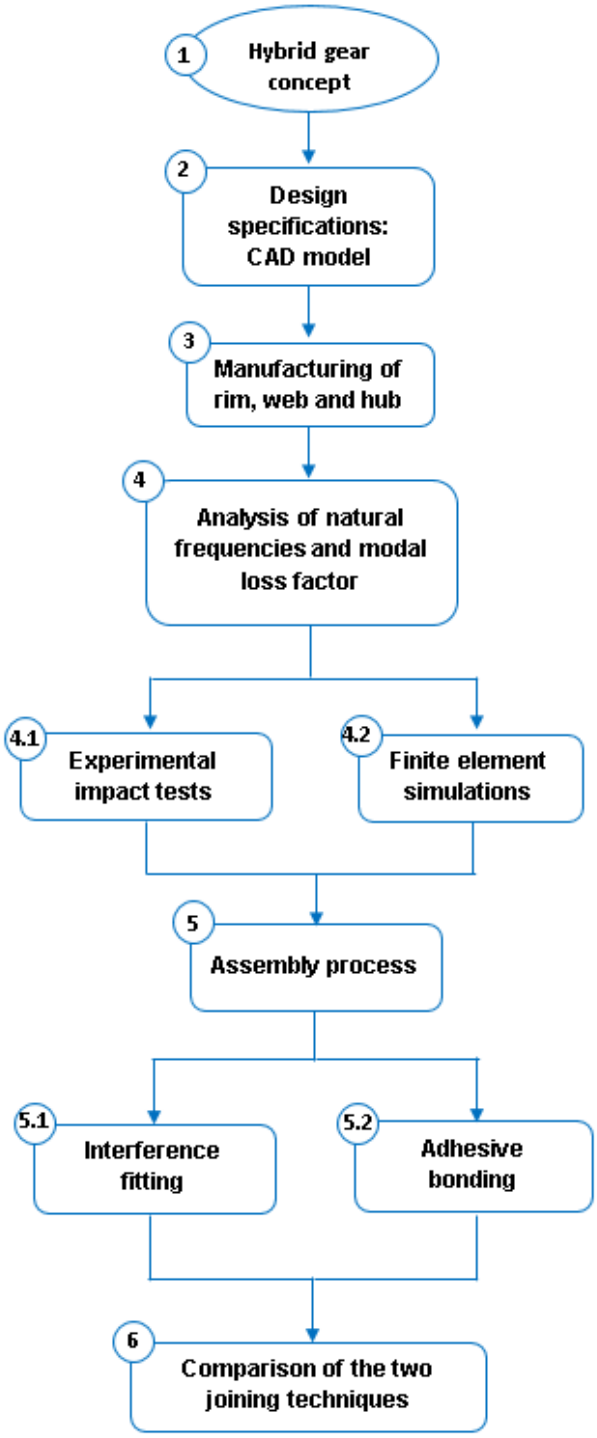

Figure 4. 1 Overview of the proposed development process for the design, manufacturing and testing of hybrid gears.

4.3 Design and manufacturing of hybrid metal-composite gears

This section describes the idea behind the design and simulation of a hybrid gear, starting from the geometry of the steel lightweight gear considered in [101], which is assumed as reference model. The CAD geometry of the hybrid gear is presented in the Section 4.3.1 while the manufacturing process is described in the Section 4.3.2.

4.3.1 CAD model

The design workflow of a metal-composite gear is based on the definition of three main areas: the teeth, the central body or web and the hub.

It is worthy to notice that the metal part is designed with small pins around the circumference of the rim and the hub to ensure mechanical locking between the metal and the composite parts. Differently from the approach described in [11], which used a hexagonal shaped web, slotted in the metal web, this joining technique enables a further reduction in weight.

The rim of the proposed hybrid gear is 23 mm thick, while the web contains a 10.5 mm thick cavity on each side of a thin-walled metal layer to accommodate the composite panels.

The complete model of the hybrid gear, built by using the commercial software Siemens PLM Software Simcenter 3D [97], was created as to have the same mass of the reference steel gear. Figure 4. 2 shows, respectively, the lightweight steel gear, used as reference gear in this work, and the proposed design of hybrid gear.

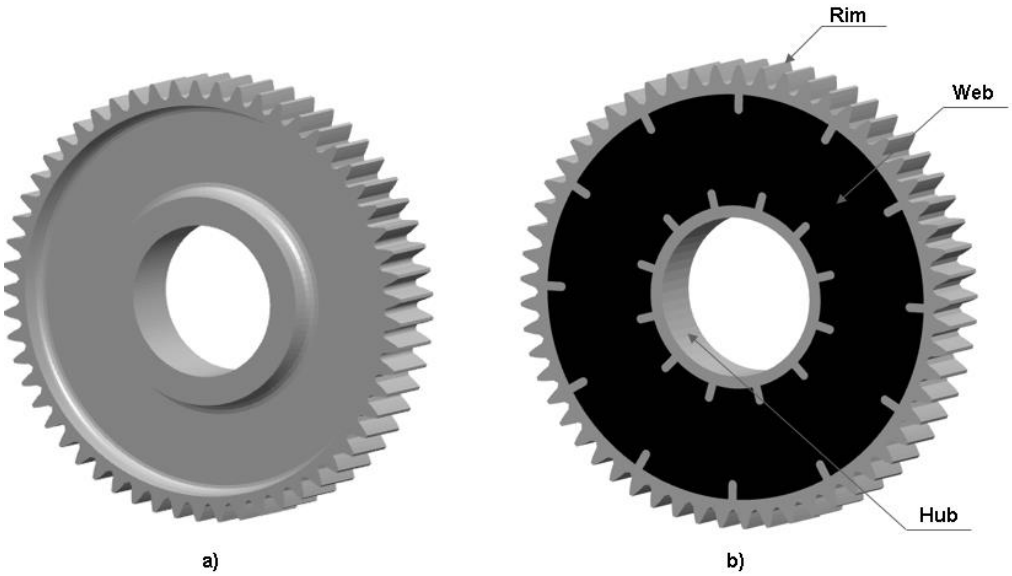

Figure 4. 2 CAD model of the lightweight steel gear a) and of hybrid gear b).

4.3.2 Hybrid metal-composite gear manufacturing

The steel rim of the hybrid gear was CNC machined according to the designed geometry (Table 4. 1), described in Figure 4. 3. A thin metal layer of 2 mm between rim and hub avoids centring problems that could be caused by the manufacturing process.

Parameter	Value
Teeth number	57
Normal module	2.6 mm
Normal pressure angle	20 deg
Face width	23 mm
Tip diameter	154 mm
Root diameter	141.70 mm
Theoretical pitch diameter	148.20 mm
Base diameter	139.26 mm

Table 4. 1 Gear specifications.

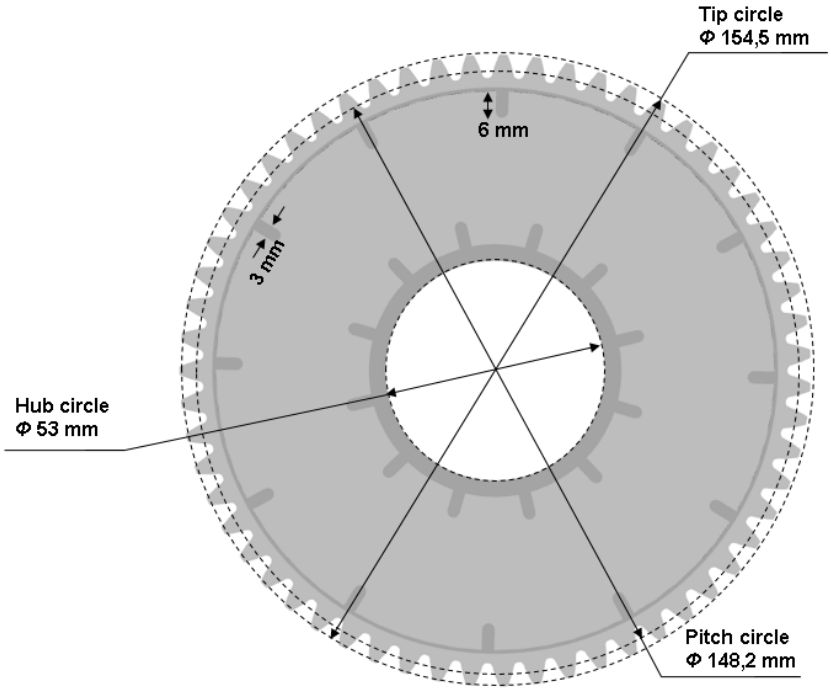

Figure 4. 3 Geometry specifications of the steel part of the gear.

The composite web was manufactured by overlapping pre-impregnated composite plies (pre-preg) manually. These are composed of an epoxy matrix and carbon fibres with the trademarks respectively of MTC400-1 and M46J. Specifically, the MTC400-1 is an epoxy

resin system that allows flexibility in component manufacture. It is characterized by a service temperature up to 200°C after post cure. The M46J carbon fibre, instead, is a high modulus fibre with enhanced tensile strength and modulus. The fibres are combined with the epoxy in a ply with a percentage in weight of 37. Physical and elastic properties of the fibres and of the resin [102], [103] are reported in Table 4. 2.

Property		**Fibre**	**Matrix**
Material type		Carbon M46J	Epoxy
Longitudinal Modulus	[GPa]	436	2.7
Transverse Modulus	[GPa]	12.35	2.7
Shear Modulus	[GPa]	24.78 Long. / 5 Transverse	1
Poisson's ratio	[-]	0.41	0.35
Density	[g/cm^3]	1.84	1.2

Table 4. 2 Physical and elastic properties of fibre and matrix.

A quasi-isotropic layup, $[0/18/36/54/72/90/108/126/144/162]_{4s}$ with thickness of 10.5 mm, was manufactured in such a way that more homogeneous properties are exhibited both in-plane and out-of-plane. The composite panels were cured by autoclave processing. The cure cycle is shown in Figure 4. 4. The pressure was kept constant at 6 bar for the entire cycle, while the cure temperature was set at 135° for 1 hour and a post-cure was executed at 180° for 2 hours. This cycle was chosen to improve compaction of the composite panels. Hence, the fatigue behaviour improves thanks to the low void volume fraction, and a high glass transition temperature (Tg) is achieved, extending the operational temperature up to 200°C and making the gear usable in particularly severe thermal conditions.

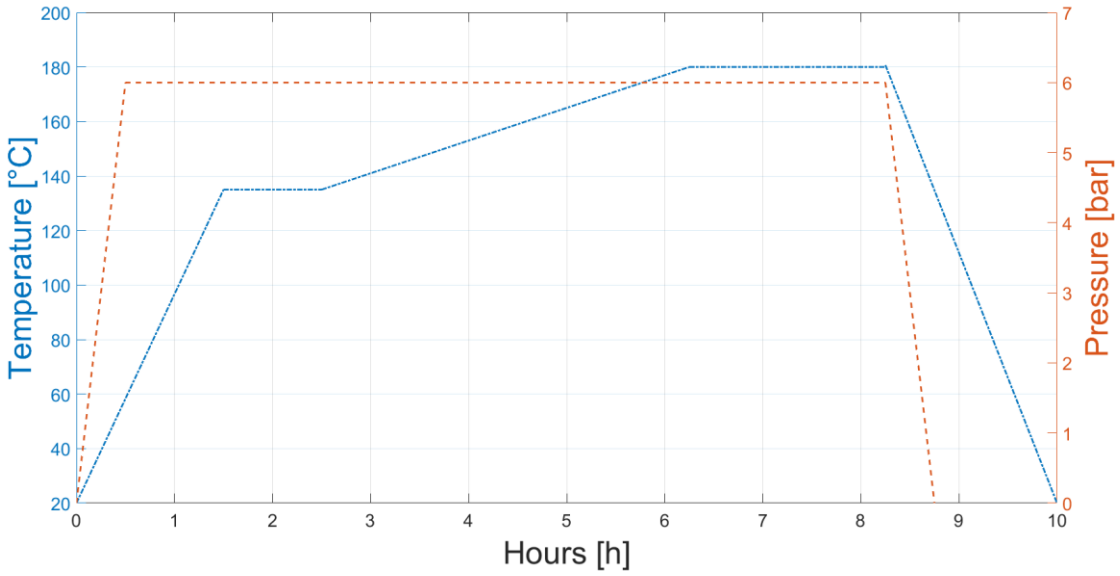

Figure 4. 4 Cure temperature and pressure profiles.

The manufactured composite panels were cut by precision waterjet to satisfy the assembly tolerances and to avoid any possible thermal degradation of the matrix.

4.4 Experimental and numerical modal analysis

In order to avoid dangerous resonance phenomena during working conditions, a critical step in the design of geared transmissions is the assessment of the dynamic stiffness properties. Especially in lightweight gears, the significant out-of-plane flexibility can result in a dynamic amplification of the system response to the bending excitation of the gear body. The knowledge of the modal properties of the individual gears is essential to make sure that the fundamental frequency is not excited by the meshing order of the gear pair. This may occur when the tooth meshing frequency approaches one of the natural frequencies of the engaging gears.

An important aspect of using composite materials is represented by damping. In a vibrating system, the phenomenon of energy dissipation into other forms of energy, e.g. heat, is referred to as damping. Experimental tests and measurements are necessary to estimate composites damping properties to be used as input for simulations aiming at analysing the dynamic behaviour of a specific structure. Various physical parameters can be considered and defined [28] to describe the complexity of the phenomena associated with energy dissipation in a vibrating system. Generally, three primary techniques can be employed to characterise the damping properties of a material [104]. The first is the

logarithmic decrement method, which is based on the transient response of the system. Herein, damping is derived from the rate at which vibration amplitude decreases during exponential decay. The second method is the Dynamic Mechanical Analysis (DMA) technique. When undergoing a cyclic load, most materials exhibit a hysteretic behaviour. The force-displacement, or stress-strain curve, in steady-state conditions takes the form of an ellipse, the area of which represents the energy dissipated by the system [105]. For low levels of damping, the loss factor of a material is calculated as the ratio between the energy dissipated per cycle of vibration and the total deformation energy [105]. The last method is the half power bandwidth method. In general, the damping in a system can be evaluated from the sharpness of the peaks in the FRF at the natural frequencies. In this case, the loss factor of a structure is defined as a function of the resonance quality factor, Q [28].

Thanks to the high damping capacity of composites [106], hybrid structures can result in a better damping capability than usual metallic components.

Section 4.4.1 describes the experimental setup used for the modal analysis, while Section 4.4.2 deals with the modal assessment by a FE techniques. Section 4.4.3 contains the experimental and numerical analysis of the steel part, while in Sections 4.4.4 the numerical prediction of the composite web modal behaviour is described. Here, two different modelling approaches were investigated and compared. The first method used to model the composite body is based on a ply-by-ply representation of the laminated gear body. The second method relies on equivalent homogeneous laminate properties, derived from analytical stress-strain constitutive relations for a generally orthotropic lamina.

4.4.1 Experimental setup

Experimental tests were carried out to characterise the modal behaviour of the hybrid gear prototypes. Specifically, the hardware instrumentation was based on a LMS Scadas system [107], and included the data acquisition system, an instrumented impact hammer (PCB Piezoelectronics, model 086C03) and a miniaturized accelerometer (PCB Piezoelectronics, model 352C22) to reduce the loading effect. The aim of the impact test was the evaluation of the FRF, defined as:

$$H(\omega) = \frac{X(\omega)}{F(\omega)} \tag{33}$$

where *F(ω)* is the input force that excites the system, which in this case is an impulse excitation applied by the instrumented hammer, while *X(ω)* is the output of the system, i.e. the acceleration measured at a point of the gear in the axial direction. Hence, the input signal, which is measured by the load cell in time domain, is converted into a signal in the frequency domain by the acquisition system. All the tests were performed in free-free boundary conditions, achieved by hanging the component using elastic wires. Figure 4. 5 shows the experimental setup.

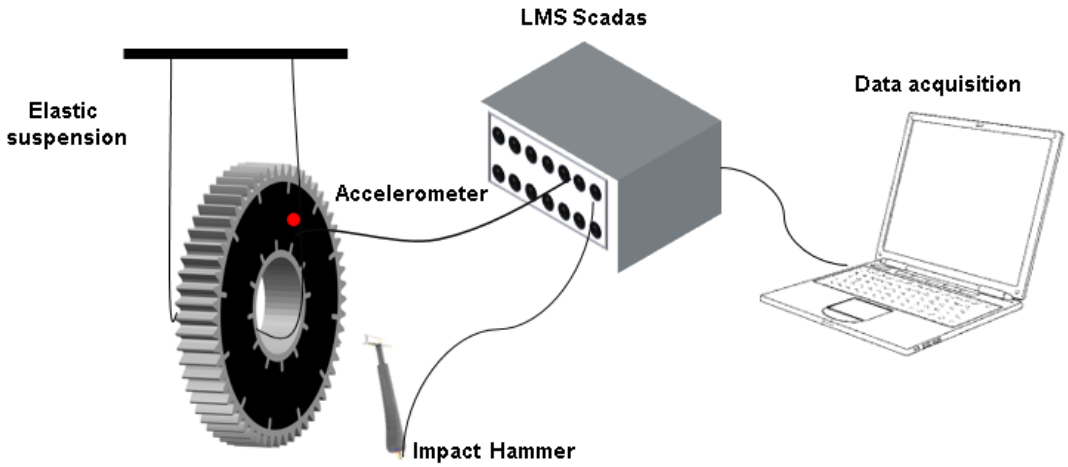

Figure 4. 5 Experimental setup used for modal characterization of the gear and of its individual components.

The FRF expresses the dimensionless acceleration-to-force ratio as a function of the frequency. Each peak allows to identify a natural frequency, to which a modal shape of the component is associated. In addition, from the measured FRF, damping properties can be analysed as well. In fact, when a structure is subjected to an impulse excitation, the peak amplitude measured at each natural frequency is affected by the energy dissipation capacity of the system. From a measured FRF, an estimation of the damping can be obtained by analysing the peak sharpness at any given natural frequency according to the half-power bandwidth method through the following equation:

$$\eta = \frac{\Delta\omega}{\omega_0} = \frac{\omega_2 - \omega_1}{\omega_0} = \frac{1}{Q} \tag{34}$$

where η is the loss factor, defined as the inverse of the Quality Factor of resonance Q, ω_0 is a given natural frequency of the system, $\Delta\omega$ is a frequency interval centred around ω_0 and corresponding to a 3dB drop from the peak value on a decibel scale. Figure 4. 6 shows how the loss factor is extracted from the measured FRF.

Four sets of impact tests were defined for the following systems: 1) the steel rim only, 2) the composite web only, 3) the hybrid gear assembled by interference fitting, and 4) the hybrid gear assembled using the adhesive layer. For each of them, natural frequencies and modal damping values were extracted, as described in the following sections. For all the tests, the measurement bandwidth, which is the frequency range to be analysed, was set in such a way that the first three non-rigid mode shapes could be excited, within an acquisition time of 10 seconds for each measurement. This value is relevant for the analysis of damping properties, since a longer acquisition time allows to capture the vibration decay after the impact more accurately.

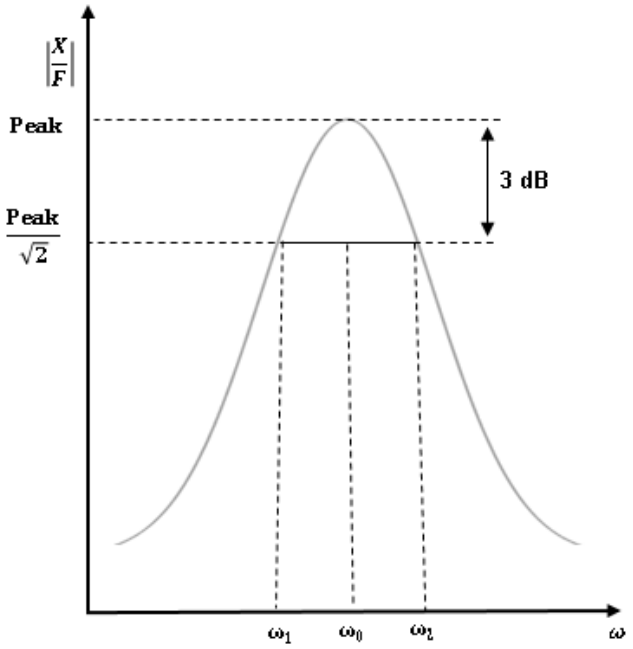

Figure 4. 6 Half-power bandwidth method *[100]*.

4.4.2 FE-based modal assessment

In order to avoid expensive prototypes and to reduce the time required for their experimental characterization, predictive tools for the analysis of the multi-material gears become essential. The FE method is employed to calculate the modal parameters of the system using numerical frequency response analyses. The commercial software Siemens

PLM Software Simcenter 3D [97] as pre-/post-processor and NX Nastran as solver were employed. In particular, modal frequency response analysis was used to compute the FRFs [108]. This method is based on the uncoupling of the equations of motion through the transformation of the system from physical to modal coordinates. The analysis starts from the definition of the equation of motion. If no damping is considered, the dynamic equilibrium equations of a discrete system can be defined as follows [100]:

$$[M]\{\ddot{x}(t)\} + [K_e]\{x(t)\} = Re\{Pe^{i\omega t}\} \tag{35}$$

where M and K_e are the mass and stiffness matrices respectively, and $Re(P)$ is the real part of the vector of the applied harmonic forces. One of the possible solutions of the previous eq. (35) can be expressed as follows:

$$\{x\} = Re\{ue^{\,i\omega t}\} \tag{36}$$

where u is the complex displacement vector. Eq. (37) is used to transform eq. (36) from physical coordinates to modal coordinates, ξ:

$$\{x\} = Re\{[\phi]\{\xi\}e^{\,i\omega t}\} \tag{37}$$

where $[\phi]$ is the modal matrix of the system. By substituting eq. (37) into eq. (35) and premultiplying by $[\phi]^T$, it is possible to express the equation of motion in terms of modal coordinates:

$$-\omega^2[\phi]^T[M][\phi]\{\xi\} + [\phi]^T[K_e][\phi]\{\xi\} = [\phi]^T\{P\} \tag{38}$$

This approach is used because it makes the mass and stiffness matrices diagonal. Hence, the equations of motion can be decoupled and written as a set of single degree-of-freedom systems as:

$$-\omega^2 m_i\xi_i(\omega) + k_i\xi_i(\omega) = p_i(\omega) \tag{39}$$

where m_i, k_i and p_i are the modal mass, stiffness and force for the i^{th} mode, respectively. If $p_i(\omega)$ is zero, the equation becomes a normal mode analysis.

To take the material damping into account, the complex stiffness formulation is used [109]. In this case, the stiffness matrix in eq. (35) takes the form:

$$[K_t] = [K_e + iK_v] \tag{40}$$

where K_v is the imaginary part of the stiffness matrix and represents the viscous contribution of the material. In this work, the damping behaviour is represented as modal structural damping, for which the following uncoupled equations of motion can be derived:

$$-\omega^2 m_i \xi_i(\omega) + (1 + iG_i)k_i \xi_i(\omega) = p_i(\omega) \tag{41}$$

where G_i is the structural damping at the natural frequency of the i^{th} mode and it takes the loss factor values η reported in Table 4. 3, Table 4. 5 and Table 4. 10. Finally, each modal response is computed as follows:

$$\xi_i(\omega) = \frac{p_i\,(\omega)}{-\omega^2 m_i + (1 + iG_i)k_i} \tag{42}$$

4.4.3 Experimental and numerical analysis of the steel part

The experimental tests were performed according to the procedure described in the previous section. In particular, the bandwidth test for the steel part was set to [0-2500] Hz interval and the FRF was evaluated as the average of 10 consecutive measurements. The position of the impact and acquisition points determines the shape of the FRF function. In order to see all the peaks corresponding to the three expected mode shapes, the impact excitation was applied on the gear tooth, while the accelerometer was placed on the opposite side, as shown in Figure 4. 7.

Figure 4. 7 Impact and acquisition points for the steel part.

The acquired data was post-processed and natural frequencies and loss factors were calculated, as reported in Table 4. 3.

Mode	Frequency [Hz]	Modal loss factor
1	1245	$0.09 \cdot 10^{-3}$
2	1610	$0.28 \cdot 10^{-3}$
3	2195	$0.84 \cdot 10^{-3}$

Table 4. 3 Frequency and loss factor values measured by impact testing of the steel part.

To enable reliable numerical modal analyses, an accurate FE model of the toothed region was created. The FE mesh of the steel part was created by using eight-node 3D solid elements. The mesh, shown in Figure 4. 8, is the result of a mesh convergence analysis. The material employed in the manufactured part was characterised properly by a tensile test, which allowed to estimate a value for the Young's modulus, E, of approximatively 220 GPa, and one for the Poisson's ratio, ν, of 0.28. Additionally, a density, ϱ, of 7.86 g/cm^3 was estimated by measuring the weight and volume. The latter was achieved by part immersion in a fluid.

An important aspect of the simulation is the proper definition of the impact and acquisition point. The first one was defined as a single node, corresponding to the location of the impacting hammer in the experimental analysis, as described in Section 4.4.1. A unitary harmonic force was set for the chosen bandwidth [108]. The output acceleration was estimated by averaging the accelerations predicted in a group of five nodes located in the region where the accelerometer was positioned in the experiments. To replicate the tests, the analysis was run in free-free conditions, disregarding the elastic wires since their contribution to the system stiffness can be considered as negligible.

Modal damping was included in the simulation by specifying the value for each natural frequency to obtain the damped FRF. Figure 4. 9 shows the comparison between the experimental and the numerical results for the steel part, while Table 4. 4 reports the percentage difference between the numerical and the experimental natural frequencies.

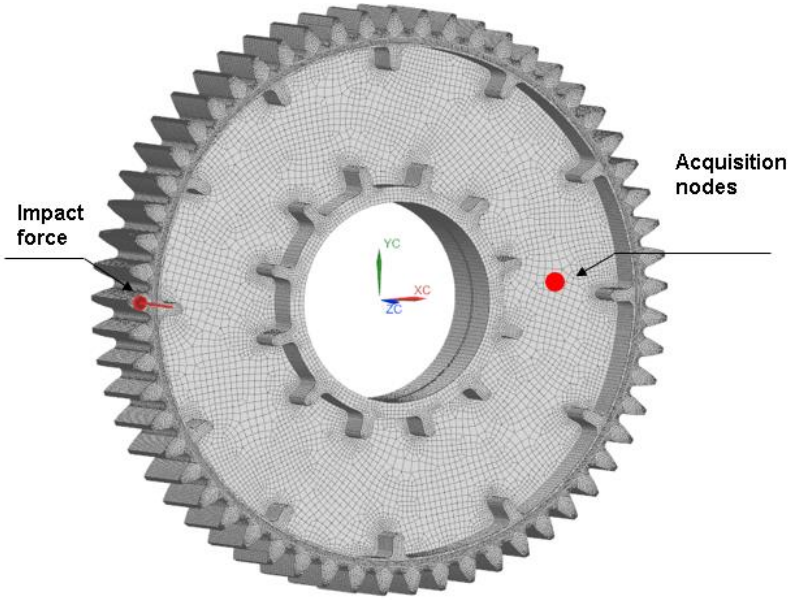

Figure 4. 8 Identification of excitation and acquisition points in the FE environment.

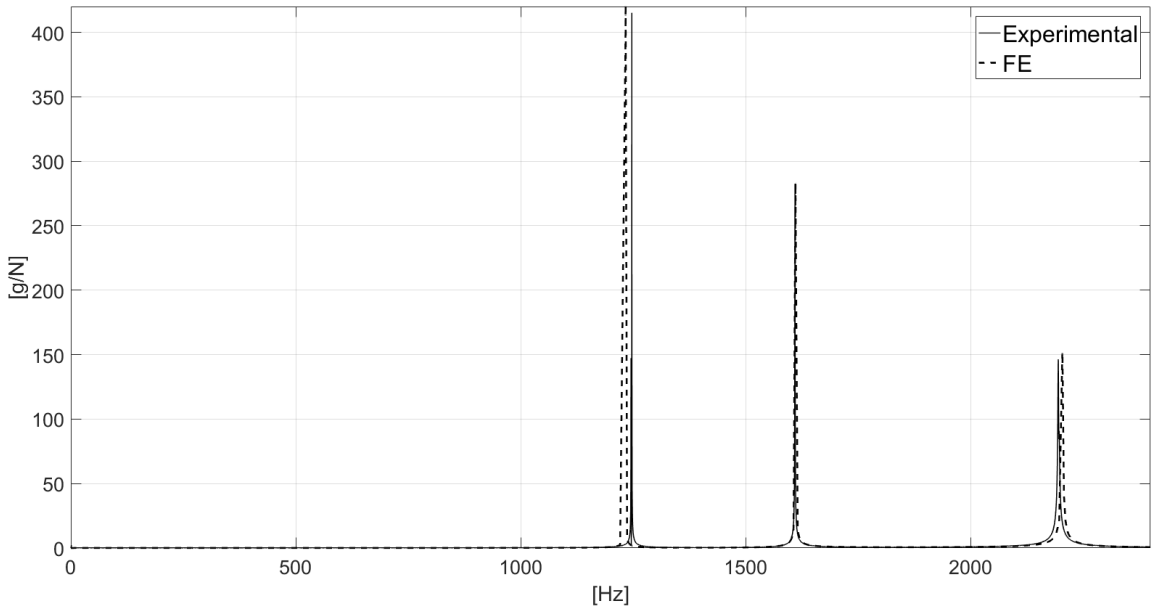

Figure 4. 9 Comparison between experimental and numerical FRFs for the steel part.

Mode	Frequency–Numerical [Hz]	Deviation [%]
1	1233	-0.96
2	1611	0.06
3	2204	+0.41

Table 4. 4 Predicted natural frequencies for the steel part of the gear and deviation from experimental values.

The FRF curves shown in Figure 4. 9 and the modal loss factors reported in Table 4. 3 clearly demonstrate the low damping capacity of steel, from which a very high quality factor of resonance can be appreciated for all the modes excited in the frequency range of interest.

It is noteworthy that the difference between numerical predictions and experimental results is less than 1%, which proves the accuracy of the proposed modelling strategy for the steel part.

4.4.4 Experimental and numerical analysis of the composite web

For the dynamic characterisation of the composite web, the approach illustrated in section 4.4.2 and based on experimental or simulated impact testing was followed. In this case,

the bandwidth was set as [0-6500] Hz in order to detect at least three modes. Figure 4. 10 shows the test configuration for the composite web, while Table 4. 5 reports the estimated values of natural frequencies and modal loss factors.

Mode	Frequency [Hz]	Modal loss factor
1	2436	$1.09 \cdot 10^{-2}$
2	2506	$7.61 \cdot 10^{-3}$
3	5451	$5.91 \cdot 10^{-3}$
4	5976	$1.29 \cdot 10^{-2}$

Table 4. 5 Frequency and loss factor values of the composite part.

Figure 4. 10 Impact and acquisition points for the composite web.

Modelling the composite web requires the characterisation of the plies' orthotropic behaviour. By applying Chamis formula for orthotropic elastic materials [20] and considering a fibre volume fraction of 52.6%, corresponding to the 37% weight fraction of the resin, the local elastic properties of the single lamina were calculated, Table 4. 6.

Elastic properties of the UD lamina	E_1 [GPa]	E_2 [GPa]	E_3 [GPa]	υ_{12} --	υ_{23} --	υ_{13} --	G_{12} [GPa]	G_{13} [GPa]	G_{23} [GPa]
	230.06	6.23	6.23	0.38	0.31	0.38	3.29	3.29	2.38

Table 4. 6 Elastic properties of the UD lamina.

The material was characterised experimentally according to ASTM D 3039 [110] tensile test standard and the analytical values were validated against experimental data. Two UD samples were made, one oriented at 0 degrees and one oriented at 90 degrees.

Then, the specimens were cut by waterjet to avoid any possible thermal degradation of the matrix and tested on an Instron® electromechanical universal testing machine at a constant velocity of 2mm/min until failure was observed. An extensometer was used to measure the deformation of the specimen in the load application direction. Figure 4. 11 shows the equipment used for experimental tests.

Figure 4. 11 Test setup.

The tensile tests were performed to characterise the composite in the longitudinal and transverse direction. The 0 and 90 degrees specimens were tested three times each to evaluate the experiment uncertainties. The extracted data were consistent and were post-processed to obtain the σ-ε curves for both cases. Figure 4. 12 and Figure 4. 13 show a

substantial correlation between the experimental Young's moduli, E_1 and E_2, and the considered analytical formulations (see Table 4. 6).

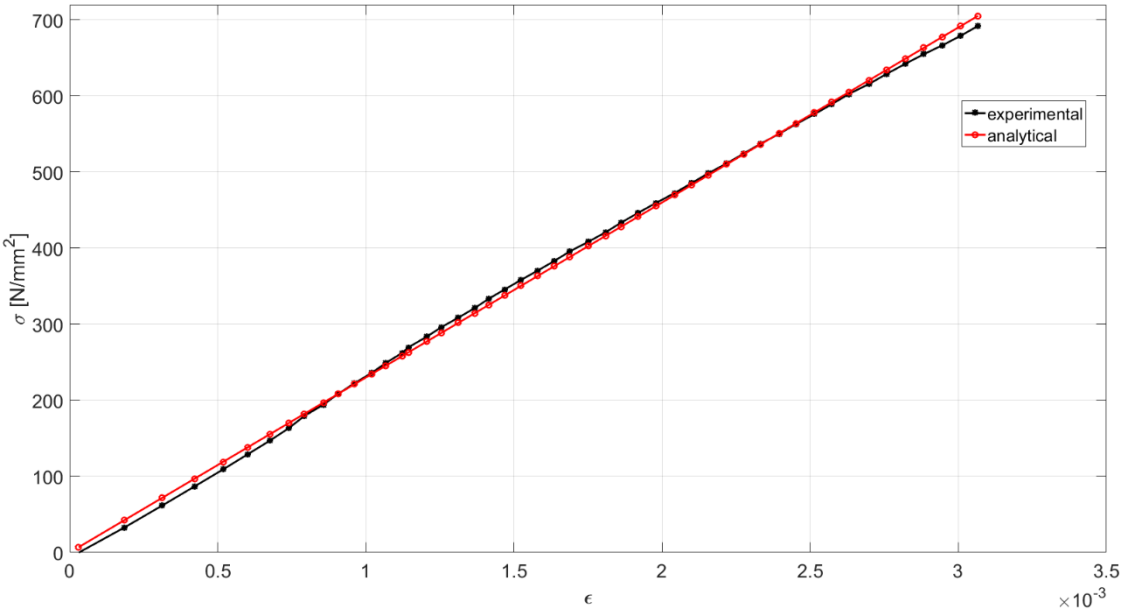

Figure 4. 12 Tensile test of the composite specimen with 0° fibre orientation.

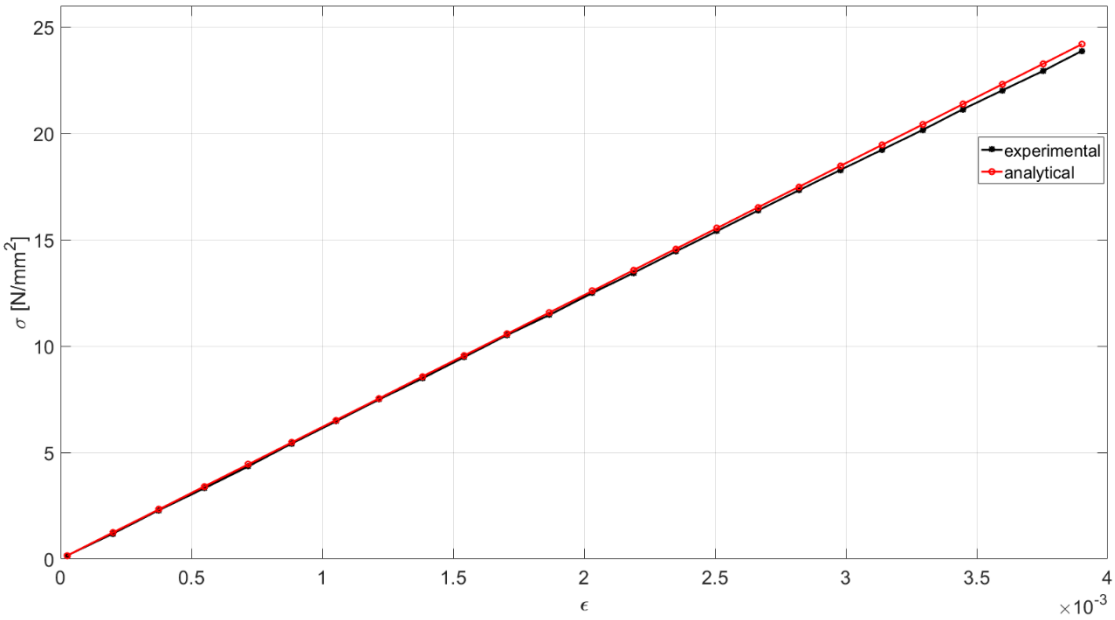

Figure 4. 13 Tensile test of the composite specimen with 90° fibre orientation.

As reported in the datasheet [111], carbon fibres are strongly anisotropic, thus exhibiting different tensile and flexural moduli. As observed in the tests, the flexural behaviour of the composite part dominates, thus requiring an accurate evaluation of the fibre flexural modulus. In the studies herein discussed, the latter was evaluated using an FE model updating process based on the results of an experimental modal analysis in free-free

conditions made on a simple UD beam of 12 plies, with 0° fibres orientation. The beam was long 220 mm, wide 15 mm and thick 4 mm, Figure 4. 14. The impact point was set at one end of the beam, while the accelerometer was placed at the opposite end. A FE model of the beam was created by using PCOMPS properties, a ply-by-ply representation compatible with solid elements [97]. For the lamina properties, it was necessary to set the x ply orientation and the z ply stack direction in accordance to a defined material coordinate system.

Fibre modulus was updated until the percentage difference between experimental and numerical frequency values became less than 1%. The resulting Young's flexural modulus along fibre direction was 185 GPa. The other material properties used in the simulation remained the same of those presented in Table 4. 6.

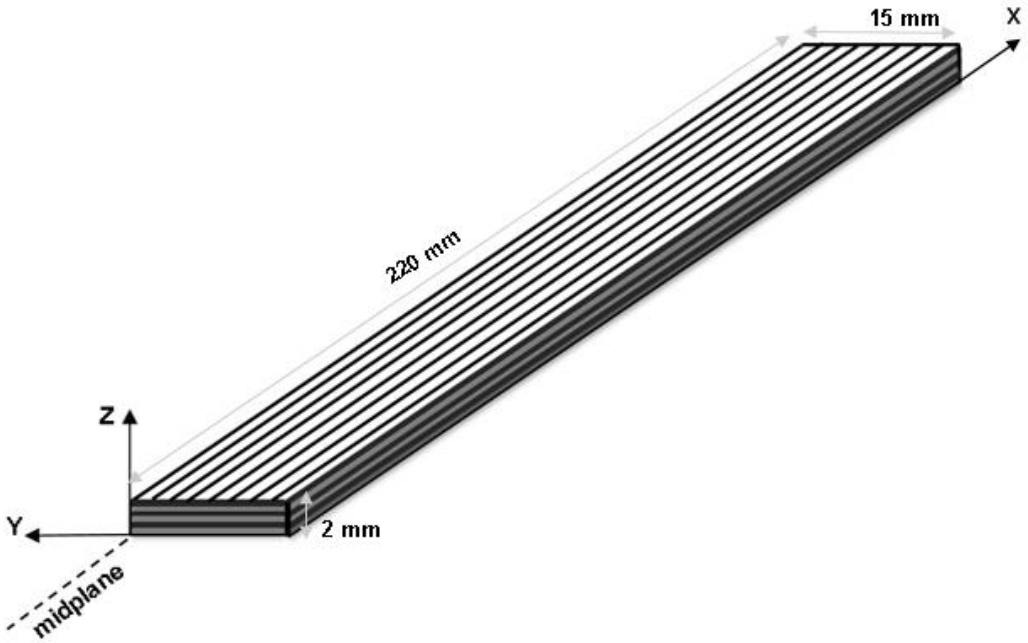

Figure 4. 14 Dimensions of the beam used for the characterization of the composite material.

Using the displayed material properties, a model of the composite web was built. The web was composed of 80 plies. The accuracy of the numerical prediction strongly relies on the property estimations for the composite material. In this case, the modal behaviour of the gear web was analysed by means of two different modelling approaches. The first was based on the virtual representation of the laminae in the composite web, by considering their disposition and orientation, as already described for the modal analysis of the beam sample. The second approach accounted for the equivalent homogeneous laminate

properties, which can be derived either by analytical or FE modelling for the considered composite made of UD plies. In this context, the analytical method, firstly presented in [21], was proven to be accurate with respect the classical laminated body problem.

The stress-strain constitutive relation for a homogeneous material composed by n laminae is based on the definition of the laminate stiffness matrix, the elements of which are given by eqs. 43-45:

$$C_{ij} = \sum_{k=1}^{n} V^k \left[C_{ij}^k - \frac{C_{i3}^k C_{3j}^k}{C_{33}^k} + \frac{C_{i3}^k \sum_{l=1}^{n} \frac{V^l C_{3j}^l}{C_{33}^l}}{C_{33}^k \sum_{l=1}^{n} \frac{V^l}{C_{33}^l}} \right] \quad \text{(i,j=1,2,3,6)} \tag{43}$$

$$C_{ij} = C_{ji} = 0 \quad \text{(i=1,2,3,6; j= 4,5)} \tag{44}$$

$$C_{ij} = \frac{\sum_{k=1}^{n} \frac{V^k}{\Delta_k} C_{ij}^k}{\sum_{k=1}^{n} \sum_{l=1}^{n} \frac{V^k V^l}{\Delta_k \Delta_l} (C_{44}^k C_{55}^l - C_{45}^k C_{54}^l)} \quad \text{(i,j=4,5)} \tag{45}$$

where $\Delta_k = \begin{vmatrix} C_{44}^k & C_{45}^k \\ C_{54}^k & C_{55}^k \end{vmatrix}$, *i,j =1,..,3* are the longitudinal, in-plane, out-of-plane and transverse directions respectively, *i,j=4,5* are the transverse shear directions and *i,j=6* the in-plane shear directions. The stress-strain relation for the homogenized material is given by eq. (1), where σ_i and ε_j are the stress and strain tensors respectively, and C_{ij} are the elements of the stiffness matrix. At this point, effective mechanical constants of the homogenous orthotropic material are given by eqs. 46-54 [22]:

$$E_x = \frac{1}{H_{11}} \tag{46}$$

$$E_y = \frac{1}{H_{22}} \tag{47}$$

$$E_z = \frac{1}{H_{33}} \tag{48}$$

$$G_{xy} = \frac{1}{H_{66}} \tag{49}$$

$$G_{xz} = \frac{1}{H_{55}} \tag{50}$$

$$G_{yz} = \frac{1}{H_{44}} \tag{51}$$

$$\upsilon_{xy} = \frac{-H_{12}}{H_{11}} \tag{52}$$

$$\upsilon_{xz} = \frac{-H_{13}}{H_{11}} \tag{53}$$

$$\upsilon_{yz} = \frac{-H_{23}}{H_{22}} \tag{54}$$

where H_{ij} are the coefficients of the compliance matrix, obtained by inverting the stiffness matrix. Table 4. 7 summarizes the elastic properties of the homogenized material that were used in the FE simulations by considering the flexural fibers modulus.

Homogenized properties	**E_1** [GPa]	**E_2** [GPa]	**E_3** [GPa]	**υ_{12}** --	**υ_{23}** --	**υ_{13}** --	**G_{12}** [GPa]	**G_{13}** [GPa]	**G_{23}** [GPa]
	66.51	66.51	6.8	0.32	0.27	0.27	25.1	2.83	2.83

Table 4. 7 Elastic properties of the homogenized laminate used in the modal analysis.

The impact and acquisition points were chosen to replicate the experimental tests, as shown in Figure 4. 15.

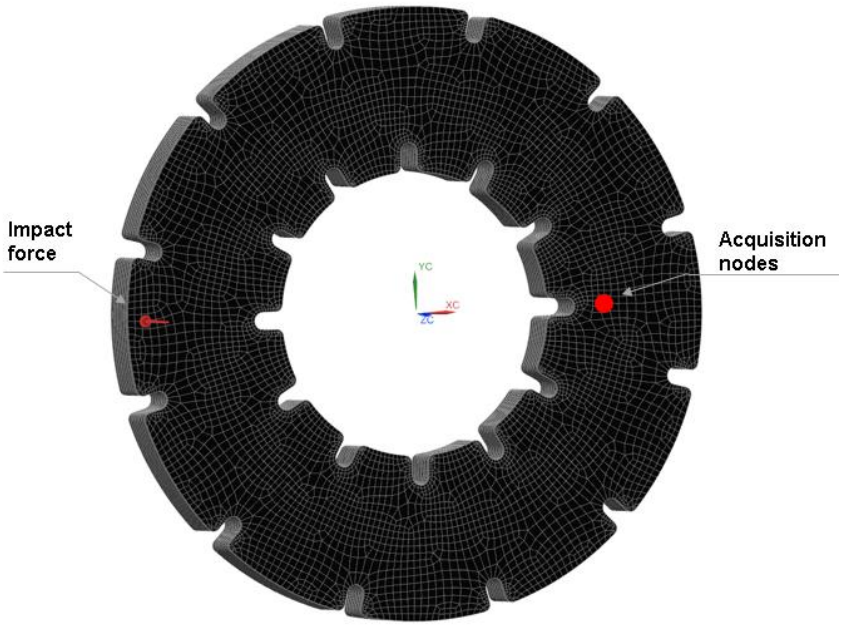

Figure 4. 15 Identification of excitation and acquisition points in FE environment for the gear web.

Figure 4. 16 shows the experimental and numerical FRFs of the composite web, while Table 4. 8 reports the percentage difference between the first four numerical natural frequencies calculated with ply-ply-ply approach and homogenized theory and the experimental evidence.

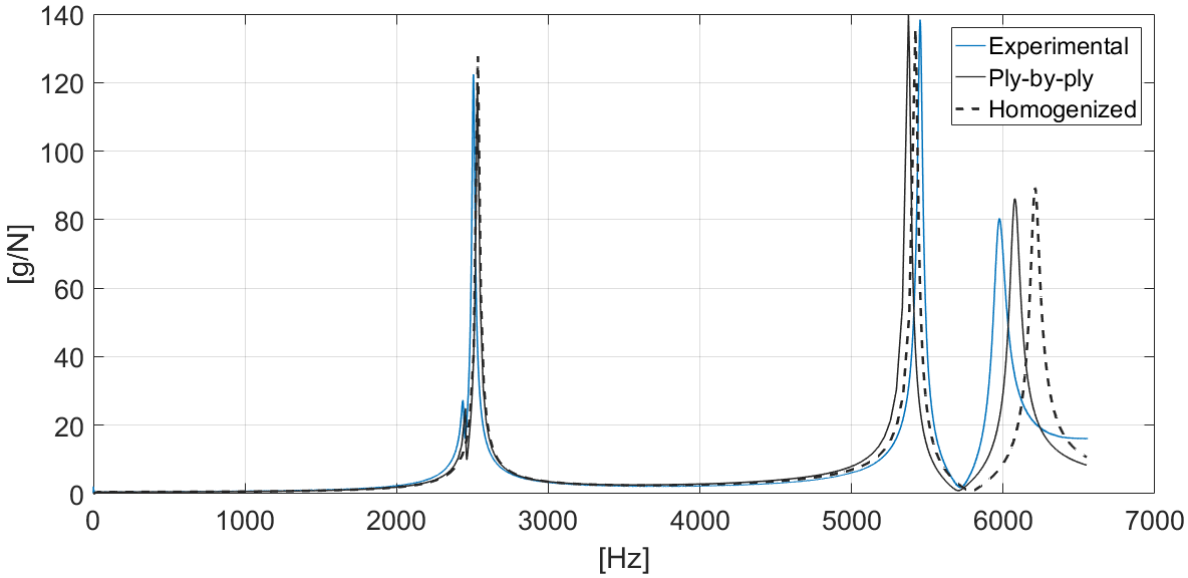

Figure 4. 16 Comparison between experimental and numerical FRFs for the composite part.

Mode	Frequency – Ply-by-ply [Hz]	Deviation [%]	Frequency – Homogenized [Hz]	Deviation [%]
1	2454	+0.7	2530	+1.0
2	2533	+1.0	2533	+1.0
3	5375	-1.3	5400	-0.9
4	6077	+1.7	6077	+3.4

Table 4. 8 Predicted natural frequencies for the gear web and deviation from experimental values.

In Figure 4. 16 two resonant peaks can be observed around 2500 Hz, corresponding to the first two non-rigid and anti-symmetric modes. The experimental results provide a validation of the FE model with both approaches, being the difference between numerical and experimental values less than 4% for all the natural frequencies in the analysed frequency range. As visible from Figure 4. 16, the homogenized theory proves to be as accurate as the ply-by-ply approach with the advantage of an additional reduction of simulation modelling effort and computational time.

4.5 Assembly process and modal characterization of hybrid metal-composite gears

4.5.1 Hybrid metal-composite gear assembled by interference fitting

In the interference fitting process, the composite web is coaxial to the rim and gradually pressed into it, in such a way that pressure-induced deformation of the web at the interface produces inter-locking between steel and composite parts. An Instron electromechanical universal machine was employed under displacement control. Figure 4. 17 shows a schematic view of the joining process, during which a maximum load of 60kN was reached, while a picture of the real assembled gear is shown in Figure 4. 18.

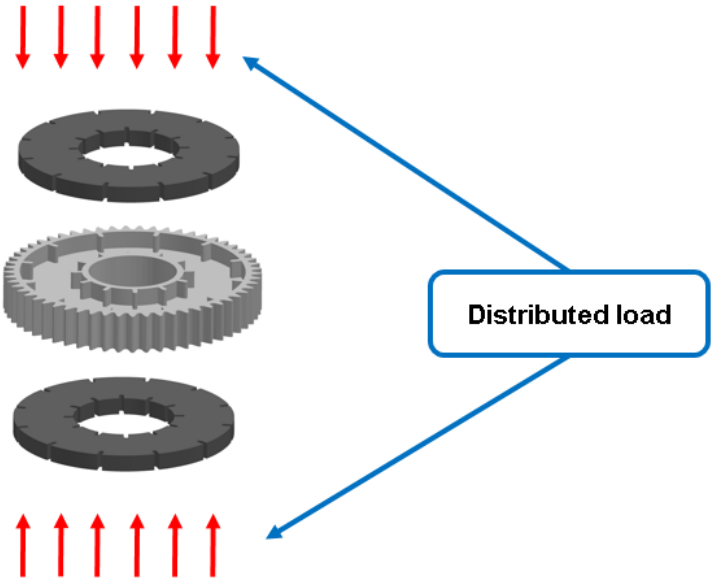

Figure 4. 17 Assembly process based on interference fitting.

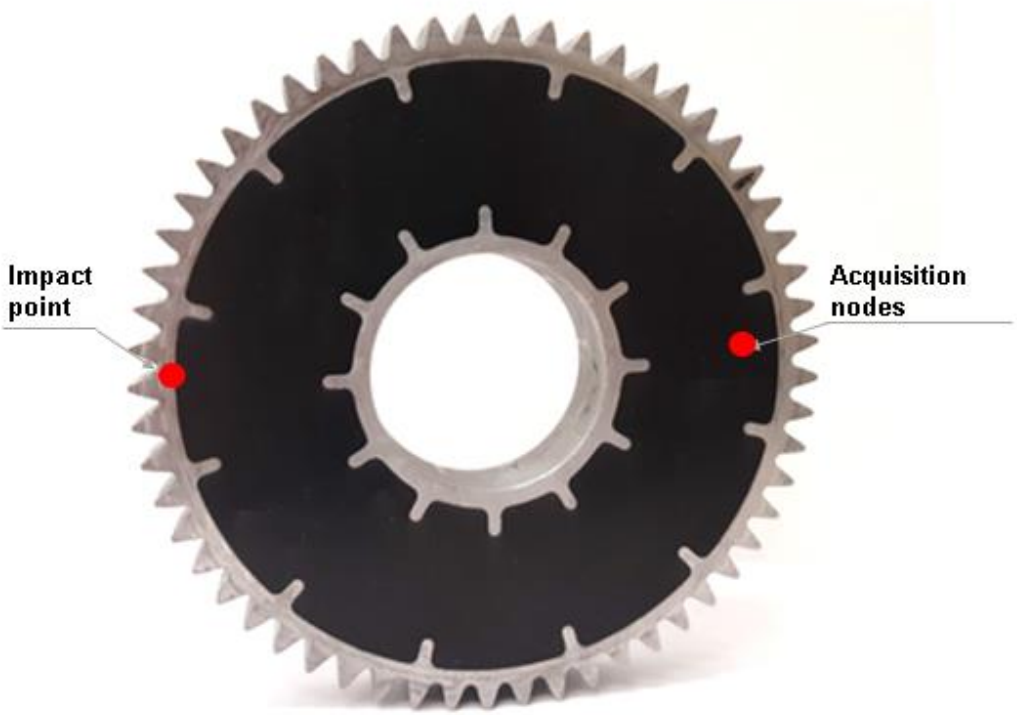

Figure 4. 18 Hybrid gear assembled by interference fitting.

The hybrid gear was tested in the [0-6500] Hz bandwidth. The impact point was set on the tooth surface and the acceleration was evaluated on the gear web, opposite to the excitation point.

On the other hand, in the FE model the behaviour of the metal-composite interface was considered as the one of an ideal joint, by neglecting its contribution to the overall compliance of the gear. Additionally, both homogenized and ply-by-ply formulations were used for the composite gear web.

Figure 4. 19 shows the comparison between experimental and numerical FRFs.

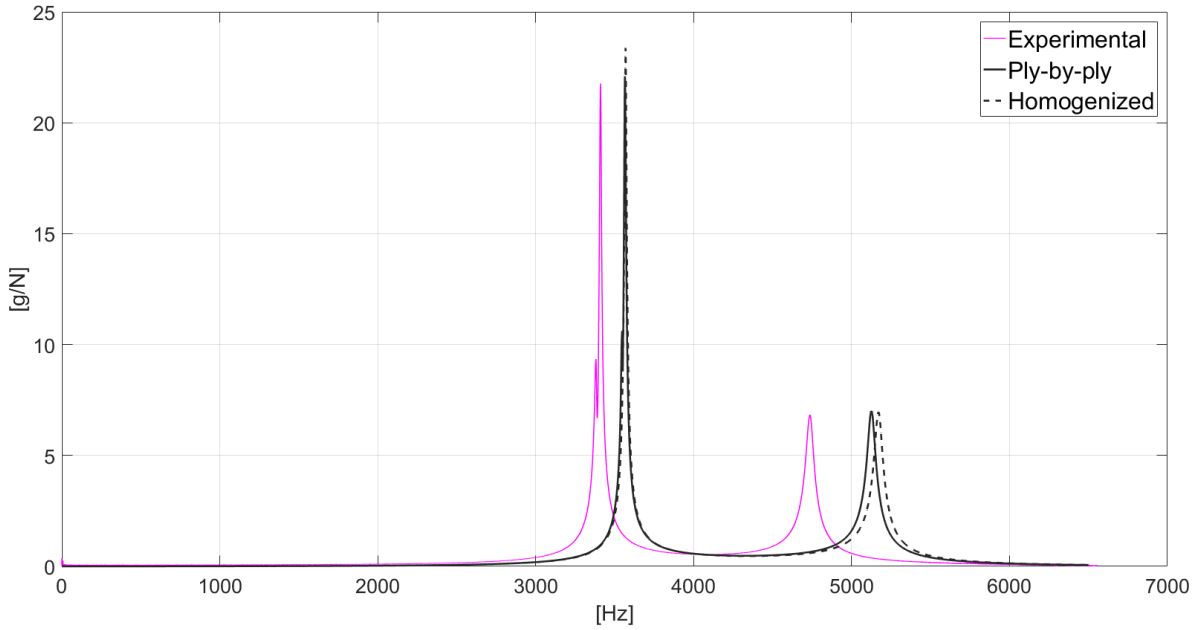

Figure 4. 19 Comparison between experimental and numerical FRFs for the hybrid gear assembled by interference fitting.

As visible from Figure 4. 19 numerical curves represent a more rigid behaviour with respect to the experimental results because the locking region was considered without imperfections. Moreover, the two numerical modelling techniques are close each other, demonstrating their efficacy in describing the gear modal behaviour.

4.5.2 Hybrid metal-composite gear assembled by adhesive bonding

In the adhesive bonding process, the joining between the metal and composite parts was performed by a commercial epoxy adhesive, namely the 3M™ D460 Scotch-Weld™ adhesive. This latter was cured at room temperature for a week. Figure 4. 20 shows an exploded sketch of the joining technique. Here, a picture of the assembled prototype is not reported since no differences with gear of Figure 4. 18 can be visually appreciated.

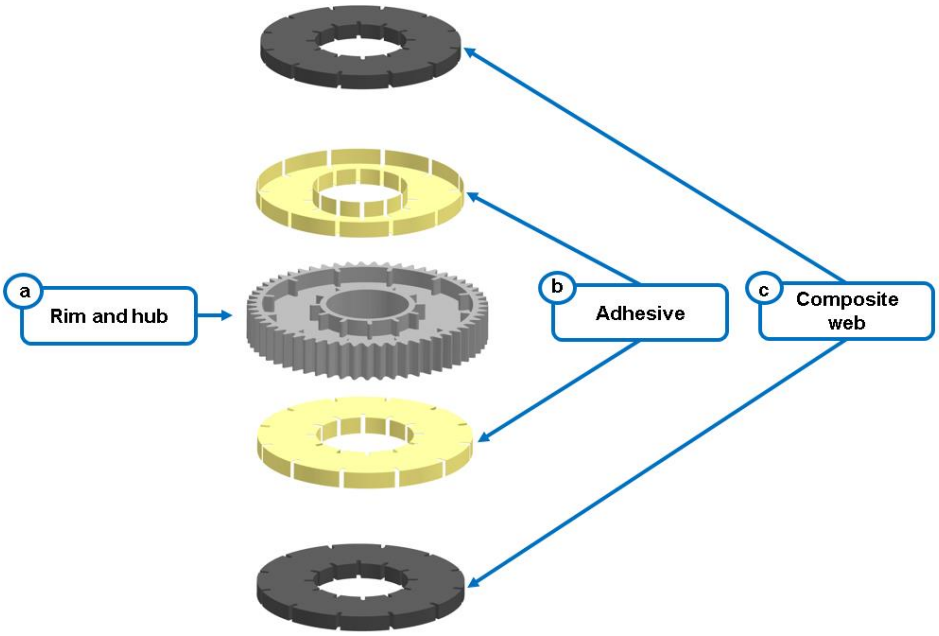

Figure 4. 20 Assembly process based on adhesive bonding

In the FE simulation, a physical layer of solid elements was employed to account for the contribution of the adhesive to the gear compliance. The adhesive was considered isotropic, with a Young's modulus of 2 GPa and a Poisson's ratio of 0.35, as per supplier data-sheet. Figure 4. 21 shows the FE model of the adhesively bonded hybrid gear, while in Figure 4. 22 numerical and experimental FRFs are reported.

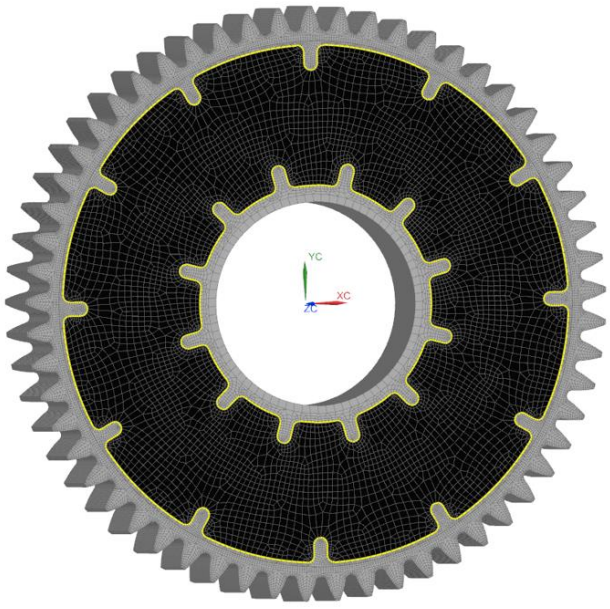

Figure 4. 21 FE model of the hybrid gear assembled by adhesive bonding.

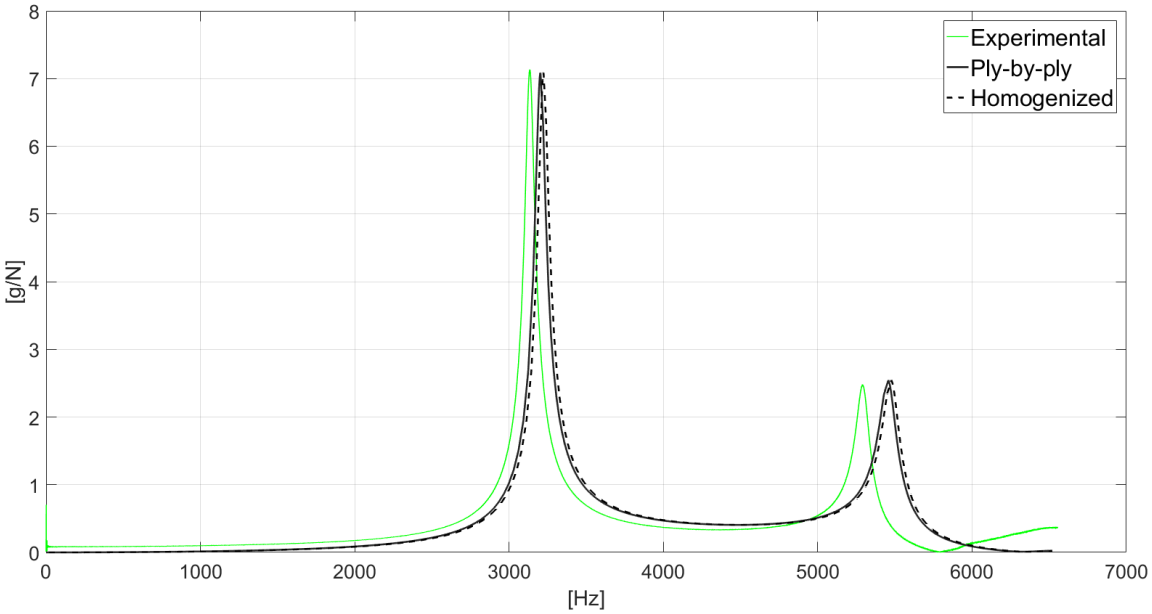

Figure 4. 22 Comparison between experimental and numerical FRFs for the hybrid gear assembled by adhesive bonding.

Here, the numerical results are much closer to the experimental evidence since the metal-composite compliance at the interface was taken into account.

4.5.3 MAC analysis

A criterion that can be used to assess the quality of the FE model with respect to experimental results is the Modal Assurance Criterion (MAC), which is a statistical indicator that provides a measure of consistency between estimates of a modal vector. The MAC is a method used to determine the similarity of two mode shapes: if the latter are identical, the MAC will have a value of one or 100%, while if they are very different the MAC will be close to zero.

The MAC value between two modes is essentially the normalized dot product of the complex modal vector at each common node. It can also be thought of as the square of correlation between two modal vectors φ_r and φ_s:

$$MAC(\{\varphi_r\},\{\varphi_s\}) = \frac{|\{\varphi_r\}^T\{\varphi_s\}|^2}{(\{\varphi_r\}^T\{\varphi_s\})(\{\varphi_s\}^T\{\varphi_r\})} \tag{55}$$

The MAC is bounded between zero and one because the vectors are normalized by the magnitude. Figure 4. 23 shows the numerical and experimental results for the first three

modes with the press-fit technology and homogenized method, which have the same shape in the adhesively bonded hybrid gear, while Figure 4. 24 depicts the MAC matrix.

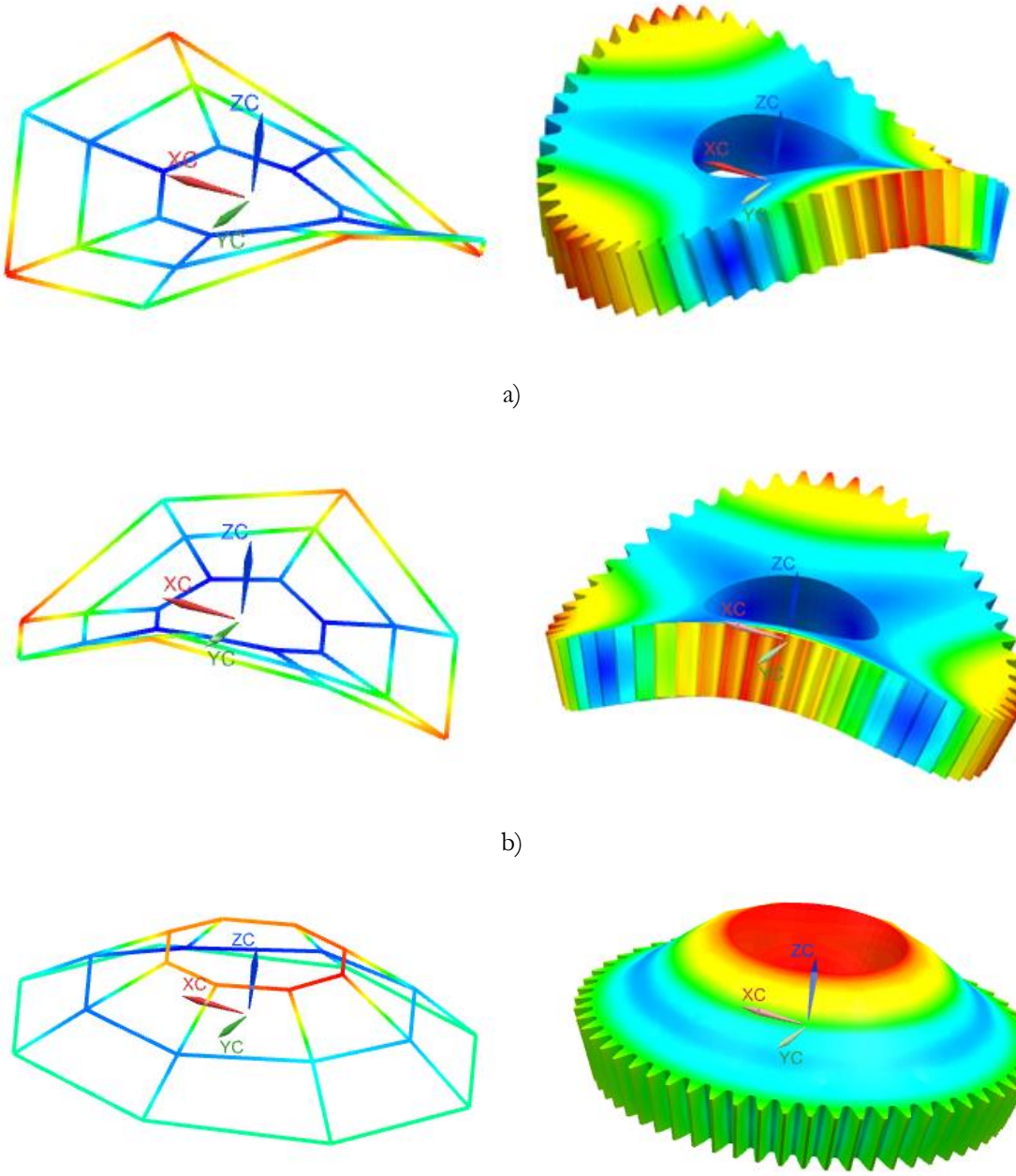

Figure 4. 23 Experimental and numerical comparison of the first a), second b) and third c) mode shape.

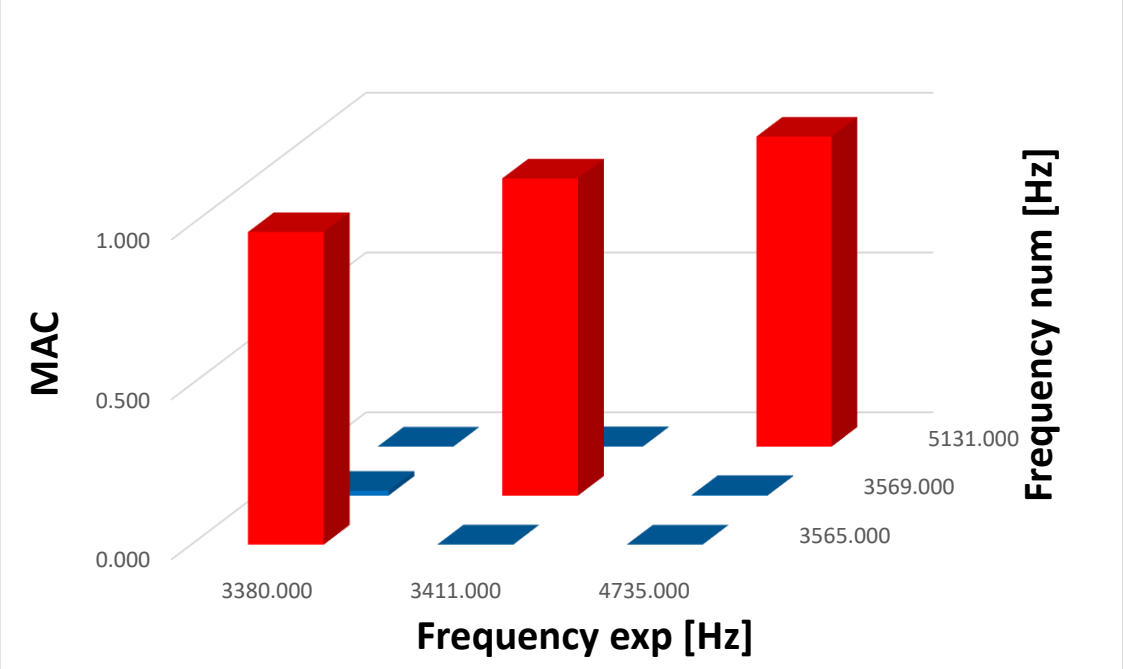

Figure 4. 24 MAC matrix comparing experimental and numerical results.

4.6 Discussion of the results

With the aim of comparing the two proposed hybrid gears against the lightweight steel gear of Figure 4. 2 in terms of dynamic stiffness, the differences between the natural frequencies measured for the former gears and those predicted for the latter one are reported in Table 4. 9. Here the homogenized

Components	Mode	Frequency – Experimental [Hz]	Frequency – Numerical (Ply-by-ply) [Hz]	Deviation [%]	Frequency – Numerical (Homogenized) [Hz]	Deviation [%]
Lightweight steel gear	1	--	1875	--	1875	--
	2	--	1878	--	1878	--
	3	--	3469	--	3469	--
Hybrid gear assembled by interference fitting	1	3380	3547	+4.9	3565	+5.4
	2	3411	3565	+4.5	3569	+4.6
	3	4735	5125	+8.2	5131	+8.3

Hybrid gear assembled by adhesive bonding	1	3138	3187	+1.6	3200	+2.0
	2	3138	3203	+2.1	3210	+2.1
	3	5298	5457	+3.0	5465	+3.1

Table 4. 9 Comparison between the lightweight steel gear and the two hybrid gears in terms of predicted/measured natural frequencies.

Both hybrid gears show increased dynamic stiffness compared to the lightweight steel gear, assumed as baseline, in the frequency range of interest. In particular, the first two natural frequencies, which correspond to a bending mode shape, are about 80% and 67% higher for the hybrid gears assembled by interference fitting and by adhesive bonding respectively. For the third natural frequency, corresponding to an axial mode shape, the difference is about 36.5% and 53% respectively.

The results reported in Table 4. 9 provide also a validation of the proposed modelling approach. The deviation of the predicted frequencies from the experimental ones is higher for the gear assembled by interference fitting gear. This is due to the fact that in the numerical model the metal-composite interface was considered as ideal, with the two parts rigidly connected to each other. In reality, a contribution to the overall compliance of the gear can be expected from the interface, due to local and unpredictably distributed imperfections in the inter-locking region.

A better agreement between simulations and experiments was achieved for the adhesively bonded gear, for which an accurate FE model, inclusive of the adhesive layer, was developed.

From Figure 4. 19 and Figure 4. 22 it is possible to notice how the homogenization and the ply-by-ply formulation match the experimental results with the same accuracy. The difference between the two approaches relies on the modelling effort and computational time, which is lower when considering the equivalent orthotropic properties of composite the web.

Additionally, in the matrix showing the MAC values for the press-fit case, it can be seen that the experimental mode shapes are correctly predicted by the FE model, due to the high values on the diagonal cell (red filled).

In order to have a direct comparison of the two joining techniques, the experimental FRFs are displayed together in the Figure 4. 25 Additionally, Table 4. 10 reports the loss factor values derived from the measured FRFs for each mode.

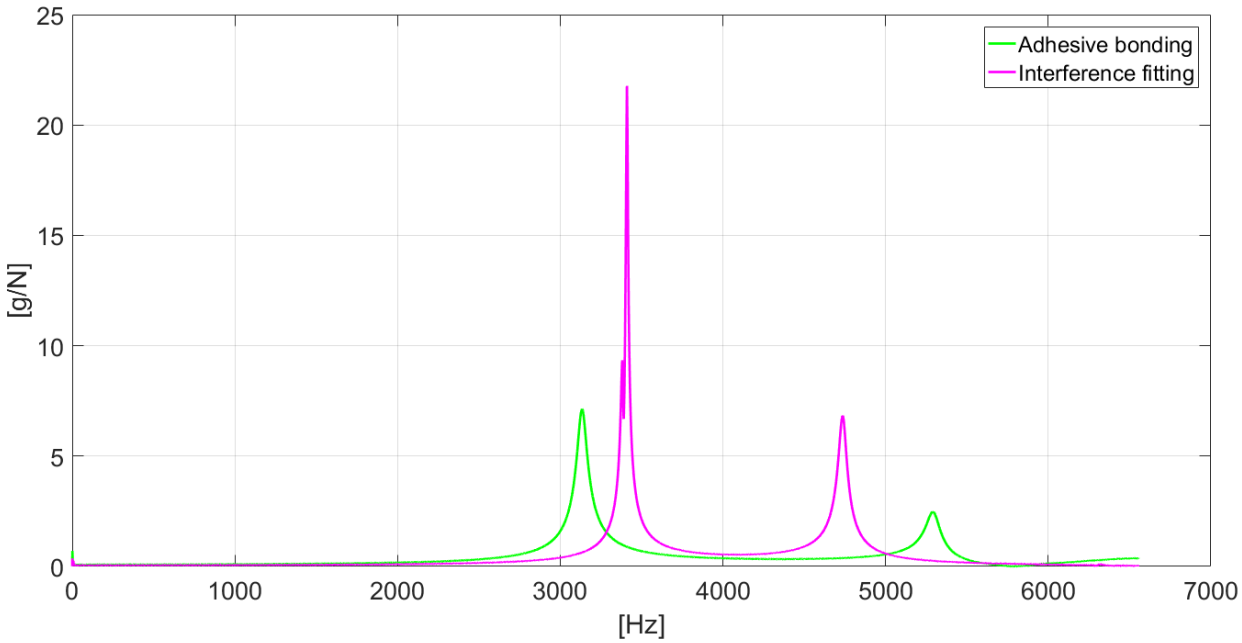

Figure 4. 25 FRFs measured for the hybrid gears assembled by interference fitting (magenta curve) and by adhesive bonding (green curve).

Components	Mode	Modal loss factor
Hybrid gear assembled by adhesive bonding	1	$2.02 \cdot 10^{-2}$
	2	$2.02 \cdot 10^{-2}$
	3	$1.65 \cdot 10^{-2}$
Hybrid gear assembled by interference fitting	1	$3.79 \cdot 10^{-3}$
	2	$3.79 \cdot 10^{-3}$
	3	$1 \cdot 10^{-2}$

Table 4. 10 Loss factor values derived from the measured FRFs.

Figure 4. 25 shows that the gear assembled by interference fitting has higher natural frequencies and lower modal damping factors than the adhesively bonded gear for the first two bending modes. In these latter, as visible from Figure 4. 23 the greatest deformation is at the interface between metal and composite and, hence, the stiffness is higher in the interference fitting technology, since no compliance is introduced.

The opposite situation occurs in correspondence of the axial mode. In fact, the adhesive restraints the out-of-plane movement of the composite web with respect to the metal

layer of the gear body, while the interference fitting does not provide any constraint in that area, allowing the composite web to deform in the axial direction.
In terms of damping, the adhesively bonded gear dissipates more energy. As visible from Figure 4. 25 and Table 4. 10, for the first and second modes, the peak amplitude exhibits a value of 7 g/N compared to 22 g/N of the gear assembled by interference fitting and the loss factor is almost ten times higher. A similar situation takes place in the third mode, although the difference is smaller. The higher effect of dissipation in the adhesively bonded gear is explainable since the viscoelasticity of the adhesive enhances the system's damping capacity significantly.

4.7 Static analysis of hybrid gears pair

In this section, the comparison between hybrid and lightweight gears is extended to the meshing analysis. The proposed approach aims at comparing a spur hybrid gear to the steel lightweight gear of equal mass in order to study the influence of the composite web on the mesh stiffness. In a FE simulation environment, the body of the gear, made of a sequence of CFRP unidirectional (UD) plies arranged in a symmetric layup and resulting in quasi-isotropic properties, is homogenized as described in the previous sections. Static non-linear FE analyses are conducted to evaluate the static transmission error (STE) curve of the hybrid gear pair and to compare it against the one achieved by a pair of steel gears with the thin-rimmed lightweight design and with the same macro-geometry properties. Additionally, a cohesive modelling technique is used to account for the damage at the metal-composite interface.

4.7.1 FE model generation of the metal and composite parts of the hybrid gear

The FE mesh of the rim was similar to the one used for the modal analysis, except for the fact that a sufficiently fine mesh was defined in the tooth regions where contact is expected to occur, so that the non-linear contact phenomena can be accurately captured. Conversely, a noticeably coarser mesh was used for the teeth far from the contact zone and for the steel body, including the hub, with the aim of limiting the computational cost of the simulations. Figure 4. 26 shows the FE mesh generated for the gear teeth and for the steel part of the body.

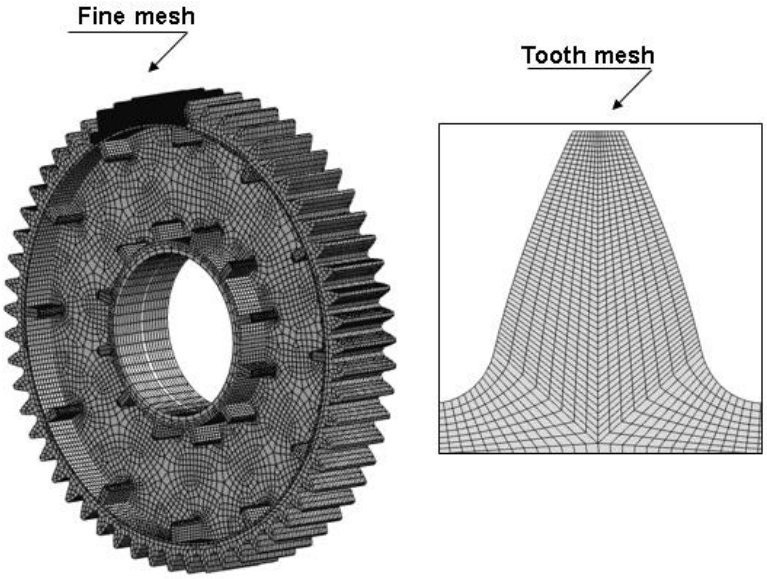

Figure 4. 26 FE model of the steel part of the hybrid gear.

Since the contact area moves cyclically from one tooth to the other during meshing, the quasi-isotropic laminate configuration guarantees a more homogeneous response of the composite web during operating conditions. In order to reduce the size of the problem and the simulation time, the analyses were carried out by considering the homogenization theory used for modal analysis, since it was proven to be as accurate as the ply-by-ply formulation.

The orthotropic elastic properties based on the eq. 46-54 and described in Table 4. 11 were defined.

Homogenized properties	E_1 [GPa]	E_2 [GPa]	E_3 [GPa]	υ_{12} --	υ_{23} --	υ_{13} --	G_{12} [GPa]	G_{13} [GPa]	G_{23} [GPa]
	81.50	81.50	6.8	0.32	0.27	0.27	30.70	2.83	2.83

Table 4. 11 Elastic properties of the homogenized laminate used for STE analysis.

Here, since the meshing load is shared in the plane of action without any out-of-plane forces since the gear is spur, the longitudinal fibre modulus was considered for the homogenized properties of the gear web.

When modelling the adhesive bond, the formulation used plays a major role. Two different approaches can be exploited depending on the main purpose of the analysis: the first one uses a physical layer of solid elements and the second one uses zero-thickness elements with cohesive behaviour [47]. The first approach is used in this work to assess

the impact of the adhesive compliance onto the gear stiffness; the second approach is generally employed to estimate the strength and the damage behaviour of the adhesive bond.

Firstly, cohesive forces at the metal-composite interface were evaluated in order to detect possible damages. The thickness of the adhesive layer was chosen as 0.25 mm both for flat and rounded surfaces and its properties were derived from [47], in which adhesive with brittle behaviour was used to build a lap joint made of metal and composite adherents. Table 4. 12 shows the adhesive properties.

Property	**XNR6823**
Young's Modulus E [MPa]	2600
Tensile failure strength σ [MPa]	57
Shear modulus G_{12} [MPa]	1000
Shear failure strength τ [MPa]	32.9
Toughness in tension G_{IC} [N/mm]	1.18
Toughness in shear G_{IIC} [N/mm]	1.5

Table 4. 12 Adhesive properties.

It is well known that for a general interface three difference fracture modes, in normal and shear directions, can occur when external tractions are applied. In particular, in the case of cylindrical gears with involute tooth profiles, the contact force is transmitted along the line of action, which is tangent to base circles of the two gears and responsible for a coupled in-plane shear and traction-compression stress field. Figure 4. 27 shows the load transfer in case of one tooth pair in contact. The cohesive theory implemented in Simcenter 3D [97], which is based on the work presented in [112], is used for the damage analysis of the adhesive layer under the described loading conditions.

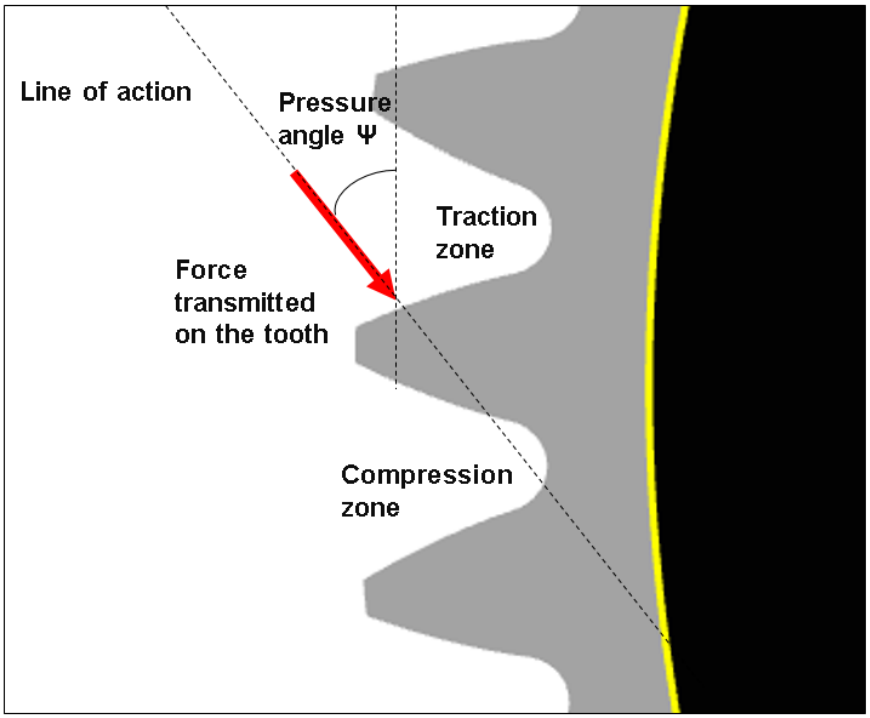

Figure 4. 27 Tooth loading condition for damage analysis: adhesive layer in yellow and composite web in black.

The potential associated to the interface model, based on the damage theory described in [113] can be written as:

$$W = \frac{1}{2}\left[k_I^0\langle\varepsilon_{33}\rangle^2_- + k_I^0(1-d_I)\langle\varepsilon_{33}\rangle^2_+ + k_{II}^0(1-d_{II})\gamma_{31}^2 + k_{III}^0(1-d_{III})\gamma_{32}^2\right] \quad (56)$$

where ε_{33}, γ_{31} and γ_{32} are the strains and d_I, d_{II}, d_{III} damage variables corresponding to modes *I, II, III* respectively; while k_I^0, k_{II}^0, k_{II}^0 are the undamaged stiffnesses of the material. It is possible to express thermodynamic forces as the derivative of Eq. 56 with respect to the three damage variables. Specifically, for a mixed mode loading, which applies in the considered case, an equivalent thermodynamic force has the following form [112]:

$$Y = \sup_{\tau \le t} G_{IC}\left\{\left(\frac{Y_I}{G_{IC}}\right)^{\alpha} + \left(\frac{Y_{II}}{G_{IIC}}\right)^{\alpha} + \left(\frac{Y_{III}}{G_{IIIC}}\right)^{\alpha}\right\}^{1/\alpha} \quad (57)$$

where *a* is a coupling coefficient among the peeling, shearing and tearing modes, considered equal to 1 in this study and G_{IC}, G_{IIC} and G_{IIIC} are the fracture toughness for the same three modes, assuming here that $G_{IIC} = G_{IIIC}$. The damage variables d_i, considered

equal to a single damage variable d, are related to the thermodynamic force through a cohesive law. This latter was chosen as to have a triangular shape between stress and the variation of the displacement. Figure 4. 28 shows the triangular law considered in the study for the case of mode I.

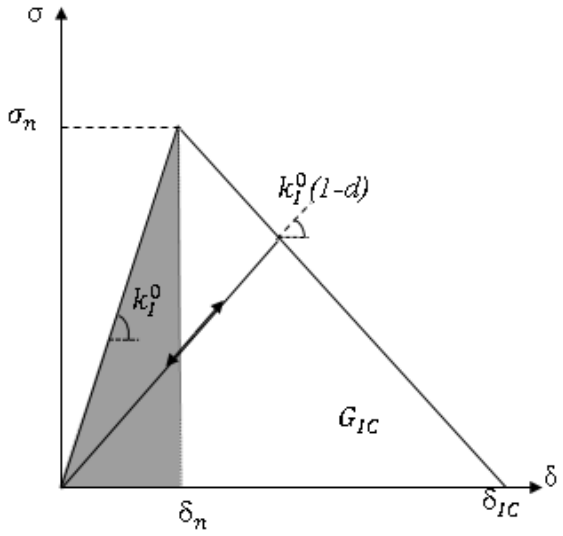

Figure 4. 28 Cohesive law for mode I *[112]*.

As visible from Figure 4. 28, the first part of the graph, represented with the grey area, is the region where no damage is detected and it corresponds to a linear increase of the stress until a maximum allowed traction value σ_n, which corresponds to the cohesive displacement δ_n, is reached. A suitable approximation of the stiffness behaviour for thin adhesive layers is E/t_a and G/t_a, that is the ratio of the Young's and shear moduli E and G, respectively, of Table 4. 12 with respect to the considered thickness t_a. If the displacement grows until δ_n, damage takes place and the stiffness reduces until the resistance of the interface becomes zero when $Gi = Gic$ for pure modes or a combination of effects through eq. 57 is reached. Although complete damage often requires much higher cohesive displacements than δ_n, in this case the design should be done in the safe grey area, due to the cyclic loading conditions in gears. Non-linear solution 401 of Simcenter Nastran [114] was used to account for cohesive behaviour of interface. Figure 4. 29 shows the magnitude of cohesive tractions for the driven hybrid gear subjected to the torque of 350 Nm, which is assumed as the heaviest load case in [101]. The two images refer to different positions along the meshing cycle, where one tooth pair and two teeth pairs are in contact, respectively.

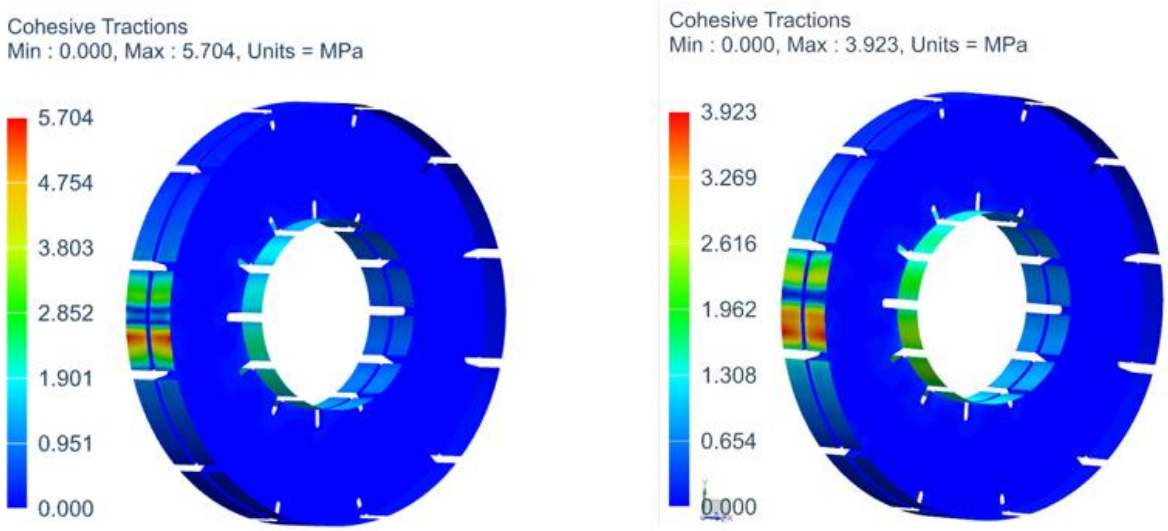

Figure 4. 29 Magnitude of the cohesive tractions for one tooth pair (a) and two teeth pairs (b) in contact.

The numerical results of Figure 4. 29 show that the maximum value of the cohesive traction is 5.7 MPa for one tooth pair in contact and 3.9 MPa in case of two teeth pairs, which are both much lower than the tensile and shear failure strength, assumed to be equal to the maximum tensile and shear cohesive strengths [47]. In fact, the results of the simulations show no damage under this loading conditions.

Once verified that the adhesive was undamaged, the bonding interface was substituted by physical layer of solid elements in order to consider its compliance in STE analyses. This approach was used for two main reasons: firstly, the application of cohesive modelling is computationally expensive because of its non-linear behaviour, which needs to be taken into account during simulations. Secondly, numerical problems, like a non-converging solution, may arise due to the impossibility in describing the adhesive behaviour under compression loads.

4.7.2 Static transmission error evaluation

When studying and designing mechanical transmissions NVH need to be considered. NVH performance of transmissions is significantly affected by internal sources of excitations, which lead to a tonal noise known as gear whine. It is a stationary noise occurring in meshing gears as a consequence of the time-varying nature of the mesh stiffness, which generates small harmonic oscillations of the transmitted torque with the same frequencies as the gear mesh frequency and its multiples [115]. From this point of view, understanding the dynamic excitations is essential to avoid undesired responses of

the system, where vibrations are transmitted from gears to shafts, bearing and gear housing, becoming dangerous for the other transmission components. The transmission error, which is the deviation of the real transmission from the ideal kinematic one, is generally considered as the main source of gear whine [115], [116]. Theoretically, this quantity would be zero if gears were rigid, teeth had perfect involute profiles and were perfectly aligned.

In real applications, these conditions are never achieved, because gears show a certain degree of compliance, the tooth profile is not a perfect involute due to manufacturing errors and misalignments between rotating shafts are frequent, especially under high operational loads. In order to reduce the TE, flank micro-modifications, such as profile relief and crowning, are very often applied to achieve a smoother load transfer between the meshing teeth [116].

In the present work, the transmission error is evaluated in static conditions, which means that no dynamic effect is taken into account in the simulations. Nevertheless, it is possible to correlate the STE peak-to-peak value to the dynamic TE. It is generally accepted to define the STE as a linear displacement of the tooth contact point along the line of action. The above-mentioned definition of the STE is often translated into formula by eq. 58 [117]:

$$STE = r_1\theta_1 - r_2\theta_2 \tag{58}$$

where r_1, r_2 and θ_1, θ_2 are the base radii and the estimated rotations of the driving and of the driven gears under a static loading torque, respectively. From the simulation point of view, it is important to capture the high deformation gradients that occur close to the contact area in the tooth. For this reason, a non-linear contact analysis was exploited by using solution 401 of NX Nastran solver [114]. Here, the supporting shafts are represented as infinitely rigid trough a central master node rigidly connected to the gear inner nodes. A torque of 350 Nm was applied to the unconstrained rotational degree of freedom (DOF) of the driving gear while the rotational DOF of the driven one was constrained. A moving reference system was used for both gears to rotate all their nodes by an angle α equal to: $\alpha=(360/z)/m$, where z is the number of teeth and m is the number of the discrete rotational positions, set equal to 30, as to span the entire meshing cycle with a sufficiently high number of estimated points. Figure 4. 30 displays the stress pattern in the contact region estimated for the hybrid gear pair in a given position along the meshing cycle.

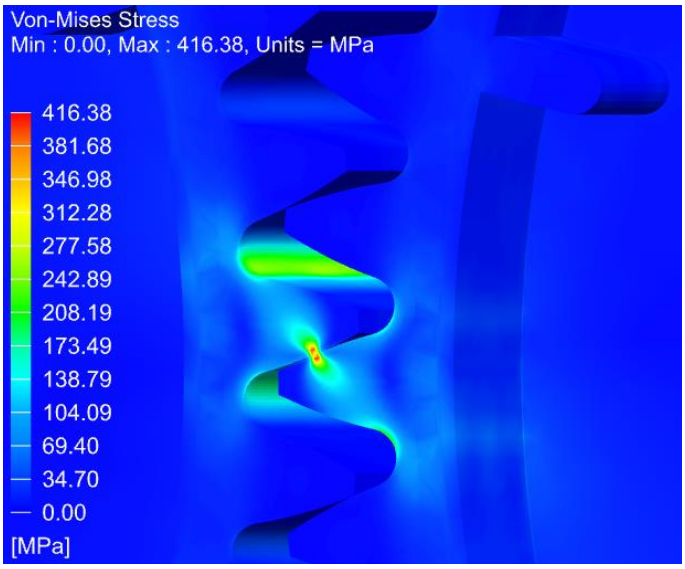

Figure 4. 30 Von Mises stress for the metal part.

In order to evaluate the STE, the results of the non-linear static simulations were post-processed and the rotation of the master node of the driving gear was used in eq. 58, where the rotation of the other gear was set to zero. Figure 4. 31 shows the STE curves estimated for the steel gear and for the hybrid gear models with homogenized composite material formulation. The curve in magenta refers to an ideal interface with press-fit technology, in which the metal-composite parts are rigidly connected to each other, while the curve in green considers an adhesively bonded model, which takes the compliance of the adhesive layer into account.

From the STE curves, the time-varying mesh stiffness of the gear pair is derived through the following equation:

$$k=\frac{T}{r_1^2\theta_1} \tag{59}$$

where T is the applied torque. Figure 4. 32 shows the mesh stiffness curve estimated for the steel gear pair, along with those calculated for all the hybrid gear pair models.

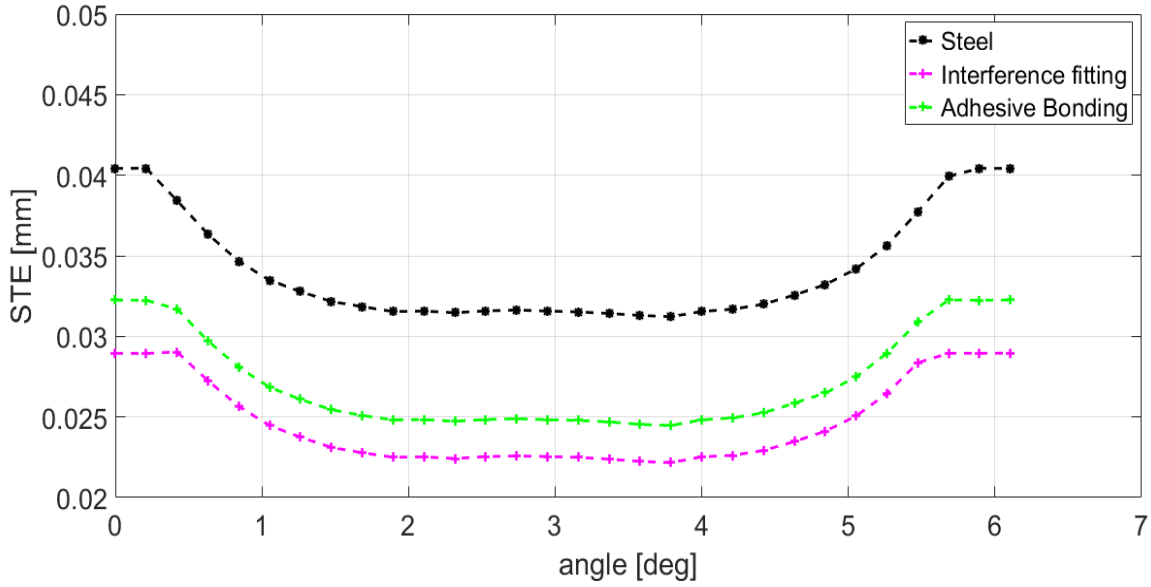

Figure 4. 31 STE of steel and hybrid gear pairs with ideal and adhesively bonded interface.

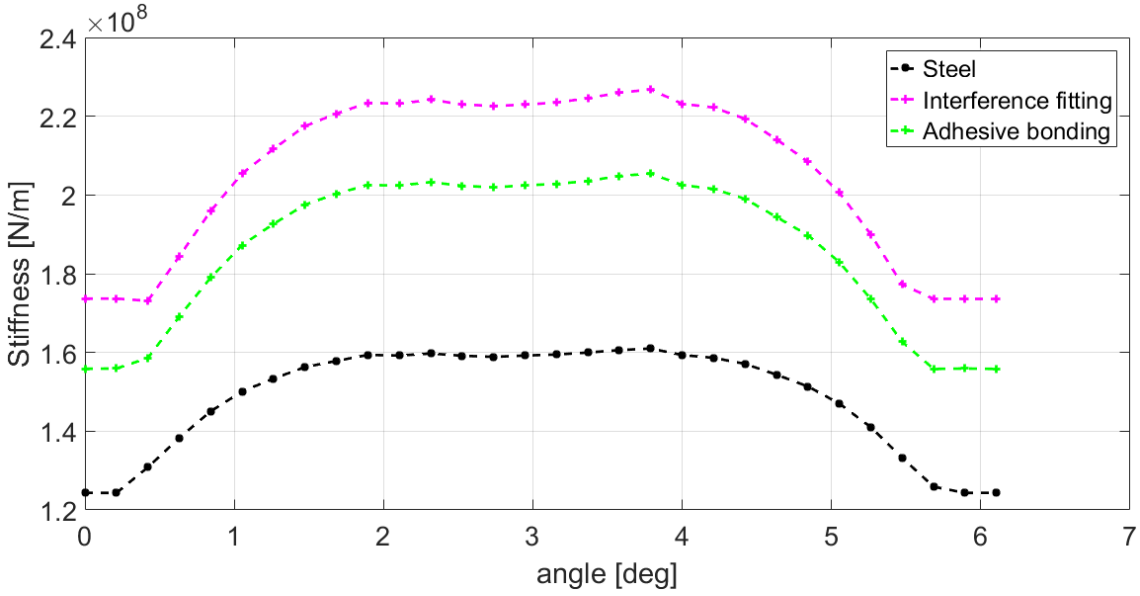

Figure 4. 32 Mesh stiffness of steel and hybrid gears with ideal and adhesively bonded interface.

Table 4. 13 summarizes the numerical results, showing that a significant enhancement in terms of both mean and peak-to-peak values of the STE can be reached in the hybrid gear pair as compared to the steel one, especially by considering interference fitting connection, which will result in an expected NVH improvement.

STE	Mean Value[mm] and percentage difference w.r.t. steel gear	Peak-to-peak value [μm] and percentage difference w.r.t. steel gear
Steel	35.8 -	9.2 -
Homogenized composite model without interface compliance	25.6 (-28.5)	6.9 (-25)
Homogenized composite model with adhesive bonding	28.4 (-20.7)	7.8 (-15.2)

Table 4. 13 Mean values and peak-to-peak comparison between steel and hybrid gear pairs.

4.8 Conclusions

In the study presented in this chapter, a comparative analysis of two different joining technologies for hybrid-metal composite gears was presented, followed by a FE analysis of gears pair during meshing. Firstly, the hybrid gear geometry was designed and, subsequently, the manufacturing procedure that led to a physical prototype was described. Two different joining techniques to connect the steel and the CFRP parts were shown. Specifically, in one case, an interference fitting solution was employed with the composite laminates inserted into the metal part of the gear using an electromechanical universal machine, which operated under displacement control. In a second case, instead, an adhesive layer was used at the metal-composite interface. Experimental impact analyses were performed to capture the differences between the two joining technologies, in terms of natural frequencies and modal loss factors, followed by a comparison based on numerical investigations. Two different formulations were used to estimate the material properties of the web: the first was based on a ply-by-ply representation while the second on material homogenization obtained through analytical formulations. Results show how the application of a composite laminate in hybrid metal-composite gear improves the modal behaviour with respect to a steel lightweight gear with the same mass. In particular,

it was shown that the press-fit technology allows to achieve a higher stiffness, while the adhesive bonding is characterized by an increased energy dissipation capacity.

As a general consideration, the study shows how both techniques are applicable in the assembly process of metal-composite parts in hybrid gears and the choice can be partly driven by the desired requirements in terms of stiffness and damping.

The meshing behaviour of the gears was evaluated in FE environment. Non-linear simulation with cohesive model was performed to verify that the adhesive strength withstood the hardest loading conditions at the interface between the metal rim and the composite body.

STE and mesh stiffness curves were evaluated for the hybrid gear pair models and compared to those estimated for the lightweight steel gear. Results demonstrated a significant reduction of the STE peak-to-peak value, which is expected to result in improved NVH performance of the hybrid gear pair.

The next chapter will be dedicated to the experimental tests of a hybrid gear pair against lightweight steel gear to show differences in terms of static and dynamic transmission error, transmitted accelerations and radiated noise.

Chapter 5

Experimental investigation on the meshing behaviour of a hybrid gear

The current chapter presents an experimental investigation of the static and dynamic meshing behaviour of a hybrid gear engaging with a metal gear and a comparison with a metal thin-rim one. In particular, the investigation is carried out on two different levels: as stand-alone components and in meshing conditions in a real test-rig. Section 5.1 describes the macro-geometry of the designed gears, which consist of a baseline steel solid gear, a steel thin-rim one and a metal-composite with the same mass of the latter, as described in Chapter 4. In Section 5.2, impact tests are carried out to compare the modal properties of the gears in terms of natural frequencies and modal damping, while Section 5.3 deals with the experimental investigation of static and dynamic transmission error, which is considered the main source of excitation, of two different gear pairs: solid-thin-rim and solid-hybrid. From the static point of view, a comparison of the meshing orders with different torques, ranging from 50 to 250 Nm, is shown for the two conditions and the main differences are highlighted. Dynamically, transmission error and accelerations are examined as main indicators of the overall system vibrations level during run-up/down events. In this case, the comparison mainly deals with the different capability to damp excitations at the different meshing orders. Finally, Section 5.4 contains the conclusions.

5.1 Macro-geometry

The gears macro-geometry used for the experimental campaign is similar to the one described in Chapter 4, Table 5. 1. The small differences come from the slight different normal module, 2.5 mm against 2.6 mm of the previously analysed gears, which enabled a reduction of costs during the manufacturing process since it is a standard value. All the consequent gear parameters result from the design requirements according to those of the test-rig, which will be described in Section 5.3.

Parameter	Value
Teeth number	59
Normal module	2.5 mm
Normal pressure angle	20 deg
Face width	24 mm
Tip diameter	154 mm
Root diameter	142.75 mm
Theoretical pitch diameter	147.50 mm
Base diameter	138.60 mm
Addendum	1*module
Dedendum	1.25*module
Tooth thickness (reference circle)	4.47 mm
Hob tip radius	1 mm

Table 5. 1 Macro-geometry of the test gears.

For the experimental campaign, based on the evaluation of the transmission error, the values of which are of the order of microns, it is necessary to have an optimum surface finishing, which requires a high-precision grinding process. This latter was determined as ISO 1328 Quality 5 standard.

Three different gears were used for the experimental investigation: the first is the solid steel one, referred to as the baseline; the second is the steel thin-rim, obtained by removing material in the body region; the third one is the hybrid, built with the same interference press-fit manufacturing process as described in Chapter 4. Here, the composite part was press-fitted into the steel gear and a thin layer of adhesive was inserted between the two materials to enable a further damping capacity. Figure 5. 1 shows the manufactured gears used for the experimental campaign.

Figure 5. 1 Three manufactured gears models.

5.2 Experimental modal analysis of gears as stand-alone components

In order to understand how the modal properties of the gears can influence the dynamic behaviour of the transmission, an experimental modal analysis was carried out, by following the same procedure described in Chapter 4. Figure 5. 2 shows the obtained FRF in a bandwidth of [0 8000] Hz, where the first two natural frequencies are shown, while Table 5. 2 highlights the natural frequencies and the damping of the three gears.

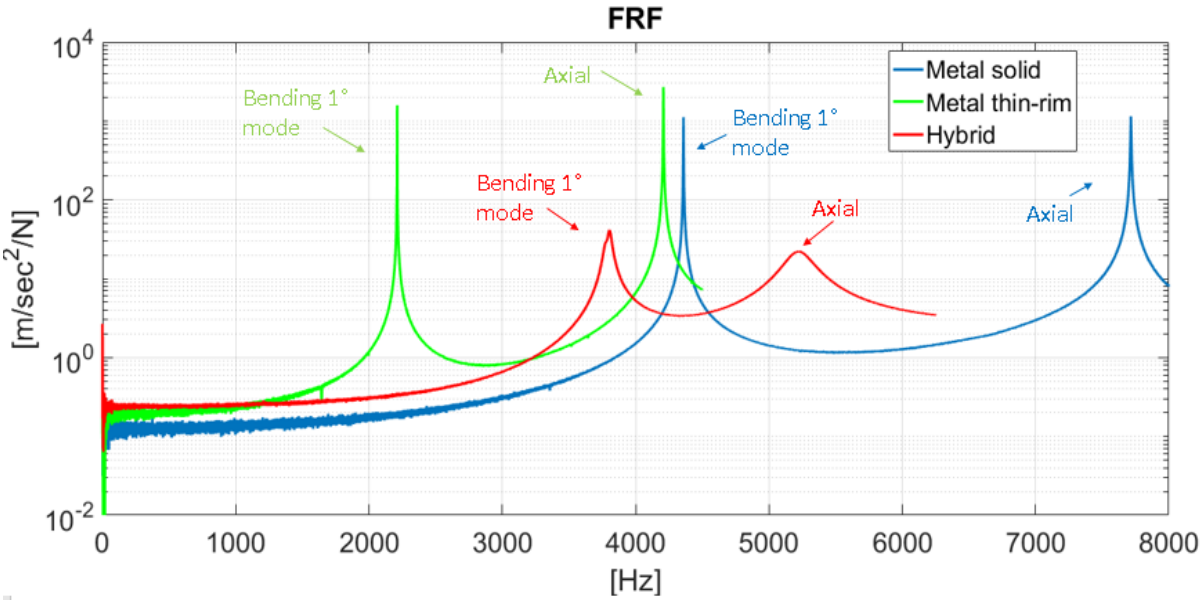

Figure 5. 2 Experimental FRF comparison.

	Mode	Frequency [Hz]	Loss factor η [-]
Steel solid	Bending 1° mode	4358	0.0002
	Axial	7712	0.0005
Steel thin-rim	Bending 1° mode	2211	0.0002
	Axial	4208	0.0003
Hybrid	Bending 1° mode	3750	0.01
	Axial	5045	0.04

Table 5. 2 Comparison of eigenfrequencies and modal damping.

As visible from Figure 5. 4 and Table 5. 2 the use of composite material in the gear body enables an increase of the natural frequency of the first bending and axial modes of 70% and 20%, respectively, compared to the steel thin-rim of the same mass. At the same time, the modal damping of the hybrid gear increases of two orders of magnitude, due to the combined effect of the composite and adhesive materials. Both these two outcomes are expected to play an important role in dynamic meshing conditions.

5.3 Experimental analysis of the gear pairs on a dedicated test-rig

The experimental investigation of hybrid metal-composite gear is based on the determination of the transmission error, both in static and dynamic conditions, which is considered as one of the main excitation sources in the system [116], acceleration values and noise level during working conditions. As described in the previous chapter, the TE is defined as the difference between the actual position of the driven gear and the position it would occupy if the gears were infinitely rigid and the tooth profiles perfectly conjugate [116]. This quantity is the result of different phenomena, which can be summarized as follows:

- the deformation of the teeth and the body, depending on the applied loads as well as actual working conditions (misalignment effects), determines a change of the pure kinematic motion between the gears;

- the local non-linear contact deformation with Hertzian type displacement field, which depends on the tooth shape and on the material;

- teeth surface deviation coming from the unavoidable manufacturing errors.

The resulting relative displacement is evaluated according to Eq. 58, where the angular displacement of the gear is converted into a linear motion along the line of action.

5.3.1 The precision gear pair test rig

Experimental activities have been performed by using a high precision gear test rig [115], the model of which is shown in Figure 5. 3.

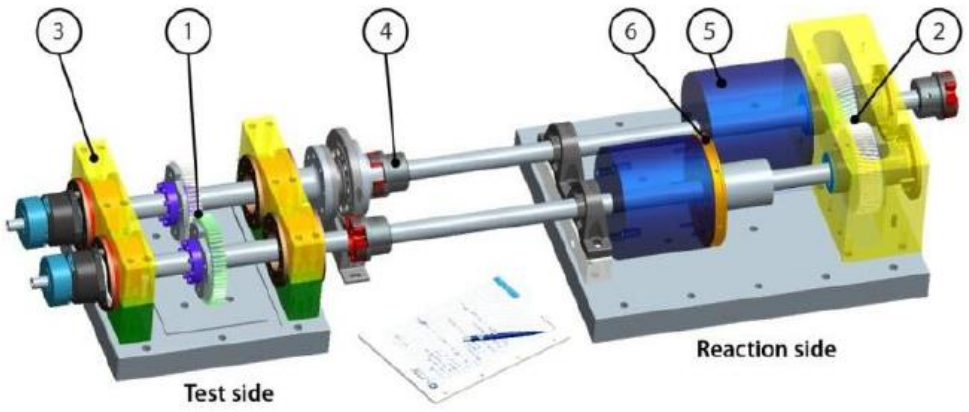

Figure 5. 3 Precision test rig, three-dimensional representation. 1. Test gears; 2. Reaction Gears; 3. Bearings support plates; 4. Flexible couplings; 5. Flywheels; 6. Clutch flange for preload. Reproduced from *[118]*.

It allows to measure different quantities, in static and dynamic working conditions, with the possibility of considering different applied loads and misalignments.
The test rig is composed by two different sides, the test and reaction sides, linked together by flexible couplings, and has a power circulation arrangement with the advantage of relatively low torque required to drive the shaft, with small electric motor and less complicated electrical system. The test rig specifications are provided in the Table 5. 3, where it is visible that there is a big range of applicable torque and angular and parallel misalignments that can be set, for the five degrees of freedom available in the relative positioning of the gears. From the functional point of view, the rotation of the gears is imposed by a 9 kW electric motor driven by a frequency inverter, which controls the speed, while the torque is inserted in the system with weights and an arm with fixed length. Such a design allows to reach a maximum allowable torque of 500 Nm.

Parameter	Range	Uncertainty
Speed	0 to 4500 rpm (0 to 75 Hz)	Measured
Torque	0 to 500 Nm	±0.05%
Angular misalignment	0 to 2 mrad	0.1 mrad
Parallel misalignment	0 to 0.3 mm	0.02 mm

Table 5. 3 Test rig specifications.

Spherical roller bearings were chosen for the shaft on the test side, by supporting radial and axial loads and allowing an angular misalignment between the axis of the inner and the outer races, while Y-bearings unit and wide-face single-row cylindrical roller bearings are mounted on the reaction side. The main goal of the bearings is to provide the highest stiffness with an infinite service life at the maximum torque. Figure 5. 4 shows the bearing installed on the test rig.

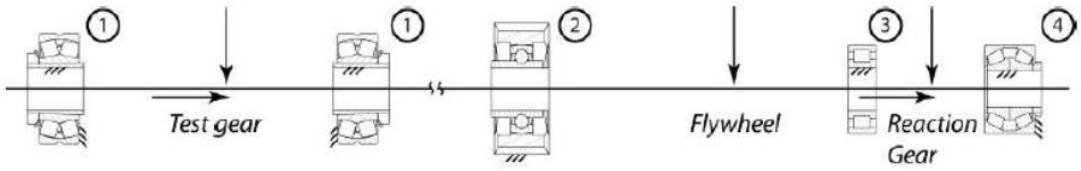

Figure 5. 4 Bearings arrangement for one shaft of the test rig. 1. High-precision spherical roller bearing; 2. Y-bearing unit; 3. Wide-face single-row cylindrical roller bearing; 4. D Double-row tapered roller. Reproduced from *[119]*.

The presence of the compliant elastomeric couplings allows to isolate the two sides from the non-torsional loads generated when the shafts are subjected to bending loads.
In order to stop the propagation of the mesh excitation coming from the reaction gears and to decouple dynamically test and reaction side, it was chosen to lower the natural frequencies of the reaction side. The natural frequencies were lowered by decreasing the torsional stiffness of the shafts while increasing the rotational inertia thanks to the use of one flywheel for each shaft.

5.3.2 Test rig instrumentation

In order to compute the TE as the difference of the measured angles of the two gears, the rotating shafts were equipped with two digital incremental encoders, namely Hidenhain ERN 120 with 5000 ppr, allowing to reach high level of accuracy.
Finally, 16 tri-axial accelerometers (PCB Piezoelectronics) were placed both on the test and reaction side and on the gear bodies to measure the transmitted acceleration from the meshing gears to the overall structure. Figure 5. 5 displays the instrumented gears and test-rig.

a)

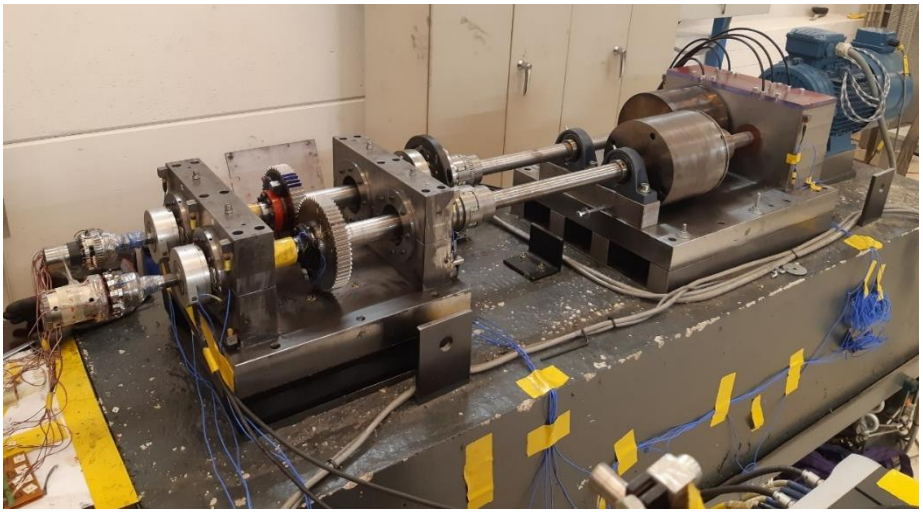

b)

Figure 5. 5 Instrumented gears a) and test-rig b).

5.3.3 Static Transmission error (STE) measurement and comparison with numerical simulations

In this section, the analysis of TE in static conditions are reported for the configurations of solid-thin-rim and solid-hybrid gear pairs and a comparison between experimental and numerical results is shown. The different curves are analysed in angle domain to remove the effect of the speed fluctuations present in the experimental data sets. The experiments were conducted with five levels of torques from 50 Nm to 250 Nm and the rotational velocity was kept at around 10 rpm to exclude any significant dynamic effect. In order to reduce the high friction coefficient, grease was applied on the teeth surfaces, since for low rotational speeds a consistent lubricant film can not be developed between the contact teeth surfaces. Data was acquired with a sampling frequency of 50 kHz. Figure 5. 6 and Figure 5. 7 show the STE curves at different torques for the thin-rim and the hybrid case, respectively. As visible from the pictures, especially in the case of solid-thin-rim gear pair, the TE presents a well-defined shape, due to the high precision reached during the manufacturing process. It is possible to investigate the effect of the applied load in changing the shape and the magnitude of the TE. From the figures, it can be visible the increase of the peak-to-peak values while increasing the torque, for both cases. It is also visible a sharp spike at the beginning of the engagement, which is related to the impacts coming from the fact that the gears are manufactured without micro-geometry modifications on teeth profiles. Additionally, the solid-hybrid gear pair shows a more modulated TE shape due to multiple causes, which determine the rise of additional orders, as visible from Figure 5. 8, where TE spectrum amplitude is compared for the two cases at the torque of 100 Nm.

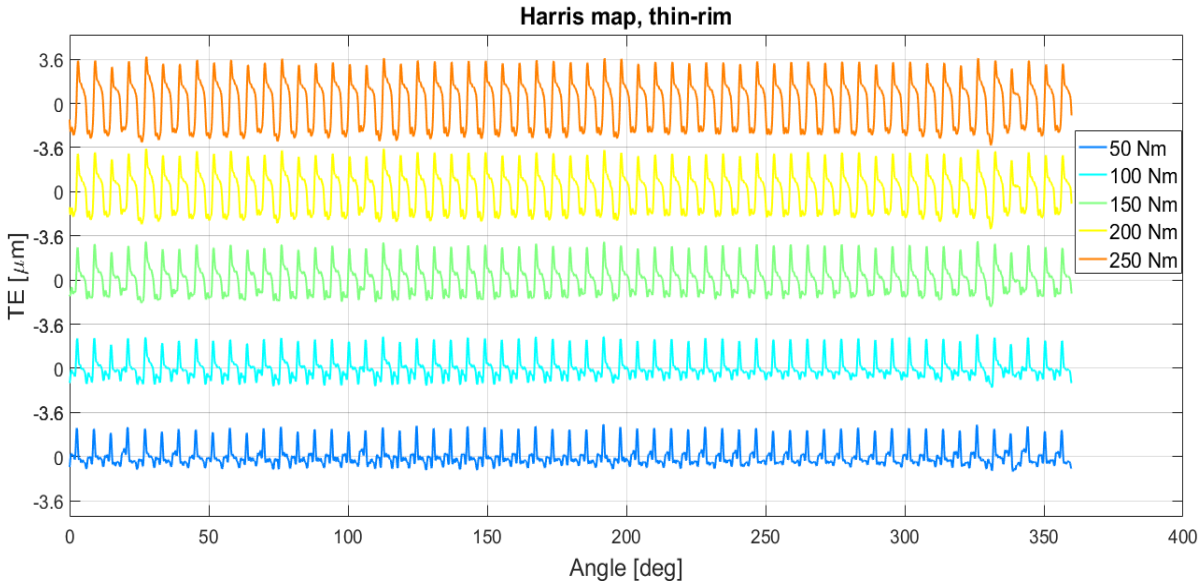

Figure 5. 6 Harris map for the solid-thin-rim gear pair.

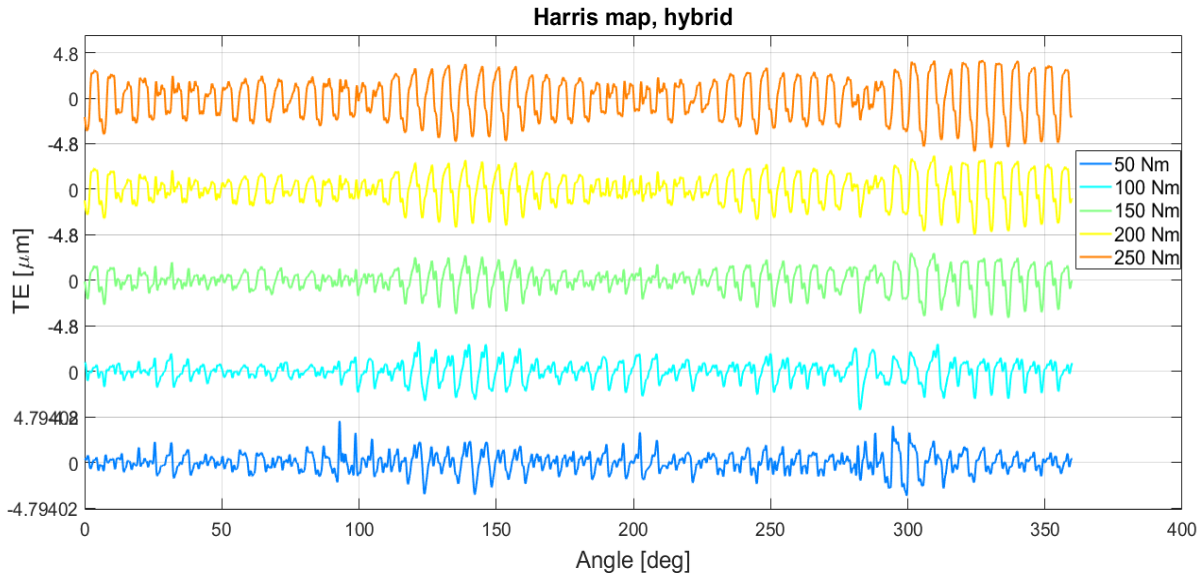

Figure 5. 7 Harris map for the solid-hybrid gear pair.

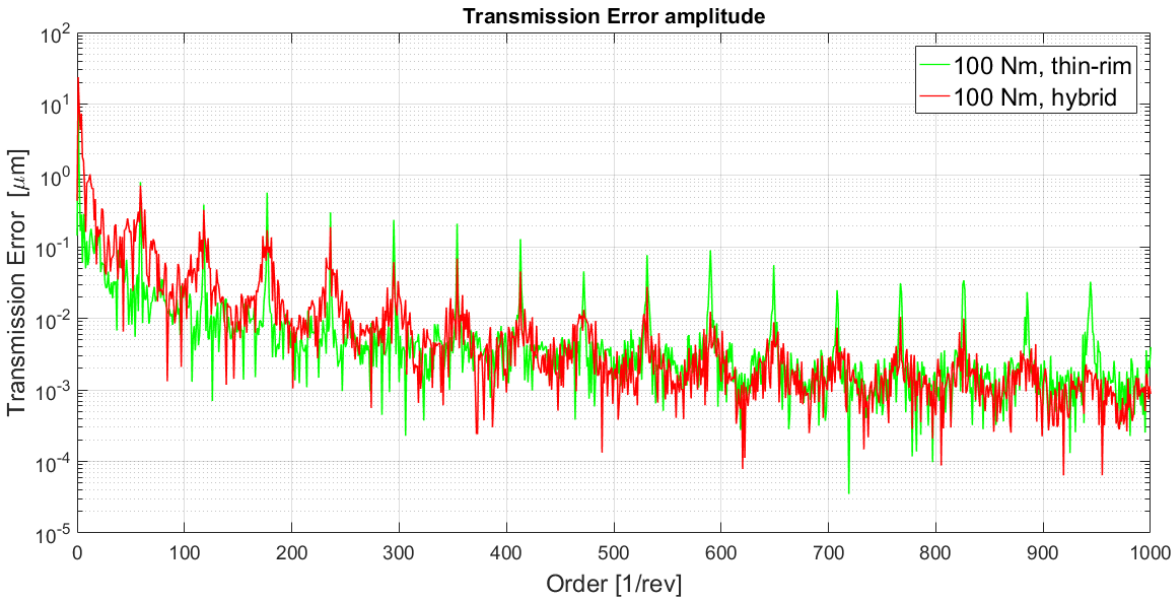

Figure 5. 8 Comparison of the TE spectrum amplitude

From Figure 5. 8 it is possible to notice how the spectrum related to the hybrid gear case is populated by a certain number of low orders with respect to the thin-rim. This is due to two main causes: the first is that the assembly between steel and composite parts creates a small body distortion, which needs to be controlled in a proper way. Additionally, even with a quasi-isotropic configuration of the laminate, there is still a small effect of the material anisotropy. This is due to the fact that, during working conditions, the loads are not perfectly in plane but misalignments can happen, which also excite the composite body in out-of-plane direction. On the other hand, the amplitude of the meshing order is lower in the case of solid-hybrid gear pair and this difference increases with the increase of the orders.

The experimental results in static conditions were compared to the numerical full non-linear FE simulations and multibody models (MB) for both cases. For the full FE analysis, the models were built in the same way as already expressed in the previous Chapter 4, while in the MB environment, a hybrid FE-analytical contact model was used, based on the work described in [83]. Here, the total deformation of the gear, caused by the tooth bending and shear loads coming from the meshing, is equivalent to the sum of a global deformation, considered linear and obtained with linear FE approach, and an analytical one, which is related to the local non-linear deformation of the tooth due to the effects of the local Hertzian contribution. Figure 5. 9 shows the decomposition of the gear displacement field.

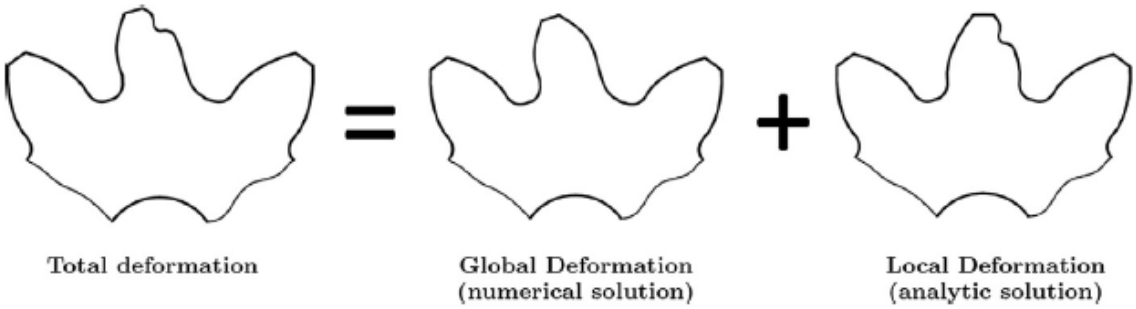

Figure 5. 9 Gear displacement field with hybrid FE analytical solution *[83]*.

Figure 5. 12 and Figure 5. 13 show the comparison of the TE shape for the applied torque of 100 Nm.

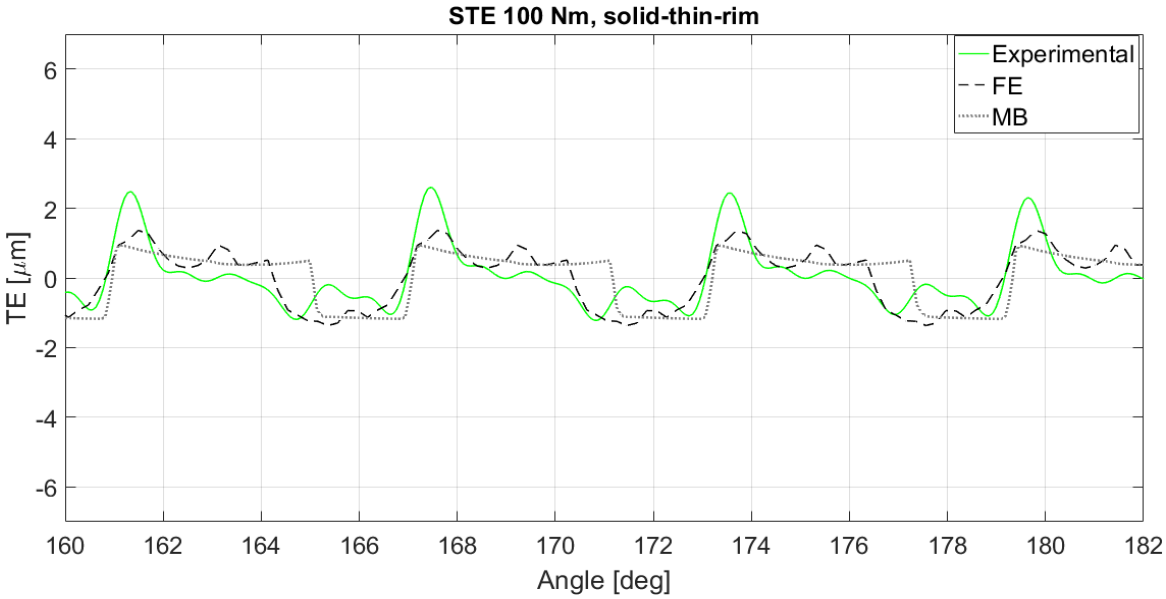

Figure 5. 10 STE shape solid-thin-rim.

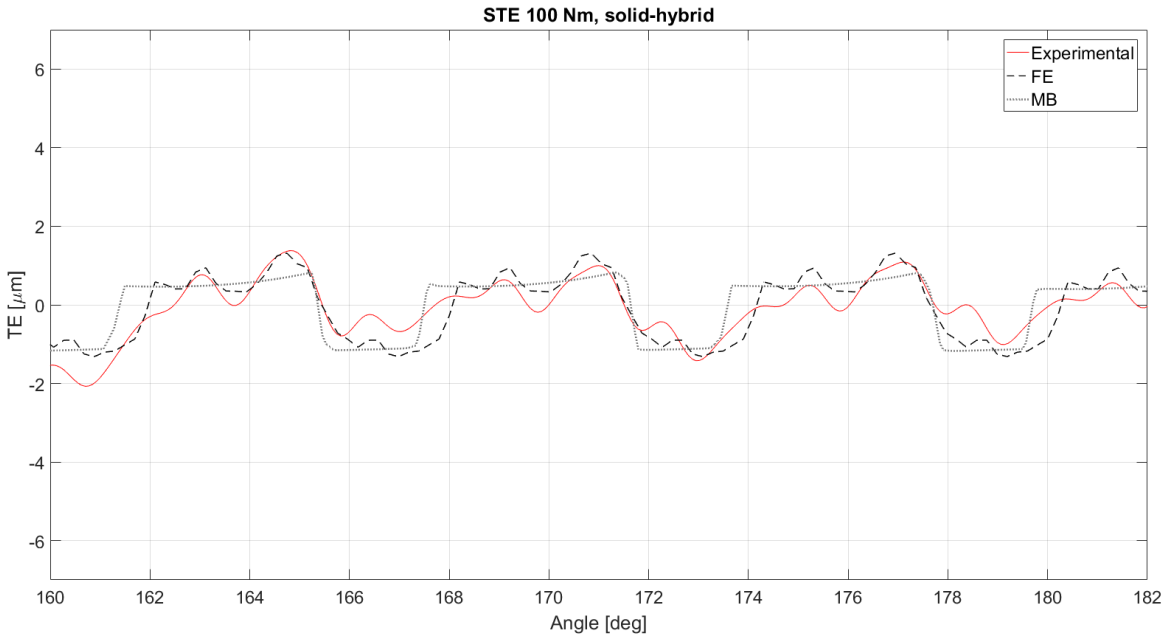

Figure 5. 11 STE shape solid-hybrid.

The advantage of using a multibody environment relies on the much lower computational cost of the simulation with respect to the full FE case, since the global displacement field is decomposed in FE linear behaviour, where less number of elements are necessary on the contact flanks, and analytical formulation. At the same time, the hybrid FE-analytical approach allows to obtain comparable accuracy with respect to the non-linear full FE method, as visible from Figure 5. 10 and Figure 5. 11.

It is worthy to highlight that the experimental/numerical validation shown in Figure 5. 11 is related to the meshing cycles where the rim distortion is negligible, while an expected worse comparison is associated with the meshing cycles where the rim distortion is significant.

In general, as visible from Figure 5. 12 and Figure 5. 13, it is possible to notice that with both FE and MB techniques the predicted TE amplitudes of the first three orders are close to the experimental ones. From the numerical analysis, a slightly worse comparison is given in the case of hybrid gear, mostly due to the small differences between the real and the calculated material properties of the composite body.

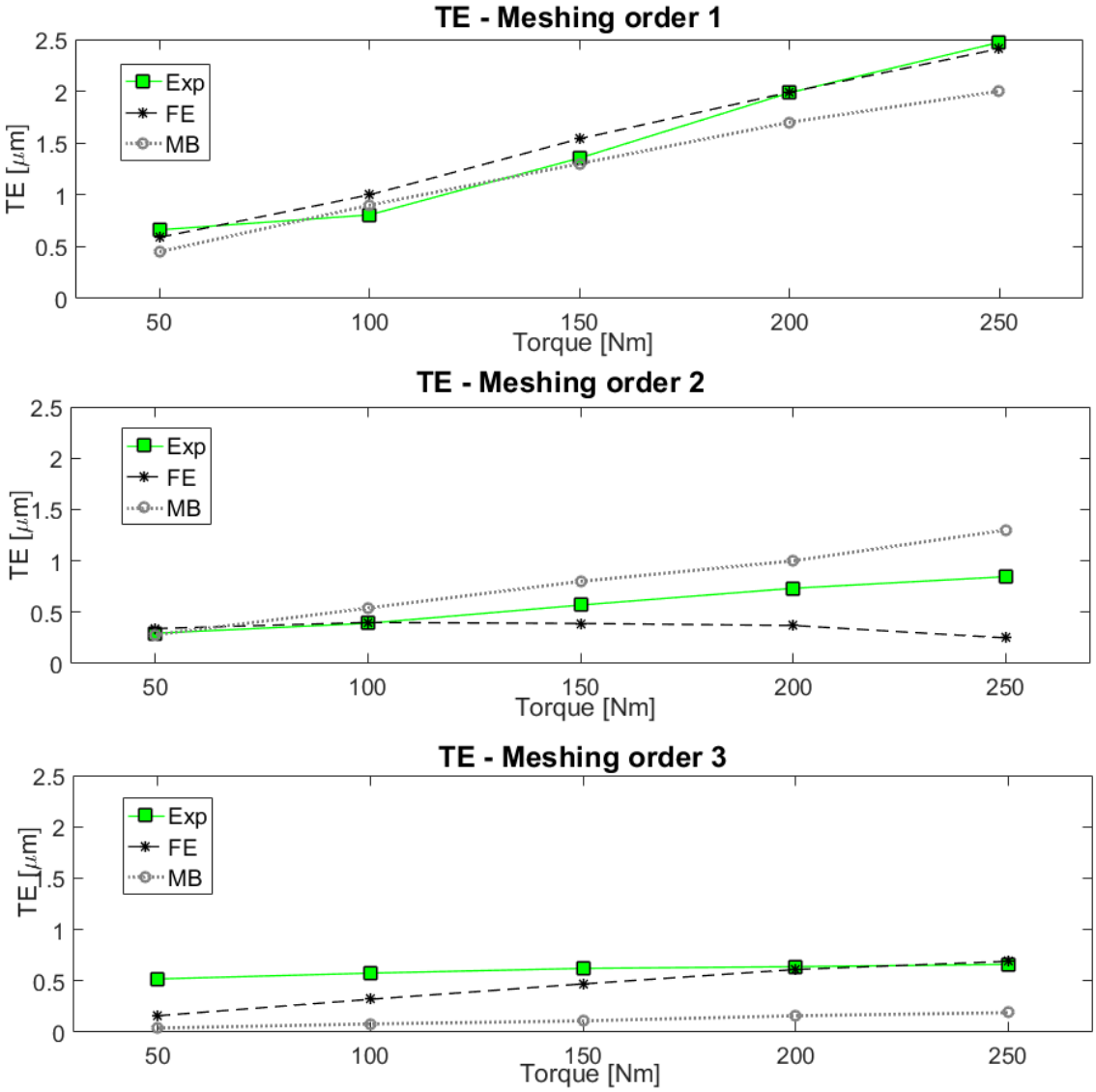

Figure 5. 12 STE order comparison between experimental and numerical results for solid-thin-rim gear pair.

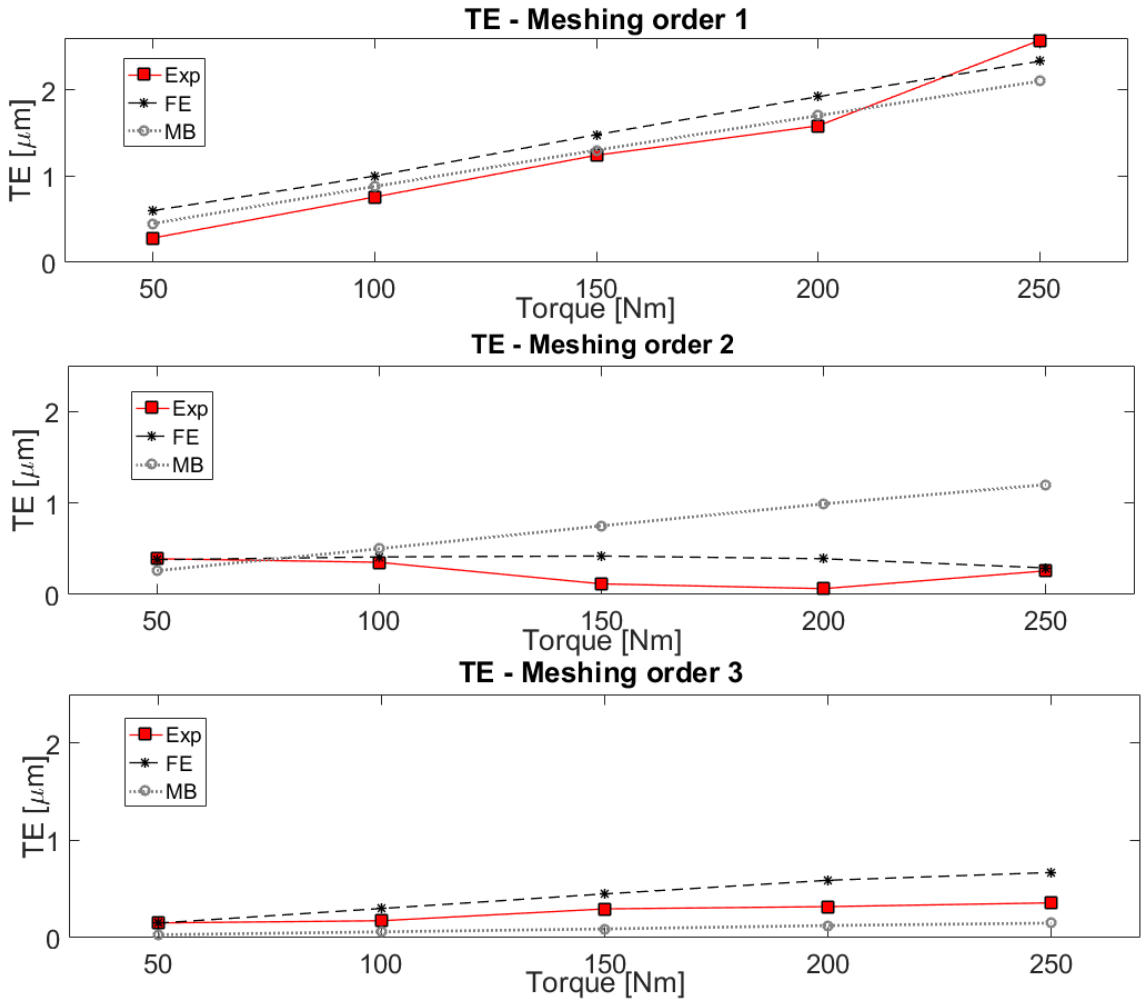

Figure 5. 13 STE order comparison between experimental and numerical results for solid-composite gear pair.

5.3.4 Dynamic analysis: run-up/down of meshing gears

The dynamic analysis of the two sets of gear pairs has been executed in a run-up/down condition in order to investigate the dynamic behaviour at different speeds.

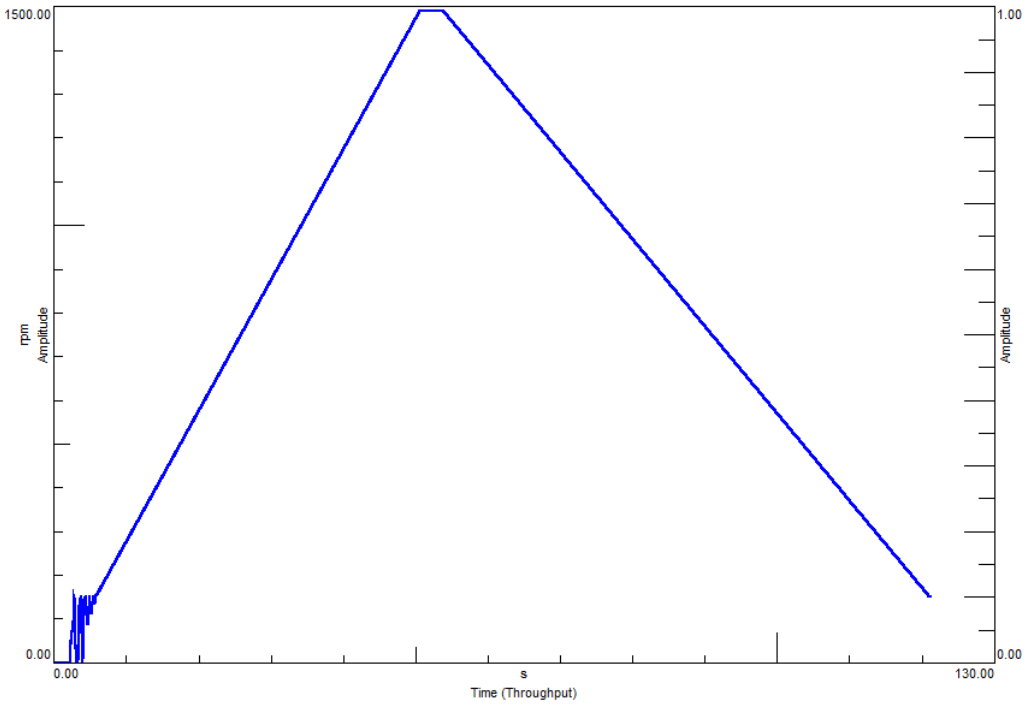

Figure 5. 14 Run-up/down of gear pairs

As visible in the Figure 5. 14 , the analysis covers the range from 0 to 1500 rpm in 50 s. The maximum speed and the slope were set to examine the dynamics of the gears without having a sharp increase of the rotational velocity, which could cause too many vibrations in the test-rig. Additionally, the first part of the run-up is characterized by a transient period in which the motor needs to overcome the overall friction of the structure before running linearly. The quantities that were analysed are the DTE, the in-plane and out-of-plane accelerations and the emitted noise level.

The DTE values were studied by means of the waterfall plot, (i.e. a 3D plot where speed, frequency and amplitude are defined), as shown in Figure 5. 15 a) and b). As visible from the graphs, at low frequencies, the hybrid gears spectrum shows higher orders amplitude as compared to the thin-rim one. On the other hand, at high frequencies the damping effect of the composite and adhesive layer is higher than the one of the steel material. It is also possible to highlight the presence of sidebands in the first two meshing orders, which determine a spread of broadband noise.

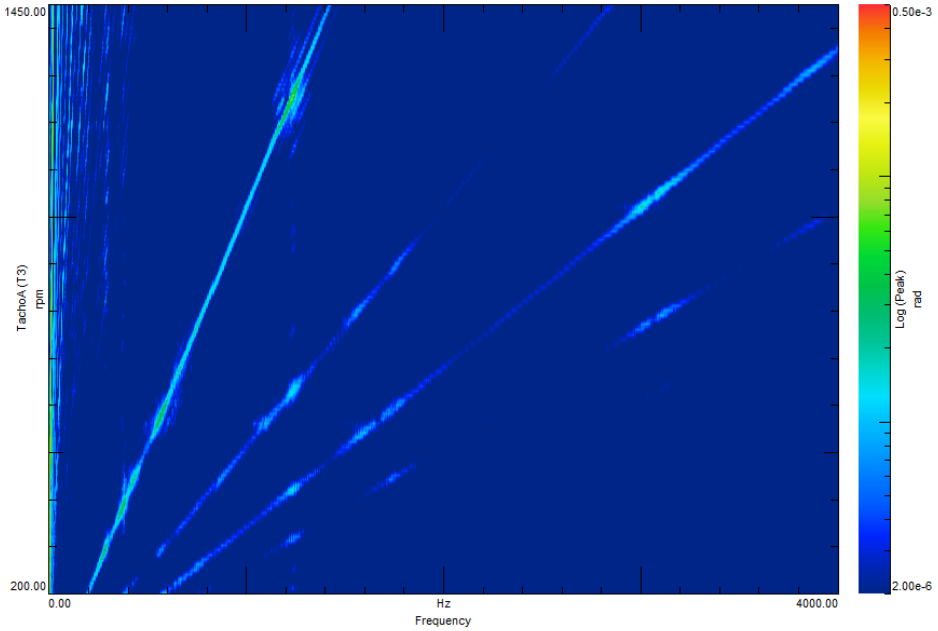

a)

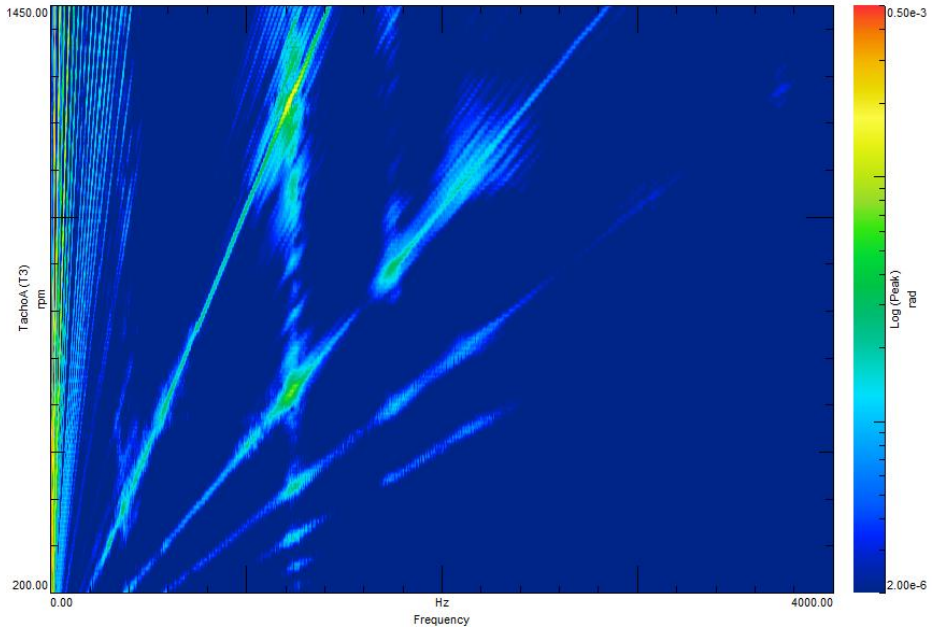

b)

Figure 5. 15 Waterfall plots of DTE of the thin-rim a) and hybrid b) gear pair.

From the amplitude point of view, the peak values are comparable, apart from those arising at the system resonance of 1200 Hz. The cause of that is not intuitive to understand and needs further analysis. From the plots, it is possible to make a one-one comparison of the two gear pairs by cutting and studying the DTE at a certain constant speed. Three levels of speeds were inspected: 60, 600, and 1450 rpm. The Figure 5. 16 a), b) and c) show the comparison.

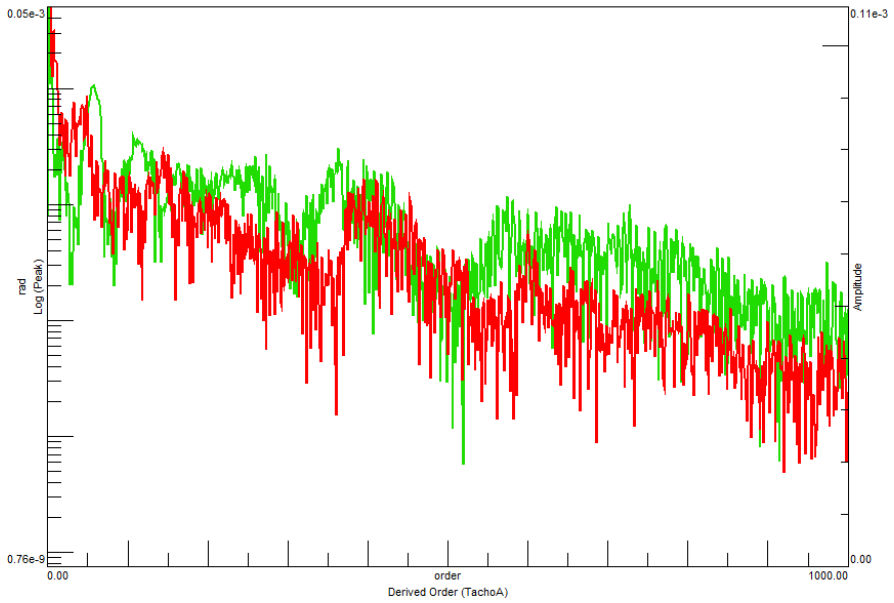
0.05e-3
0.11e-3
rad
Log (Peak)
Amplitude
0.76e-9
0.00
0.00
order
1000.00
Derived Order (TachoA)

a)

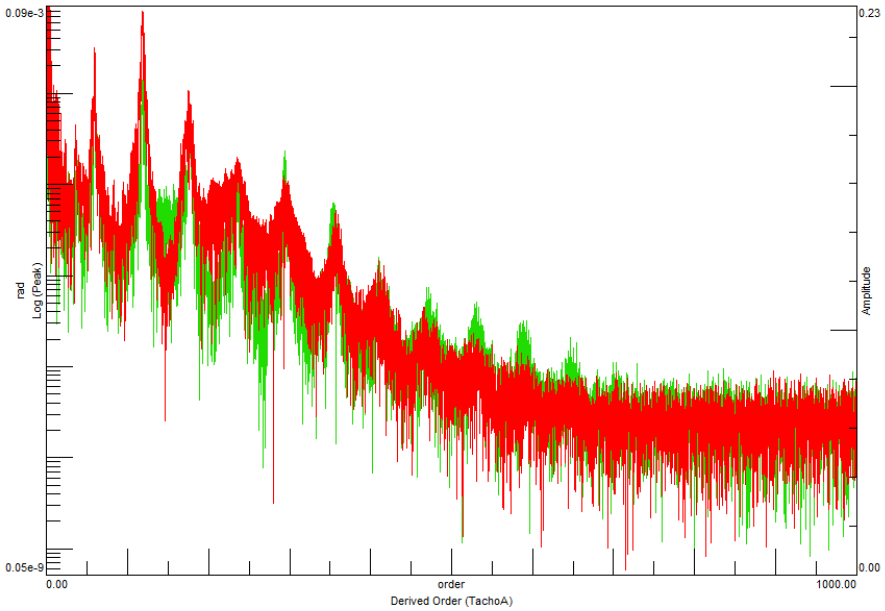
0.09e-3
0.23
rad
Log (Peak)
Amplitude
0.05e-9
0.00
0.00
order
1000.00
Derived Order (TachoA)

b)

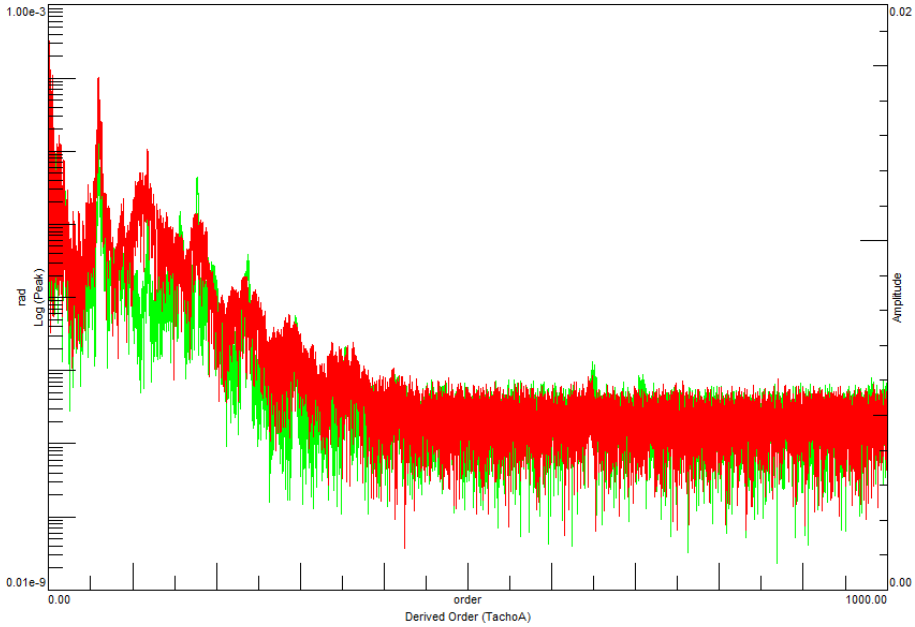

c)

Figure 5. 16 DTE comparison of thin-rim (green) and hybrid (red) at constant speed of 60 rpm a), 600 rpm b), 1450 rpm c).

As visible from Figure 5. 16 a), the DTE content of the thin-rim gear is always higher than the one of the hybrid. By increasing the speed, the amplitude of the first meshing orders starts increasing, while high meshing orders remain below. One possible reason of this behaviour can be found in the dynamic imbalance of the hybrid gear body, which becomes significant at higher speeds.

With regard to the acceleration values, the analysis considered the in-plane and out-of-plane accelerations of the steel solid gear body. In this way, the results were consistent since the accelerometer position did not change in the two tests. Figure 5. 17 a) and b) show the position of the accelerometer in the case of solid-thin-rim and solid-hybrid gear pair, respectively.

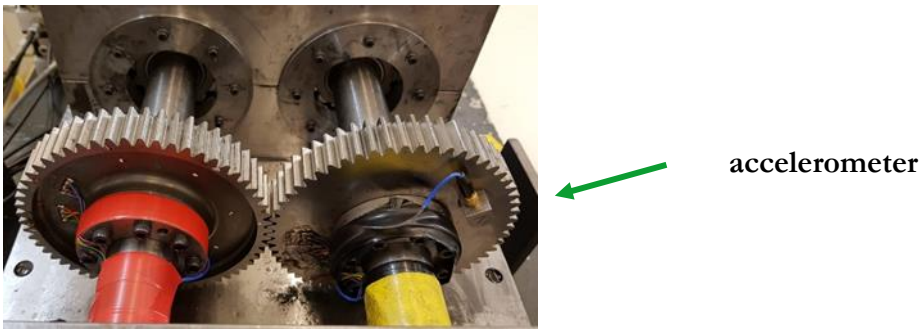

a)

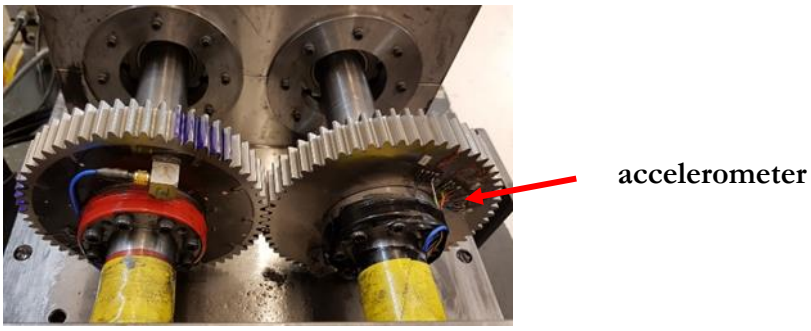

b)

Figure 5. 17 Accelerometer position in solid-thin-rim a) and solid-hybrid b) gear pair.

The waterfall plots of the in-plane acceleration, displayed in Figure 5. 18 a) and b), are considered in the range of [0 20000] Hz in order to analyse a good number of meshing orders in the audible spectrum.

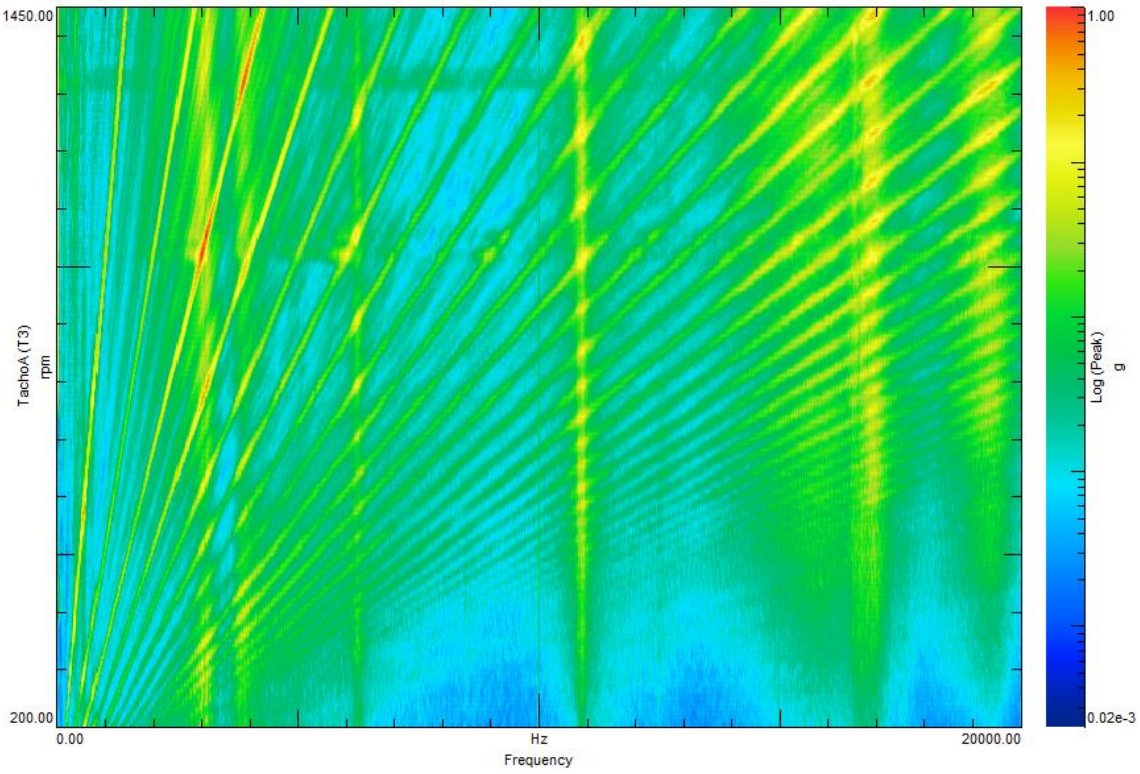

a)

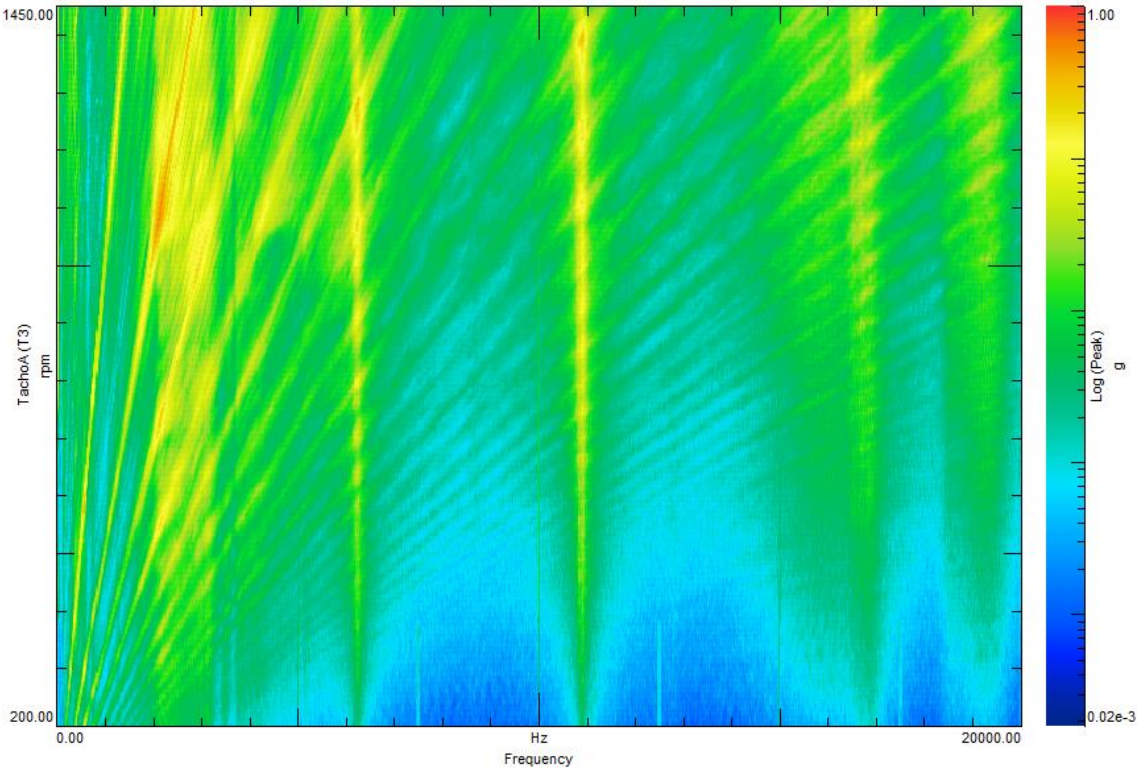

b)

Figure 5. 18 Waterfall plots of acceleration for the thin-rim a) and hybrid b) gear.

As visible from the plots, the maximum of the acceleration is different in the two cases, with respect to the amplitude and the position in the meshing orders. In the solid-thin-rim, it appears at the third meshing order and it is higher than that one of the solid-hybrid gear, which appears at the second meshing order. Additionally, it can be visible the different behaviour of the gear sets, going from low to high frequencies, where hybrid gear behaves better with a reduction of the signal amplitude. Figure 5. 19 shows the envelope of the acceleration signal in time domain. As visible from the graph, the overall acceleration values are lower in the case of hybrid for the run-up/down condition, suggesting that the gear is more capable to damp the system excitation. Similar consideration can be expressed for the out-of-plane acceleration values.

Finally, the noise in dB level was examined with a microphone in the same frequency range (Figure 5. 20 a and b). It is possible to notice that, at low frequencies, the noise coming from the hybrid gear has larger broadband than the thin-rim case, while at high frequencies the level of the tonal noise of thin-rim is higher than the one of the hybrid.

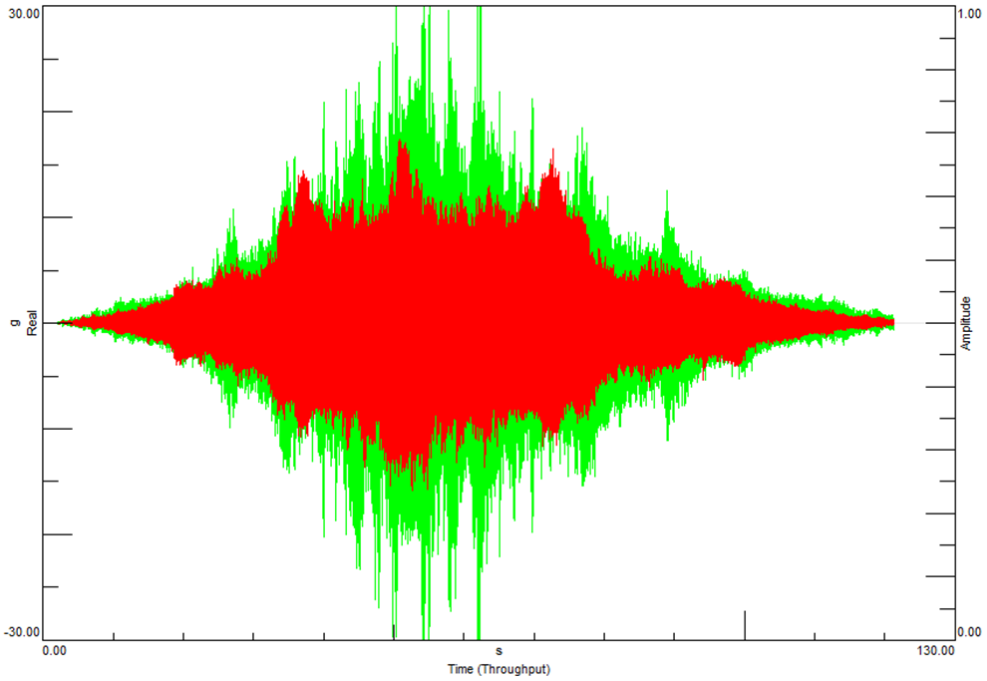

Figure 5. 19 Acceleration in time domain, lightweight in green and hybrid in red.

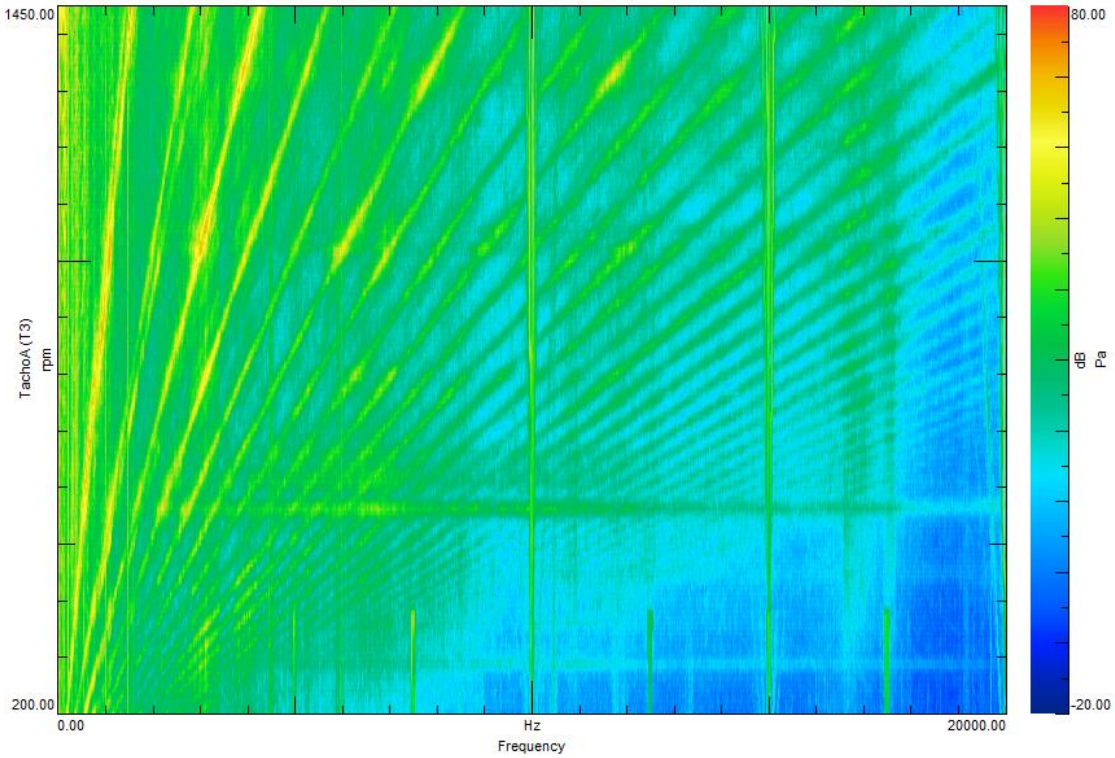

a)

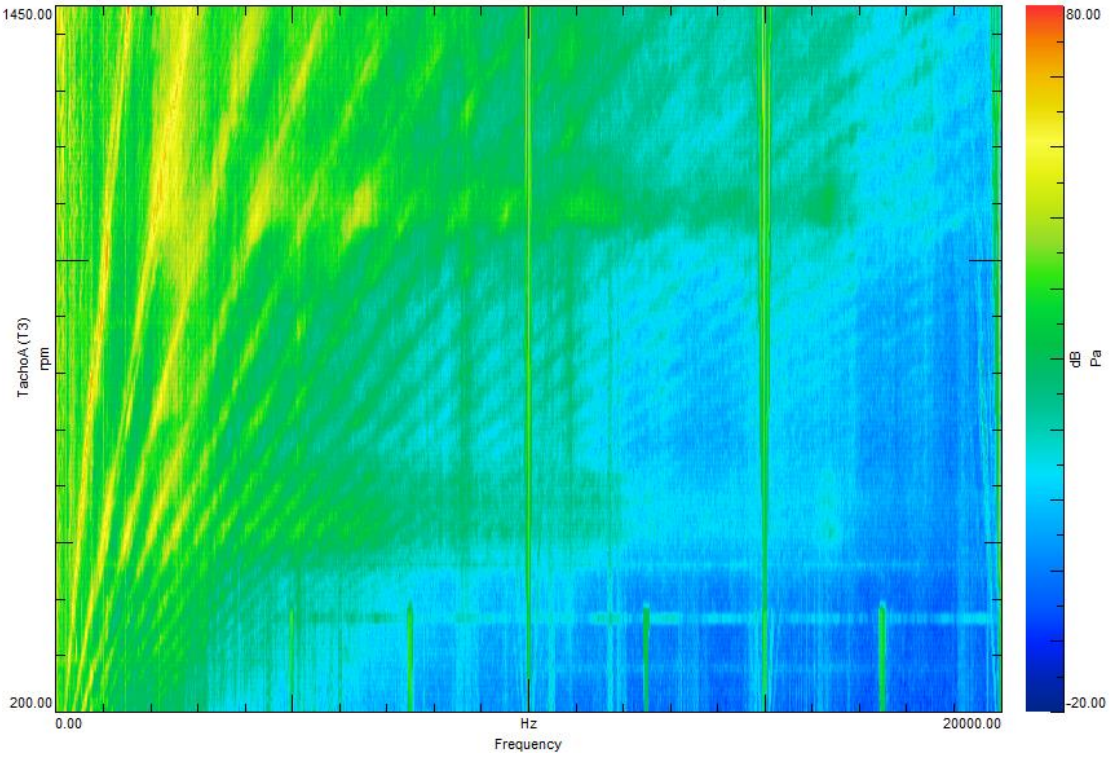

b)

Figure 5. 20 Noise level of the lightweight a) and hybrid b).

5.3.5 Conclusions

In this Chapter, an experimental investigation of solid-hybrid gear pairs has been conducted and a comparison with the solid-thin-rim gear pair has been carried out. The analysis was divided in two parts: static and dynamic. In the first case, the amplitudes of the meshing orders have been examined for different torques, showing that the hybrid case is capable to obtain a reduction of the STE values, especially at high orders. Additionally, it was noticed that the STE spectrum of hybrid contained more sidebands and more pronounced peak amplitudes at low orders. These effects are most likely depending on two main causes: the assembly process and the anisotropy of the composite material. Non linear FE and MB simulations show the good comparison with experimental tests for both cases for the first three meshing orders.

Dynamically, the main considered quantities were the TE, accelerations and noise level. The results coming from the TE analysis showed a similar trend of the static analysis, although at high speed the unbalance coming from the assembly process in hybrid gear was not negligible. From the acceleration signals, the overall behaviour of solid-hybrid

gear pair was generally better than the solid-thin-rim case. Finally, the noise analysis indicated the capability of the hybrid gear to reduce the noise at high frequency, while having a more broadband content at lower ones.

Chapter 6

Conclusions

The main objective of the PhD thesis hereby presented was the investigation and development of new strategies for the design, simulation and testing of multi-material gears made of metal rim and composite body. On the simulation side, a predictive model, based on a FE multi-scale approach, was proposed for the analysis of material properties of the composites to be used in subsequent static and dynamic simulations aiming at in-depth analysis of the mechanical behaviour of transmissions. On the testing side, hybrid gears have been tested as stand-alone components and at gear pair-level to study their NVH performances in comparison with classical steel-thin-rim gears.

The first part demonstrates the investigation the mechanical behaviour of hybrid gears by means of a FE approach. In fact, the simulation tools represent a fundamental part of product design and development, since they can replicate working conditions of the system with high accuracy, thus allowing the identification of potential issues and relevant mitigation actions, almost completely removing the need for expensive and numerous physical prototypes. In this context, the proposed approach, based on the Simcenter™ VMC ToolKit, part of Siemens PLM Software [25], allows to reduce modelling efforts and the number of physical tests on coupons made for composite materials characterization, offering a substantial cost reduction. The methodology presented in the dissertation relies on the multi-scale modelling of composite materials at different scales, from micro to macro, by considering a representative unit cell (RUC). The analysis of the RUC involves the consideration of fibre volume fraction, interweaving yarns geometry (i.e. their cross-sections, width, thickness and spacing) and the interaction between yarns and matrix. A homogenization procedure was used to evaluate elastic material properties in an efficient and accurate way. Results, obtained by performing modal analysis, showed the good capability of the method to match previously published experimental studies. The main advantage of this technique is, therefore, the possibility to establish a complete and general simulation framework, which can be applied for several composite materials and hybrid gears with different geometrical shape, like circular, bevel, etc.

The second part of the work deals with the manufacturing and testing of a new hybrid gear model as stand-alone component. The metal-composite gear was designed as to maximize the use of composite with respect to the metal in the gear body, thus enabling the maximum weight reduction from the baseline solid gear. Here, the issues relative to the manufacturing process were analysed and two different joining techniques were considered for N&V improvement: interference press-fit and adhesive bonding. The impact testing of the two models showed that it is possible to obtain a gear with an increased dynamic stiffness compared to the steel thin-rim one. In particular, the tests demonstrate how it is possible to achieve a percentage increase of the first eigenfrequency of around 80% and 67% for the interference press-fit and adhesive bonding technique, respectively. From the damping point of view, the new solution presents an increase of the modal loss in both configurations. In particular, the assembly with adhesive layer between composite and steel showed the highest modal loss factor thanks to the coupled contribution of glue and composite in damping the system resonances. A FE model of the hybrid gears was built to replicate the impact tests. Here, the analysis was carried out by using two different formulations for composite materials. The first dealt with a ply-by-ply representation of the gear body, while the second was based on the material homogenization of the composite part obtained through analytical formulations. The latter proved to be as accurate as the ply-by-ply technique with further reduction of computational time and modelling effort. Numerical and experimental results were compared by means of a MAC analysis, which showed perfect correlation, proving the accuracy of the proposed method.

The homogenization theory was, then, used in non-linear simulations where the static transmission error of a hybrid gear pair was compared to that related to a steel thin-rim gear pair. Results demonstrated significant reduction of the peak-to-peak, around 25% with interference press-fit and 15% with adhesive joining. Additionally, a cohesive model was used to take into account the damage at the interface between composite and steel part during working conditions. In particular, the cohesive theory implemented in Simcenter 3D [97] allowed to consider the damage of the interface in accordance with the real loading conditions between gears. Non-linear simulations were, then, used to verify that the adhesive strength withstood the hardest loading conditions, proving the good design of the gear.

Both concepts proved manufacturable and the analyses showed improvements with respect to the baseline steel gear. Moreover, the two concepts further proved to be potential solutions, depending on operational requirements priorities of stiffness or damping.

The last part of the thesis contains a static and dynamic experimental comparison between two gear pairs: the first is composed by a steel solid gear and a steel thin-rim one; the second by the same solid gear and a hybrid one with the same mass of the thin-rim. The test were performed in a dedicated test-rig where different torques and rotations were applied. The work focused on the analysis of transmission error, accelerations and noise levels. Firstly, all the tests with hybrid gears didn't show a visible damage at the interface between composite and steel, even when gears passed through the system resonances. This proved the quality of the joining technique. The static TE showed that an improvement of the amplitude meshing order was possible thanks to the use of high stiffness and strength composite materials in a quasi-isotropic configuration, even if the TE shape of the hybrid gear presented a more pronounced modulation due to the additional low orders derived from the assembly process, which needed to be more controlled.

Additional FE non-linear static analysis and multibody technique were used to validate experimental STE for the first three meshing orders, showing the good capability of the methods to represent the physical system. In particular, the full MB approach demonstrated a higher computational efficiency than FE with comparable accuracy when comparing STE experimental shape and orders.

During speed sweep condition, at low rotational speed, the experimental evidence was in agreement with static tests, while at higher speed there was an amplification of the TE peak-to-peak, partially due to the distortion of the gear rim induced by the manufacturing process. This will require further investigation. From the acceleration point of view, a noticeable reduction of the *g* amplitude was measured, especially at higher frequencies (5000-20000 Hz), due to the combined damping effect of composite and adhesive. This effect was observed for the in-plane and out-of-plane accelerations, even if with different percentage of reduction. Another visible phenomenon from the waterfall plots was a more spread vibration level in hybrid gears with respect to the thin-rim. This trend is also visible in the noise analysis, where a tonal noise appears in the steel thin-rim gear, while a broadband noise appears in the hybrid one.

To conclude, it is possible to highlight some major benefit resulting from the application of composite materials to the gears. Firstly, the multi-material design allows to improve the strength-to-weight ratio, which is a fundamental driver, especially in the aerospace sector. The use of high stiffness and strength laminates can improve the performances of the entire system, both in terms of dynamic stiffness and in damping behaviour. Energy dissipation becomes particularly relevant in cases where the dynamic excitations are so high that they affect the global performance of the system, like durability or noise radiation. In these situations, the option of composites can represent a great help for the designers in the development of a new product.

It can be noticed that the described research is mainly focused on the application of the composites in spur gears, in order to develop a general methodology, which can be applied to different geometry and materials. The proposed CAE based approach for the design, simulation and manufacturing of hybrid gears can be usefully considered in its entirety for transmissions with helical gears, mainly used in automotive gearboxes, and for bevel gears, typical of the aerospace sector. In these cases, an important aspect to examine is the complexity of the web geometry for its correct joining with the metal rim and hub.

On the other hand, the choice of composites over other materials has been mainly driven by the fact that CFRP allows to reach the maximum power-to-weight ratio, extremely important for the reduction of the fuel consumptions and CO_2 emissions in the transportation sectors, without compromising the working conditions. Nonetheless, the developed methodology of hybrid gears can be easily integrated with the application of additional materials like lightweight metals (e.g. aluminium), when high power transmission in lighter components is required, or polymers (e.g. phenol resin), used achieve a further N&V reduction, while diminishing, at the same time, the dynamic stiffness. In these two cases, a fundamental step of the analysis can be related to the consideration of the materials thermo-mechanical behaviour in the proposed design approach.

6.1 Future steps

From the thesis, it is clear that multi-material design has high innovative potential in the field of mechanical transmissions.

Additional experimental campaigns are needed to better understand all the phenomena so far arisen during the tests and provide validation data for future modelling techniques.

In this context, an important research path to improve the modelling of multi-material structures is the application of parametric model order reduction. This technique, based on the reduction of the parametric models of composites, which relies on the inclusion of a set of mode shapes in the considered reduction space, can lead to a decrease in the computational cost of the simulation, while maintaining a good accuracy.

Another potential extension of this work is mostly related to the optimization of the composites in the gear body. Here, the shape, the plies number and orientation, the polymeric matrix can be used as input for a multi-objective optimization for stiffness, strength and damping values, depending on the target application. Moreover, the multi-material approach can be easily extended to helical gears, where the out-of-plane stiffness and damping of the composites can increase their potential benefit for NVH behaviour.

Appendix A

Publications list

Articles in International Journals

F. Cosco, G. Serratore, P.G. Catera, F. Gagliardi, E. Luberto, D. Mundo, Experimental assessment of stiffness and energy dissipation properties of disk-shaped polymer-based composite specimens by in-plane torsion testing, Polymer Testing 2020.

P.G. Catera, D. Mundo, F. Gagliardi, A. Treviso, A comparative analysis of adhesive bonding and interference fitting as joining technologies for hybrid metal-composite gear manufacturing, International Journal on Interactive Design and Manufacturing 2020.

P. G. Catera, D. Mundo, A. Treviso, F. Gagliardi, A. Visrolia, On the design and simulation of hybrid metal-composite gears, Applied Composite Materials, (2019) 26: 817-833.

P. G. Catera, F. Gagliardi, D. Mundo, L. De Napoli, A. Matveeva, L. Farkas, Multi-scale modelling of triaxial braided composites for FE-based modal analysis of hybrid metal-composite gears, Composite Structures 2017, 182, 116-123.

Articles in International Conferences

N. Contartese, P. Catera, D. Mundo, Static mesh stiffness decomposition in hybrid metal-composite spur gears, The 15th IFToMM World Congress, 30th June-4th July 2019, Cracow, Poland.

D. Mundo, S. Shweiki, P. Catera, On the Impact of Transmission Error on the Dynamic Behaviour of Geared-Linkages, The 4th Conference on Mechanisms, Transmissions and Applications, 3rd -5th July 2017, Trabzon, Turkey.

M. Vivet, R. Adduci, P. Catera, G. H. K. Heirman, D. Mundo, T. Tamarozzi, W. Desmet, Global mesh stiffness calculation for lightweight spiral bevel gears, ISMA 2016, International Conference on Noise and Vibration Engineering, 19th -21th September 2016, Leuven, Belgium.

Oral presentations in International Conferences

P. G. Catera, D. Mundo, A. Treviso, F. Gagliardi, A. Visrolia, Static Transmission error evaluation in hybrid metal-composite spur gear pairs, 21st International Conference on Composite Structures, 4th -7th September 2018, Bologna, Italy.

Bibliography

[1] E. Union, REGULATION (EC) No 443/2009, setting emission performance standards for new passenger cars as part of the Community's integrated, 2009.

[2] M. F. Ashby, Technology of the 1990s: Advanced materials and predictive design. Philosophical Transactions of the Royal Society of London, A322,393-407.

[3] A. A. Griffith, The phenomena of rupture and flow in solids. Philosophical Transactions of the Royal Society, 221A, 163–198., 1920.

[4] S. Lin and S. Poster, "Development of a Braided Composite Drive Shaft with Captured End Fittings, presented at he 60th Annual Forum of the American Helicopter Society International," June 2004.

[5] T. Cecil, R. Ehinger and C. and Kilmain, "Application and Configuration Issues of Resin Transfer Molded Composite Transmission Housings – A Program Review, presented at the 63rd Annual Forum of the American Helicopter Society International," May 2007.

[6] P. Velex and A. Singh., "Top gear," *Journal of Mechanical Design,* 2010, 1-2, 132.

[7] S. Shweiki, Analysis of Static and Dynamic Meshing Behaviour of Lightweight Gears, Doctoral Thesis, University of Calabria, 2019.

[8] Y. Cai, "Simulation on the rotational vibration of helical gears in consideration of the tooth separation phenomenon," *Journal of Mechanical Design,,* 1995, 460-469, 117.

[9] A. Palermo, D. Mundo, R. Hadjit and W. Desmet, "Multibody element for spur and helical gear meshing based on detailed three-dimensional contact calculations," *Mechanism machine Theory,* 2013, 13-30, 62.

[10] T. Lin, H. Ou and R. Li, "A finite element method for 3D static and dynamic contact/impact analysis of gear drives," *Computational Methods in Applied Mechanics and Engineering,* 2007, 1716-1728, 196.

[11] R. Handschuh, G. Roberts, R. Sinnamon, D. Stringer, B. D. Dykas and L. W. Kohlmann, "Hybrid Gear Preliminary Results—Application of Composites to Dynamic Mechanical Components," *NASA/TM-217630,* July 2012.

[12] J. C. Gerdeen and R. A. L. Rorrer, Engineering design with polymers and composites, CRC Press, 2nd edition, 2011.

[13] J. M. Berthelot, Mechanics of composite materials and structures, Vallouise, France, 2015.

[14] R. Gibson, Principles of composite material mechanics, CRC Press, Taylor & Francis Group, 2016, 4th edition.

[15] S. Timoshenko, "On the correction factor for shear of the differential equation for transverse vibrations of prismatic bar," *Philosophical Magazine,* 6 (41):295, 1921.

[16] R. Midlin, "Influence of rotatory inertia and shear on flexural motions of isotropic, elastic plates," *Journal of Applied Mechanics,* 18:31-38, 1951.

[17] J. N. Reddy, Mechanics of Laminated Composite Plate and Shells: Theory and Analysis., Springer, 2nd edition, 2003.

[18] E. Carrera, "Cz0 Requirements-models for the two dimensional analysis of multilayered structures," *Composite Structures,* 37(3/4):373-383,1997.

[19] A. Treviso, Finite Element models for the dynamic analysis of composite and sandwich structures, Doctoral Thesis, University of Calabria, 2015.

[20] C. Chamis, "Mechanics of composite materials: past, present and fuure," *Journal of Composites, technology and research,* 11, No. 1 (March 1989), 3-14.

[21] P. C. Chou, J. Carleone and C. M. Hsu, "Elastic Constants of Layered Media," *Journal of Composite Materials,* 6(1), 80–93, 1972.

[22] T. Bogetti, C. Hoppel and W. Drysdale, "Three-dimensional effective property and strength prediction of thick laminated composite media," *U.S. Army Research Laboratory,* October 1995.

[23] R. F. El Hajjar, S. S. Shams and D. J. Kehrl, "Closed form solutions for predicting the elastic behavior of quasi-isotropic triaxially braided composites," *Composite Structures,* 101 (2013) 1–8.

[24] S. Jacques, I. D. Baere and W. V. Paepegem, "Application of periodic boundary conditions on multiple part finite element meshes for the meso-scale homogenization of textile fabric composites," *Composites Science and Technology,* 92 (2014) 41–54.

[25] L. Farkas, K. Vanclooster, H. Erdelyi, R. Sevenois and S. V. Lomov, "Virtual material characterization process for composite materiasl: an industrial solution," *ECCM17 – 17th European Conference on Composite Materials, Munich, Germany,* 26 - 30th June 2016.

[26] A. R. Melro, P. P. Camanho and S. T. Pinho, "Generation of random distribution of fibres in long-fibre reinforced composites," *Composites Science and Technology,* 68 (2008) 2092–2102.

[27] S. Jacques, "Development of a framework for the construction of meso-scale finite element models of textile composites," *Ghent University Faculty of Engineering and Architecture, PhD Thesis,* 2014.

[28] C. Sun and Y. P. Lu, Vibration Damping of Structural Elements, Prentice Hall PTR, 1995.

[29] R. Gibson, "Damping Characteristics of Composite Materials and Structures," *Journal of Materials engineering and Performance,* volume 1, 1992.

[30] P. Kim, "A Comparative Study of the Mechanical Performance and Cost of Metal, FRP, and Hybrid Beams," *Applied Composite Materials,* 5: 175–187, 1998.

[31] E. Sarlin, Y. Liu, M. Vippola, M. Zogg, P. Ermanni, J. Vuorinen and T. Lepistö, "Vibration damping properties of steel/rubber/composite hybrid structures," *Composite Structures,* 94 (2012) 3327–3335.

[32] W. V. Liebig, V. Sessner, K. A. Weidenmann and L. Kärger, "Numerical and experimental investigations of the damping behaviour of hybrid CFRP-elastomer-metal laminates," *Composite Structures,* 202 (2018) 1109–1113.

[33] D. H. Cho, D. G. Lee and J. H. Choi, "Manufacture of one-piece automotive drive shafts with aluminum and composite materials," *Composite Structures,* Vol. 38, No. l-4, 309-319, 1997.

[34] H. S. Kim and D. G. Lee, "Optimal design of the press fit joint for a hybrid aluminum/composite drive shaft," *Composite Structures,* 70 (2005) 33–47.

[35] J.-H. Bae, K.-C. Jung, S.-H. Yoo, S.-H. Chang, M. Kim and T. Lim, "Design and fabrication of a metal-composite hybrid wheel with a friction damping layer for enhancement of ride comfort," *Composite Structures ,* 133 (2015) 576–584.

[36] G. Zhu, G. Sun, Q. Liu, G. Li and Q. Li, "On crushing characteristics of different configurations of metal-composites hybrid tubes," *Composite Structures,* 175 (2017) 58–69.

[37] G. Suna, Z. Wanga, H. Yu, Z. Gong and Q. Li, "Experimental and numerical investigation into the crashworthiness of metal-foam-composite hybrid structures," *Composite Structures,* 209 (2019) 535-547.

[38] R. Kalhor, H. Akbarshahi and S. W. Case, "Numerical modeling of the effects of FRP thickness and stacking sequence on energy absorption of metal–FRP square tubes," *Composite Structures,* 147 (2016) 231–246.

[39] P. Tran, S. Linforth, T. D. Ngo, R. Lumantarna and T. Q. Nguyen, "Design analysis of hybrid composite anti-ram bollard subjected to impulsive loadings," *Composite Structures,* 189 (2018) 598–613.

[40] S.-W. Jeon, Y. H. Cho, M.-G. Han and S.-H. Chang, "Design of carbon/epoxy–aluminum hybrid upper arm of the pantograph of high-speed trains using adhesive bonding technique," *Composite Structures,* 152 (2016) 538–545.

[41] M.-G. Han, Y. H. Cho, S.-W. Jeon and S.-H. Chang, "Design and fabrication of a metal-composite hybrid pantograph upper arm by co-cure technique with a friction layer," *Composite Structures,* 174 (2017) 166–175.

[42] S.-W. Lee, Y. H. Cho, J.-H. Kim and S.-H. Chang, "Mechanical performance evaluation of composite hybrid pantograph upper arm under environmental cyclic conditions: Experimental verification," *Composite Structures,* 210 (2019) 599-607.

[43] S. H. Chang, P. J. Kim, D. G. Lee and J. K. Choi, "Steel-composite hybrid headstock for high precision grinding machines," *Composite Structures,* 53 (2001) 1-8.

[44] B. J. Kim, a. S. Kim and D. G. Lee, "Design of hybrid steel/composite circular plate cutting tool structures," *Composite Structures,* 75 (2006) 250–260.

[45] S.-K. Cho, H.-J. Kim and S.-H. Chang, "The application of polymer composites to the table-top machine tool components for higher stiffness and reduced weight," *Composite Structures,* 93 (2011) 492–501.

[46] J.-H. Kim and S.-H. Chang, "Design of l-CNC machining centre with carbon/epoxy composite–aluminium hybrid structures containing friction layers for high damping capacity," *Composite Structures,* 92 (2010) 2128–2136.

[47] T. Ribeiro, R. Campilho, L. d. Silva and L. Goglio, "Damage analysis of composite–aluminium adhesively-bonded single-lap joints," *Composite Structures,* 136 (2016) 25–33.

[48] F. Lambiase and D.-C. Ko, "Feasibility of mechanical clinching for joining aluminum AA6082-T6 and Carbon Fiber Reinforced Polymer sheets," *Materials and Design,* 107 (2016) 341–352.

[49] S. Pitta, V. d. l. M. Carles, F. Roure, D. Crespo and J. I. Rojas, "On the static strength of aluminium and carbon fibre aircraft lap joint repairs," *Composite Structures,* 201 (2018) 276–290.

[50] H. Tang and L. Liu, "A novel metal-composite joint and its structural performance," *Composite Structures,* 206 (2018) 33–41.

[51] G. Heirman, N. Cappellini, F. P. J. v. Wermeskerken and A. Toso, "A gear contact model to analyse the dynamics of transmissions with lightweight, flexible gears," *VDI International Conference on Gears,* Munich, Germany, October 5-7, 2015.

[52] A. Toso, F. v. Vermeskerken, N. Cappellini and G. Heirman, "On the effect of lightweight gear blank topology on transmission dynamics," *ASME 2015 International Design Engineering Technical Conferences & Computers and Information in Engineering Conference IDETC/CIE 2015,* Boston (MA), USA, August 2-5, 2015.

[53] M. Vivet, R. Adduci, P. Catera, G. Heirman, D. Mundo, T. Tamarozzi and W. Desmet, "Global mesh stiffness calculation for lightweight spiral bevel gears," *Proceeding of International Conference on Noise and Vibration Engineering,* (ISMA 2016), Leuven (Belgium), 19-21 September 2016.

[54] R. F. Handschuh, K. Laberge, S. DeLuca and R. Pelagalli, "Vibration and Operational Characteristics of a Composite-Steel (Hybrid) Gear," *NASA/TM—2014-216646,* June 2014.

[55] R. C. S. M. Sean Gauntt, "Design Optimization of a Hybrid Spur Gear," *Conference: Vertical Flight Society Forum 75,* May 2019.

[56] K. E. LaBerge, S. Berkebile, R. F. Handschuh and G. Roberts, "Hybrid Gear Performance Under Loss-of-Lubrication Conditions," *73rd American Helicopter Society Annual Forum,* 9-11 May 2017, United States.

[57] K. E. LaBerge, R. F. Handschuh, G. Roberts and S. Thorp, "Performance Investigation of a Full-Scale Hybrid Composite Bull Gear," *AHS 2016 Forum,* 17-19 May 2016, West Palm Beach, FL, United States.

[58] K. E. LaBerge, J. Johnston, R. Handschuh and G. Roberts, "Evaluation of a Variable Thickness Hybrid Composite Bull Gear," *AHS 2017 Forum,* 14-17 May 2018, Phoenix, Arizona, United States.

[59] R. K. Naffin, U. Ulun, C. Garmel, N. McManus, Z. Hu, W. Ohlerking and D.E.Mayers, "RTAPS (Research and Technology for Aerospace Propulsion Systems): Simulation of Structural Loads within a Hybrid Gear Resulting from Loading at the Gear Teeth," *NASA/CR-2017-218945,* December 2017.

[60] B. M. Abramov, "Vibration of gear transmissions caused by varying rigidity of meshing," *Trud. Sem. Tear. Mash. Mekh,* 21.86 (1960).

[61] M. Utagawa, "Dynamic Loads on Spur Gear Teeth," *Bulletin of JSME,* 1.4 (1958), 397-403.

[62] S. L. Harris, "Dynamic loads on the teeth of spur gears," *Proceedings of the Institution of Mechanical Engineers,* 172 (1958), 87–112.

[63] R. W. Gregory, S. L. Harris and R. G. Munro, "Dynamic Behaviour of Spur Gears," *Proceedings of the Institution of Mechanical Engineers,* 178 (1963), 207–226.

[64] J. Helsen, F. Vanhollebeke, B. Marrant, F. D. Coninck, D. Vandepitte and W. Desmet, "Updated wind turbine gearbox multibody model with optimized

flexible housing to deliver inputs for acoustic calculations," *Proceedings of the Multibody Dynamics Thematic Conference ECCOMAS,* 2011.

[65] A. Kahraman and R. Singh, "Non-linear dynamics of a spur gear pair," *Journal of Sound and Vibration,* 142.1 (1990), 49 –75.

[66] H. Özgüven and D. Houser, "Dynamic analysis of high speed gears by using loaded static transmission error," *Journal of Sound and Vibration,* 125.1 (1988), 71 – 83.

[67] M. Kubur, A. Kahraman, D. M. Zini and a. K. Kienzle, "Dynamic Analysis of a Multi-Shaft Helical Gear Transmission by Finite Elements: Model and Experiment," *Journal of Vibration and Acoustics,* 126.3 (2004), 398–406.

[68] S. Li., "Experimental investigation and FEM analysis of resonance frequency behavior of three-dimensional, thin-walled spur gears with a power-circulating test rig," *Mechanism and Machine Theory,* 43.8 (2008), 934 –963.

[69] Y. Cai and T. Hayashi, "The Linear Approximated Equation of Vibration of a Pair of Spur Gears (Theory and Experiment)," *Journal of Mechanical Design ,* 116.251 (1994), 558–564.

[70] G. Blankenship and A. Kahraman, "Steady state forced response of a mechanical oscillator with combined parametric excitation and clearance type non-linearity," *Journal of Sound and Vibration,* 185.5 (1995), 743 –765.

[71] A. Kahraman and G. Blankenship, "Interactions Between Commensurate Parametric And Forcing Excitations In A System With Clearance," *Journal of Sound and Vibration,* 194.3 (1996), 317 –336.

[72] A. Andersson and L. Vedmar., "A dynamic model to determine vibrations in involute helical gears," *Journal of Sound and Vibration ,* 260.2 (2003), 195 –212.

[73] H. Özgüven, "A non-linear mathematical model for dynamic analysis of spur gears including shaft and bearing dynamics," *Journal of Sound and Vibration,* 145.2 (1991), 239 –260.

[74] P. Velex and M. Maatar, "A Mathematical Model for Analyzing the Influence of Shape Deviations and Mounting Errors on Gear Dynamic Behaviour," *Journal of Sound and Vibration,* 191.5 (1996), 629 –660.

[75] S. Shweiki, J. Korta, A. Palermo, R. Adduci and D. Mundo, "Combininf finite element analysis and analytical modelling for efficient simulations of non-linear gear dynamics," *VII European Congress on Computational Methods in Applied Sciences and Engineering,* Crete Island, Greece, 5–10 June 2016.

[76] J. Korta, A. Palermo, D. Mundo and S. Shweiki, "Combining Finite Element and Multibody Modeling Techniques for Time-Efficient Simulation of Nonlinear

Gear Dynamics," *SIMUL 2015 : The Seventh International Conference on Advances in System Simulation.*

[77] J. Wang and I. Howard, "Finite Element Analysis of High Contact Ratio Spur Gears in Mesh," *Journal of Tribology,* 127.3 (2005), 469 –483.

[78] V. Abousleiman and P. Velex, "A hybrid 3D finite element/lumped parameter model for quasi-static and dynamic analyses of planetary/epicyclic gear sets," *Mechanism and Machine Theory,* 41.6 (2006), 725 –748.

[79] S. Vijayakar, "A combined surface integral and finite element solution for a three-dimensional contact problem," *International Journal for Numerical Methods in Engineering,* 31.3 (1991).

[80] B. K. Han, M. K. Cho, C. Kim, C. H. Lim and J. J. Kim, "Prediction of vibrating forces on meshing gears for a gear rattle using a new multi-body dynamic model," *International Journal of Automotive Technology,* 10.4 (2009), 469–474.

[81] Z. Neusser, M. Sopouch, T. Schaffner and H.-H. Priebsch, "Multibody Dynamics Based Gear Mesh Models for Prediction of Gear Dynamics and Transmission Error," *SAE Technical Paper. SAE International,* Apr. 2010.

[82] "Boosting productivity in gearbox engineering. \protect\unhbox\ voidb @ x \ penalty \ @M \ https : / / community . plm . automation . siemens . com / siemensplm/attachments/siemensplm/Simcenter_event_tkb/117/2/Siemens-PLM-Boosting-Productivity-in-Gearbox-E," *Siemens PLM Software,* 2017.

[83] S. Shweiki, A. Rezayat, T. Tamarozzi and D. Mundo, "Transmission Error and strain analysis of lightweight gears by using a hybrid FE-analytical gear contact model," *Mechanical Systems and Signal Processing,* 123, 2019, 573-590.

[84] I. Gonzalez-Perez, J. L. Iserte and A. Fuentes, "Implementation of Hertz theory and validation of a finite element model for stress analysis of gear drives with localized bearing contact," *Mechanism and Machine Theory,* 46, 6 (2011) 765–783.

[85] P. Davoli, E. Conrado and K. Michaelis, "Recognizing gear failures," *Machine Design,* 79 (June 2007), 64–67.

[86] "ZF 8HP 8-Speed Automatic Transmission, Product Brochure".

[87] P. G. Catera, F. Gagliardi, D. Mundo, L. D. Napoli, A. Matveeva and L. Farkas, "Multi-scale modelling of triaxial braided composites for FE-based modal analysis of hybrid metal-composite gears," *Composite Structures ,* pp. 116-123, 2017, 182.

[88] C. Ayranci and J. Carey, "2D braided composites: A review for stiffness critical applications," *Composite Structures,* 85, 1, September 2008, 43-58.

[89] M. Shokrieh and M. Mazloomi, "An analytical method for calculating stiffness of two-dimensional triaxial braided composites," *Composite Structures,* 92, 12, November 2010, 2901-2905.

[90] J. D. Littell, W. K. Binienda, W. A. Arnold, G. D. Roberts and R. K. Goldberg, "Effect of microscopic damage events on static and ballistic impact strength of triaxial braid composites," *Composites Part A: Applied Science and Manufacturing,* 40, 12, December 2009, 1846-1862.

[91] C. Cater, X. Xiao, R. K. Golberg and L. W. Kohlman, "Improved subcell model for the prediction of braided composite response," *NASA/TM-2013-217875, June 2013*.

[92] X. Li, "Mesomechanical model for failure study of two dimensional triaxial braided composite materials," *Ph.D dissertation,* December 2010.

[93] C. Zhang and W. Binienda, "A meso-scale finite element model for simulating free-edge effect in carbon/epoxy textile composite," *Mechanics of Materials,* 76, September 2014, 1-19.

[94] C. Zhang, "Multi-scale characterization and failure modeling of carbon/epoxy triaxially braided composite," *Ph.D dissertation,* December 2013.

[95] C. Zhang, N. Li, W. Wang, W. K. Binienda and H. Fang, "Progressive damage simulation of triaxially braided composite using a 3D meso-scale finite element model," *Composite Structures,* 125, July 2015, 104-116.

[96] L. Xu, S. J. Kim, C.-H. Ong and S. K. Ha, "Prediction of material properties of biaxial and triaxial braided textile composites," *Journal of Composite Materials,* 46, 18, 2012.

[97] "Siemens PLM software's Simcenter".

[98] P. Catera, D. Mundo, F. Gagliardi and A. Treviso, "A comparative analysis of adhesive bonding and interference fitting as joining technologies for hybrid metal-composite gear manufacturing," *International Journal on Interactive Design and Manufacturing (IJIDeM),* 2020.

[99] P. G. Catera, D. Mundo, A. Treviso, F. Gagliardi and A. Visrolia, "On the Design and Simulation of Hybrid Metal-Composite Gears," *Applied Composite Materials,* Vols. Issue 3, 26, pp. 817-833, 2019.

[100] J. H. Ginsberg, "Mechanical and Structural Vibrations: theory and applications," *John Wiley and sons,* 2001.

[101] S. Shweiki, A. Palermo and D. Mundo, "A Study on the Dynamic Behaviour of Lightweight Gears," *Shock and Vibration,* 2017.

[102] C.-M. Kuo, "Elastic bending behavior of solid orthogonal woven 3-D carbon-carbon composite beams," *Composite Science and Technology,* 68, 2008, 666-672.

[103] www.torayca.com.

[104] S. Adhikari, "Structural Dynamic Analysis with Generalized Damping Models, Analysis," *John Wiley & Sons, Inc.,* 2014.

[105] H. Abramovich, D. Govich and A. Grunwald, "Damping measurements of laminated composite materials and aluminum using the hysteresis loop method," *Progress in Aerospace Sciences,* 78, 2015, 8-18.

[106] A. Treviso, B. V. Genechten, D. Mundo and M. Tournour, "Damping in composite materials: Properties and models," *Composite Part B,* 78, 2015, 144-152.

[107] "Siemens LMS Scadas system".

[108] "Basic Dynamic Analysis User's Guide, Siemens NX Nastran".

[109] S. Mahmoudi, A. Kervoelen, G. Robin, L. Duigou, E. Daya and J. Cadou, "Experimental and numerical investigation of the damping of flax–epoxy composite plates," *Composite Structures,* 208, 2019, 426-433.

[110] "ASTM D 3039. Standard Test Method for Tensile Properties of Polymer Mtrix Composite Materials".

[111] "M46J. technical datasheet, Toray Composite Materials America Inc.".

[112] M. Bruyneel, J. P. Delsemme, P. Jetteur and F. Germain, "Modeling interl-laminar failure in composite structures: illustration on an industrial case study," *Applied Composite Materials,* 16, 2009, 149-162.

[113] O. Allix and L. P., "Interlaminar interface modelling for the prediction of laminated delamination," *Composite Structures,* 22, 1992, 235-242.

[114] "NX Nastran, Multi-Step Nonlinear User's Guide".

[115] A. Palermo, L. Britte, K. Janssens, D. Mundo and W. Desmet, "The measurement of Gear Transmission Error as an NVH indicator: Theoretical discussion and industrial application via low-cost digital encoders to an all-electric vehicle gearbox," *Mechanical Systems and Signal Processing,* 110, 2018, 360-389.

[116] J. Smith, "Gear noise and vibration," *2nd ed. Marcel Dekker, Inc,* 2003.

[117] J. A. Korta and D. Mundo, "Multi-objective micro-geometry optimization of the gear tooth supported by response surface methodology," *Mechanism and Machine Theory,* 109, 2017, 278-295.

[118] S. Shweiki, "Static and dynamic characterization of a precision gear test rig and its application to the measurement of gear Transmission Error," *Master's Degree Thesis,* University of Calabria, 2015.

[119] A. Palermo, J. Anthonis, D. Mundo and W. Desmet, "A novel gear test rig with adjustable shaft compliance and misalignments. Part I: Design," *Proceedings of the CMMNO,* 2013.

[120] F. C. Baccar, M. S. Abbes and M. Haddar, "Effect of spalling or tooth breakage on gearmesh stiffness and dynamic response of a one-stage spur gear transmission," *European Journal of Mechanics - A/Solids,* 27.4 (2008), 691 –705.